ABSTRACT

Title of Document: THE HYDROLOGIC AND WATER QUALITY PERFORMANCE OF THE SLIGO-DENNIS BIORETENTION CELL.

Jennifer M. Olszewski, Master of Science, 2010

Directed By: Professor Allen P. Davis
Civil and Environmental Engineering

Bioretention cells have been found to improve the hydrologic and water quality performance of impervious areas such as parking lots. The current study recorded hydrologic data from a bioretention cell in Silver Spring, MD, over a period of 2 years, collecting water quality data from 14 storm events. Data showed the cell completely captured storm events that produced less than or equal to 1.27 cm of rainfall, after which a linear relationship between cell outflow and cell inflow was observed. The cell was found to reduce the site CN from 96 down to 79 and to have a CN of 96 when assessed as a separate land use. The hydrologic performance was also compared to that of a forested stream near Baltimore, MD. While the cell performed similarly volumetrically for storms producing less than or equal to 2 cm of rainfall, the Sligo-Dennis flow-durations were typically half the length and double the flowrate of those of the forested stream.

THE HYDROLOGIC AND WATER QUALITY PERFORMANCE OF SLIGO-DENNIS BIORETENTION CELL.

By

Jennifer Marie Olszewski

Thesis submitted to the Faculty of the Graduate School of the
University of Maryland, College Park, in partial fulfillment
of the requirements for the degree of
Master of Science
2010

Advisory Committee:
Professor Allen P. Davis, Chair
Professor Alba Torrents
Professor Richard McCuen

Dedication

Dedicated to the continued fight to save the Beautiful Chesapeake Bay to all those working towards its restoration. The Bay has fueled my passion for environmental engineering over the past 5 years and is a main factor in my love of the field.

Acknowledgements

Thank you to all my mentors, family, and friends. A special thanks to Dr. Allen P. Davis for guiding through two years of rain garden research; always pushing me to look deeper. I will forever have a passion for and a true belief in the impact of these seemingly little gardens. My experience would not have been the same without Dr. Alba Torrents and Dr. Eric A. Seagren. From real-world chemistry problems to aeration raps, your classes got me excited about environmental engineering and never failed to challenge me. And I owe a sincere thanks to Dr. McCuen for believing in me even when I did not believe in myself.

To all my lab mates, Carmen Franks, Poornima Natarajan, Sean O'Neil, Hunho Kim for patiently helping me out in the lab and for being my friends. I extend a special thanks to Phillip Jones for teaching me the ropes even after graduating.

To my environmental engineering twin, Jason Louis Becker, it has been one great adventure, and I don't know how I will go to class without you. Thank you for being there through all the highs and lows. To all my friends, Jessica Rajkowski, Luke Johnson, Erica Espenak, Caitlin Dietsche, Livia Ehardt, Abi Kallushi, Mark Patrick, and John Chai for your unwavering faith in my abilities.

Thank you to my parents, for being proud of me for simply doing my best. Mom, thank you for instilling me with a passion and a deep respect for nature that has sparked my passion in environmental engineering. Dad, thank you for teaching me to be an engineer and to always be creative in my solutions.

Table of Contents

List of Tables

List of Figures

Chapter 1: Introduction

1.1 Impacts of Urban Stormwater

Urban ecosystems typically rely on a system of pipes to remove rainwater from impervious surfaces such as roads, parking lots, and roofs as quickly and as efficiently as possible. This design ensures public safety and health by preventing urban flooding. Due to the high percentage of impervious surfaces and the efficiency with which water is removed, very little infiltration into the ground occurs before this water runs off into surrounding areas. As a result, urban runoff delivers excess water to surrounding ecosystems. Because urban runoff moves rapidly, it also introduces energy to surrounding ecosystems, which allows the water to move a greater amount of pollutants and nutrients.

Many studies have shown that urban areas negatively impact both the hydrology and water quality of surrounding streams and other natural water bodies (Barco et al. 2009). High energy runoff causes flashier hydrographs and is the source of many of the symptoms associated with the "Urban Stream Syndrome" (Walsh et al. 2005). Symptoms of this syndrome include channelization of streams and rivers, increased nutrient loading, and decreased biotic diversity (Walsh et al. 2005). While the loss of meanders in a stream reduces areas of denitrification, increased nutrient loadings can further increase phosphorous and nitrogen levels. Excess nutrients can lead to eutrophication and eventual dead zones if left alone. Eutrophication, in turn, can reduce biodiversity and overall natural water health.

As development increases worldwide, urban runoff is becoming more and more of a problem. Fewer forests and riparian buffers lead to less rain absorption before urban runoff reaches streams. With fewer buffers, more water with more pollutants, higher temperatures, and higher flowrates enters natural waters. Smaller storm events have the potential to more greatly impact surrounding ecosystems due to this reduction in infiltration through impervious areas. What once was a 1-year event could now have the impact of a 3-year flood on the same area after development.

Bioretention cells or "Rain Gardens" are one method of slowing down and filtering urban runoff before it reaches surrounding ecosystems. These cells are part of the LID (Low Impact Development) effort to reduce the effect of development on the environment by the most natural means possible. LID designs emphasize simplicity and incorporating green space within development and around impervious surfaces. Following this idea, bioretention cells are gardens with multiple layers of media for infiltration.

Bioretention cells are designed to manage runoff from impervious surfaces like parking lots and roofs. They are placed down gradient from a given drainage area and runoff is directed into the cells. Once the runoff enters the cell, it infiltrates down through the media. If the storage capacity of the cell is met or if the runoff arrival rate is faster than the cell infiltration rate, ponding will occur, as shown at the top of the cell in Figure 1.1. The storage capacity refers to the maximum amount of water a bioretention cell can hold. Once this value is met, the cell begins to produce outflow. This outflowing water can leave through infiltration to surrounding soils, an underdrain, and/or through overflow. Only larger storms with excessive ponding

promote overflow. One study found only 0.8% of all inflow to a bioretention cell produced overflow; all other water left through subsurface flow (Dietz and Clausen 2005). Water exiting through subsurface flow is filtered in the cell, which promotes pollution removal, outflow volume and flowrate reduction, and allows the runoff to cool off (Davis 2005).

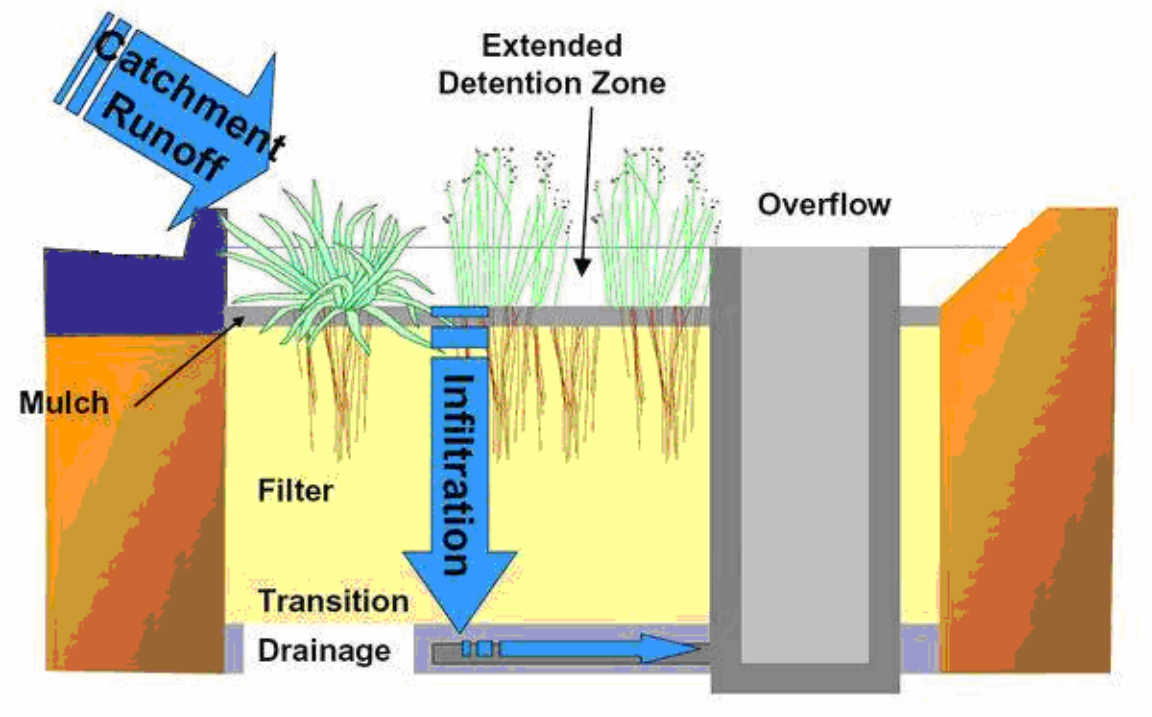

Figure 1.1. Diagram shows movement of runoff from impervious drainage area into and through Bioretention cell. Runoff infiltrates down through the cell. If the storage capacity of a cell is met water can leave through an underdrain if present and/or can overflow once ponding at the surface has reached a maximum.

1.2 Literature Review

1.2.1 Bioretention Cell Design

Bioretention cells use both infiltration and media storage to mitigate runoff volume. A typical cell consists of a 7.5-cm top layer of mulch, an 80-cm layer of permeable soil made up of a mixture of clay, silt and sand, a 15-cm layer of sand, and

a bottom 40-cm layer of gravel (Anacostia Low Impact Development 2005). This layering design allows for water storage in the upper, less permeable soil as well as infiltration in the lower sand and gravel layers. Once upper layers are saturated, water will begin to pond on the surface of the cell. Most cells are designed to allow for 15-30-cm of ponding before overflow of runoff occurs. Some cells also have underdrains that minimize overflows and reduce ponding.

Many facilities are sized using the Prince George's County Bioretention Manual to size bioretention facilities (PGC Bioretention Manual 2007). Facilities are sized based on the post and pre-development Curve Number (CN) values for the drainage area, a design storm, and a pre-development peak flow (PGC Bioretention Manual 2007). Other sizing methods use the rational method by multiplying the "C" value for the drainage area by 5-7% of its area (Dietz and Clausen 2005). Regardless of the method, facilities are sized relative to how much runoff they will receive and how much volume is required to store a given design storm size.

1.2.2 Bioretention Cell Hydrologic Performance

Overall, bioretention cells have been found to perform well hydrologically. One study done at the University of Maryland found that 18% of 49 storm events were completely captured by the lined cells being monitored. In addition, peak flows were reduced by 44-63% and were delayed significantly, usually by a factor of 2 (Davis 2008). A study in North Carolina found similar reductions, reporting that all outflow volumes were less than 50% of the inflow volumes in unlined bioretention cells over the course of a year (Hunt et al. 2006). A peak reduction of 96% was seen

in storm events producing less than 4-cm of rainfall in a study done by Hunt et al (2008).

Because cell runoff storage depends on the saturation of the cell, environmental factors such as temperature and antecedent dry time can play a role in cell performance. One study in Norway found that the hydraulic retention time of a bioretention cell was positively correlated to the air temperature (Muthanna et al. 2007). The same study also observed an overall average peak flow reduction of 42%, and a 27% peak flow reduction for all storm events occurring in temperatures <0°C. Reduced infiltration due to frozen media as well as reduced evapotranspiration were listed as possible causes for poorer winter performance (Muthanna et al 2007). Another study done in North Carolina also found higher cell outflow:runoff from the drainage area being served ratios in winter months. This difference was partially attributed to decreased evapotranspiration during winter months (Hunt et al. 2006).

1.2.3 Bioretention Cell Water Quality Performance

Pollutant studies consistently show bioretention cells reduce Total Suspended Solids (TSS) and metals content. While removals of TSS and metals are consistently around 55-99%, those for phosphorous and nitrogen vary greatly (Davis et al. 2009). Media make-up may play a large role in these inconsistencies. One study that monitored the performance of two bioretention cells found that one cell promoted denitrification while the other did not. Organic material in the media, flow characteristics, and perhaps age were cited as possible reasons for these differences (Li and Davis 2009). Organic material in anoxic conditions allows for denitrification.

Different flow paths may allow for areas of extended saturation, perhaps leading to anoxic, denitrifying conditions in lower levels of the media. More mature plants and older cells may also promote greater denitrification.

Phosphorous removal via bioretention has been reported as inconsistent throughout the literature. Because phosphorous usually attaches to particulates, it should be removed in the upper layer of the cell along with TSS. In the field, however, phosphorous is much less predictable. Retention percentages range from -105% (Dietz and Clausen 2005) to 59% (Davis et al. 2003). Negative retention values represent phosphorous export. A number of studies reported phosphorous export most likely due to high phosphorous levels in bioretention media (Dietz 2007). Media with low phosphorous saturation levels (Hunt et al. 2006) and existing soil disturbance (Dietz and Clausen 2005) were also cited as possible causes of phosphorous export.

Infiltration can provide filtration of total suspended solids (TSS) and adsorption of metals; nutrient removal can also be promoted, which depends on biological activity. Larger particles may become captured in the top layer (5-20-cm depth), requiring periodic cleaning or removal and replacement of the top media layer (Davis et al. 2008). One study measured that the top layer of mulch retained 98%, 36%, and 16% of inflowing Cu, Pb, and Zn (Dietz and Clausen 2006). Native, water-loving vegetation enhance evapotranspiration, aid in infiltration and increasing the permeability of the media, as well as encourage biological activity and eventual, possible denitrification (Wolf and Lundholm 2008). A study on green roofs also found facilities with older, more established vegetation saw greater porosity, organic

matter content, and water holding capacity than newly installed facilities (Getter et al. 2007). Specific plant type depends on location; more research is needed to determine optimal performance.

Cells with ISZs (internal storage zones) or IWS (internal water storage) may also promote greater denitrification, especially in warmer and humid months, by creating lower, anoxic layers of saturated media (Passeport et al. 2009). These storage zones consist of an underdrain with an upturned, 90-degree elbow at its end. Water remains the lower layer of the cell when the water level is below that of the upturned elbow, creating anaerobic conditions (Hunt et al. 2006). This design is shown in Figure 2.1.

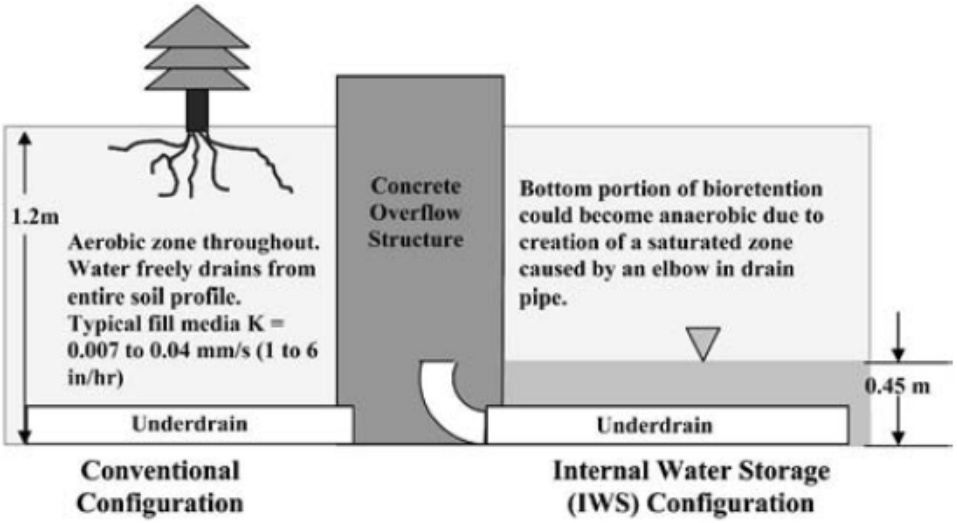

Figure 1.2 A conventional underdrain is shown on the left and an IWS underdrain is shown on the right. Water remains in lower level of the cell in the IWS configuration due to the upturned elbow. This saturated area may promote anaerobic zone in cell, allowing for denitrification (Hunt et al. 2006).

Different carbon sources and electron donors can affect the ability of a cell to denitrify (Kim et al. 2000). A laboratory column study found using newspaper as a carbon source promoted 100% NO_3-N removal (Kim et al. 2000). In general,

however, achieving these conditions has proved to be challenging in bioretention cells.

Nitrate removal especially is difficult to achieve in the field. While a study done in Haddam, Connecticut showed NO_3-N reductions of 87% in cells with ISZ's (Dietz and Clausen 2006), others found very little change in NO_3-N concentration. A study in North Carolina found no significant nitrogen reduction in a cell equipped with an ISZ. Furthermore, NH_4^+-N and TKN levels in outflowing water were greater than those measured in cells with conventional underdrains in the same study. These results may have been due to an extensive anaerobic zone in the lower levels of the cell. Too many anaerobic regions can prevent nitrification of NH_4^+-N to NO_3-N, leaving most nitrogen in the NH_4^+-N and TKN forms (Hunt et al. 2006).

Another study found 84.6% retention of NH_4^+-N, which was attributed to both adsorption to the negatively charged soil as well as nitrification. No significant removal was seen for NO_3-N, suggesting very little denitrification was occurring (Dietz and Clausen 2005). While it was not a focus of the current study, the behavior of nitrogen in bioretention cells is a very important area of research because it is difficult to remove consistently.

1.2.4 Factors Affecting Bioretention Performance

Vegetation appears to play a large role in bioretention cell performance. Evapotranspiration, which accounted for 15-20% of all inflow loss in one study done in North Carolina, plays an important role in cells (Davis et al. 2009). Most cells consist of a variety of trees and shrubs. One study showed that grassed cells

performed just as well, if not better than typical cells by reducing water volume and peak flow as well as pollutant content (Passeport et al. 2009). The Prince George's Bioretention Manual suggests plants tolerant of expected pollutant loads, fluctuating soil moisture, ponding, and a range of soil pHs (PGC Bioretention manual 2007). Native species that fit these criteria were strongly recommended versus invasive species such as English Ivy (PGC Bioretention manual 2007). How to best apply vegetation to optimize hydrologic performance and nutrient uptake requires more research (Davis et al. 2009).

Surrounding media may also affect performance. Cells placed in media with lower permeability and hydraulic conductivity (clays) may have more need for an underdrain than those placed in more permeable and sandy media (PGC Bioretention Manual 2007). Surrounding media may affect how a bioretention cell drains and how much water is lost to groundwater recharge.

1.3 Research Goals

This study will focus on the performance of a bioretention cell in Silver Spring, MD. A previous study on this cell showed good removal of TSS, metals, phosphorus, and nitrogen, performing better than another, smaller cell located at the University of Maryland. While both cells treated similar storm events, the Silver Spring cell had a greater storage capacity and therefore allowed for greater media contact time for small events (Li and Davis 2009). Higher organic matter content in the Silver Spring cell may have also been responsible for its greater nitrogen removal

(Li and Davis 2009). Water quality data performance, especially nitrogen and phosphorous in the current study, will be compared to these data.

Bioretention cells offer localized solutions to urban runoff. If parking lot and road runoff could be directed into and managed by bioretention cells, the causes of the Urban Stream Syndrome may be greatly reduced. However, the exact effectiveness of these structures is not known. The main goal of this research is to better understand the long-term, hydrologic performance of bioretention cells and how their performance compares with that of pre-development areas.

Many studies of bioretention cells assess performance solely on percent reductions from inflowing water to outflowing water. While these reductions are important, their comparison with pre-development values is an important measure of the effectiveness of bioretention cells. There is a gap in research between how a cell will perform and what impact its performance will have on a watershed. The success of a bioretention cell is generally regarded as reducing post-development conditions to states similar to predevelopment conditions. Success the Chesapeake Bay watershed is usually constituted as meeting or working towards meeting pre-development conditions. Reaching pre-development conditions is difficult and ambitious, especially when bioretention cells serve only small portions of a watershed. As a result, their impact is not always seen downstream. Seeing how bioretention cells perform compared to relevant forested watersheds could prove helpful in implementing cells on a watershed level.

This study aimed to establish a storage capacity for the cell in order to better understand its performance. To do so, the relationships between rainfall depth, cell

inflow volume, and cell outflow volume were plotted and analyzed. By defining a cell storage capacity, the cell could be characterized by the storm events it completely captured. Furthermore, this storage could be compared with other land uses and used to design future bioretention cells based on pre-development storm capture.

In order to achieve the stated goal, CN's were also estimated for both the Sligo-Dennis drainage area with the mitigation of the cell and for the bioretention cell itself. These estimates were then compared with designated CN's for alternative land uses such as woods and pavement. The CN obtained for the site was also compared with that of the original Sligo-Dennis parking lot to show the volumetric improvement provided by the cell.

In addition to comparing the volumetric performance of the cell with pre-development land uses, this study also aimed to evaluate the overall hydrologic regime of the cell. Data, were therefore, obtained from a forested stream located 72 km north of the cell. Flows, lag times, flow durations, and overall flow volumes were analyzed for each site and compared. Through this comparison, this study hopes to compare the hydrologic regimes of the cell and the forested stream, determining how well the bioretention cell mimics pre-development hydrology.

Chapter 2: Methods and Materials

2.1 Sligo-Dennis Bioretention Cell

2.1.1 Bioretention Site Description

The current study follows the performance of a bioretention cell installed in August, 2005 at the base of the Dennis Avenue Health Center parking lot. This facility is located on Dennis Avenue, right off of Georgia Avenue in Silver Spring, MD, shown in Figure 2.1. As part of Anacostia River LID Development, the cell was installed to mitigate and treat runoff from the Health Center parking lot, which has a drainage area of about 0.37 ha. On a larger scale, the cell and its drainage area are part of the Sligo Creek watershed, which is a tributary of the Northwest Branch of the Anacostia River. Figures 2.1 and 2.2 show the cell, its drainage area, and its location.

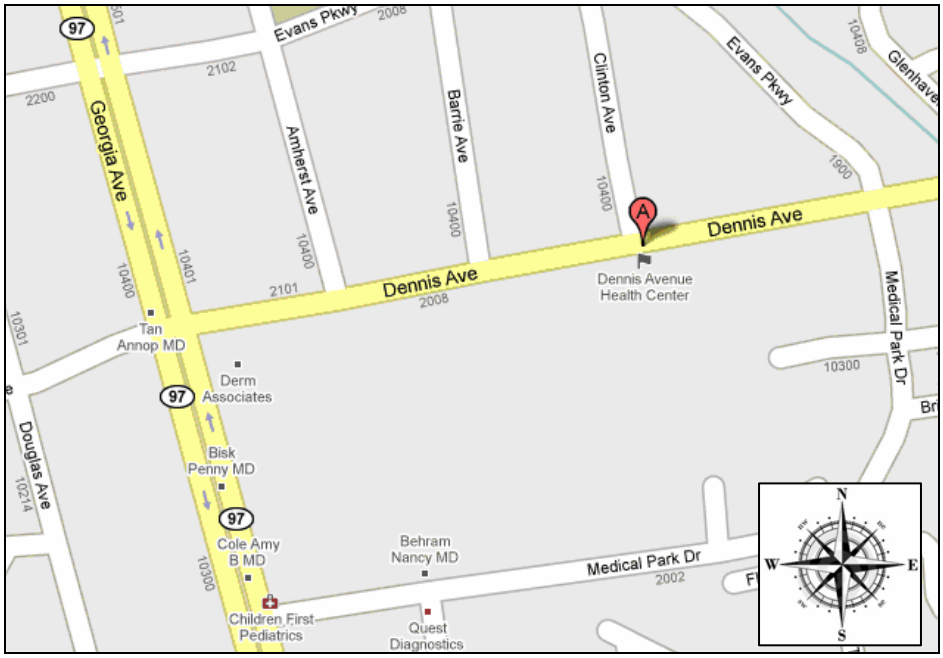

Figure 2.1 Site Location, Georgia Avenue on the left and Sligo Creek in the top right corner (www.googlemaps.com).

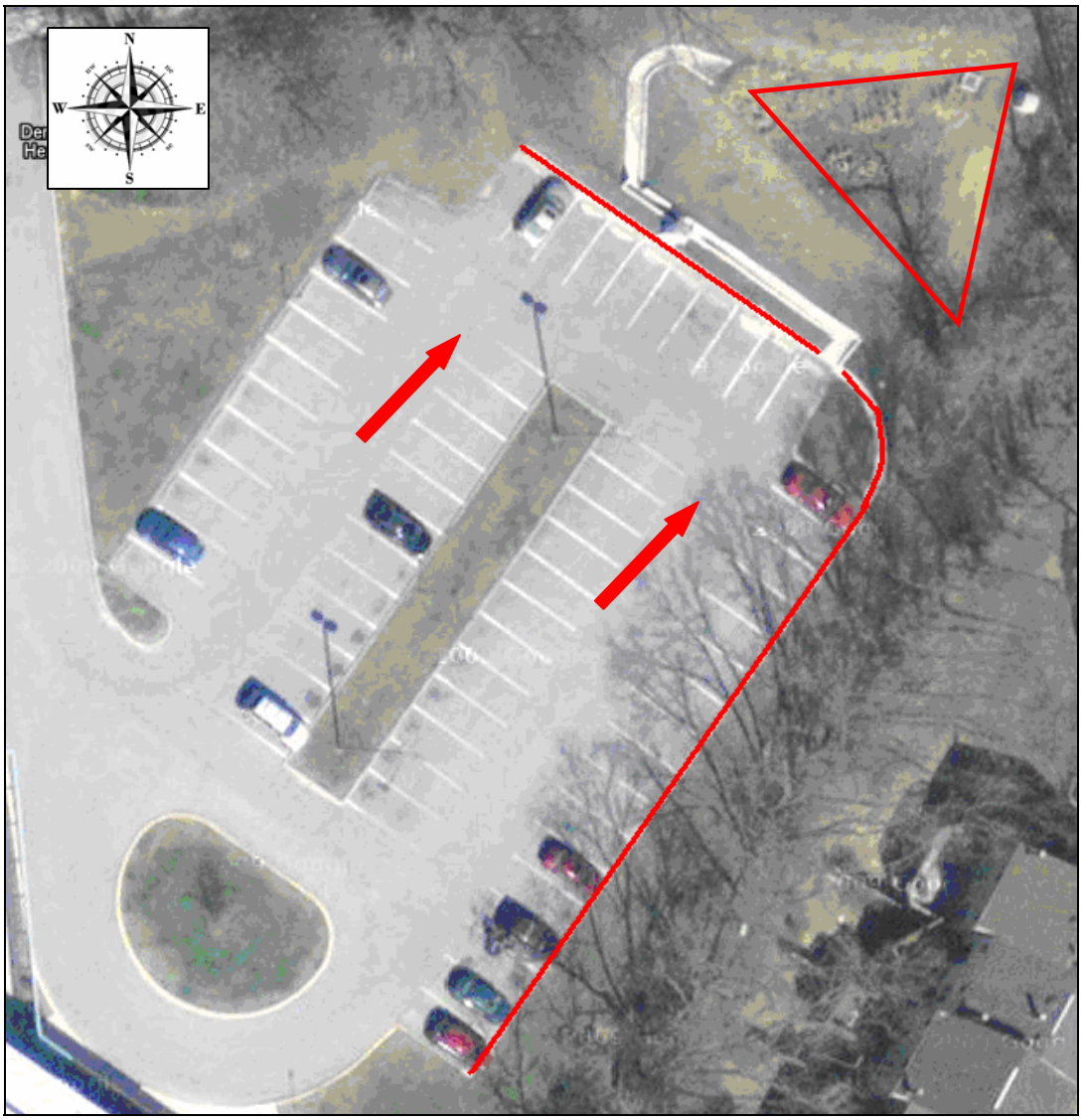

Figure 2.2 Arial View of Sligo-Dennis Bioretention Cell (inside the red triangle) and the parking lot it serves. The arrows show direction of runoff in the parking lot and the red outlines show where curbs guide runoff into the channel (www.googlemaps.com).

During and after a storm event, runoff travels through sheet flow on the parking lot in the direction of the arrows shown in Figure 2.2. The runoff is also guided by curbs shown in red along the perimeter of the parking lot (see Figure 2.3) and channeled into the cell flume at the northeast corner of the parking lot. At this corner, the curbs open up into the flume that directs the water in the northwest

direction, curving back to enter the triangular bioretention cell at its western corner. An underdrain and an overflow drain are situated at the east corner of the cell. Runoff flows from the west to the east/southeast of the cell.

A system of five (15 cm) perforated pipes drains the cell. These pipes are installed in the bottom, coarse aggregate layer of the cell, which are attached to the monitored, 15 cm outflow underdrain, and eventually the existing stormwater system. All pipes are shown in black and white lines in Figure 2.3. A larger black and white line extends out from the site, which represents the existing stormwater system. Five vertical observation wells are connected to the drains and are evenly distributed over the cell. Observation wells are denoted as outlined circles in Figure 2.3. This drainage system ends at the bottom of a grated manhole, represented by the outlined square at the top left of Figure 2.3. The underdrain is equipped with a 15-cm volumetric weir (Thel-Mar) to which an Teledyne ISCO 730 Bubbler Module is attached and used to record water level data. The manhole grate also serves as an overflow for the cell if ponding exceeds 30 cm.

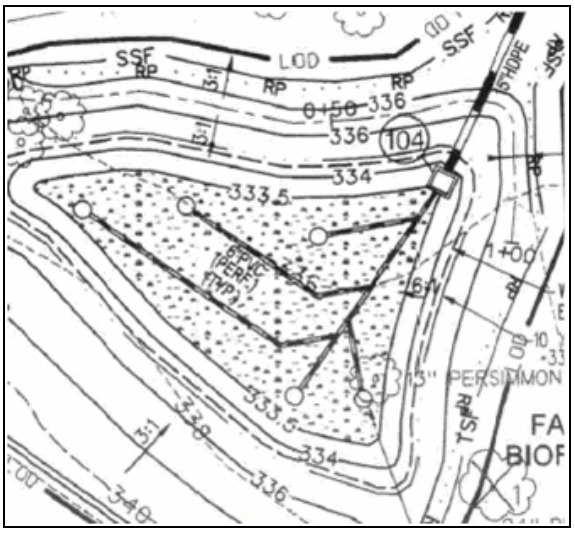

Figure 2.3 Underdrain system of bioretention cell. Observation wells are outlined circles, pipes are black and white lines, and the grated manhole/overflow is in an outlined square (blueprints).

The cell media has an area of about 102 m^2, which is about 2.8% of the entire drainage area and just below the typical 3-5% range (Davis 2008). It also has a depth of 0.9 m, which consists of four layers. The cell blueprints specified the following layers and media types. The top layer was designed with a 3:1 slope on the sides with a level bottom. This top layer was filled with 8 cm of hardwood mulch. The next layer down is a permeable soil mixture 76 cm deep. This soil mixture was specified to consist of one third C33 sand, one third high grade compost, and one third soil made up of no more than 10% clay, 30-55% silt, and 35-60% sand. Below the soil mixture is a 15 cm layer of sand for infiltration. This sand is silica based, washed ASTM C33 Fine Aggregate Concrete Sand, which meets ASTM C-33 gradation. Under the sand is a 38 cm layer of coarse aggregate. In total, the bioretention cell has a depth of about 0.9 m and a total volume of 91.8 m^3. Figure 2.4 shows a cross-section of the cell and its layered components.

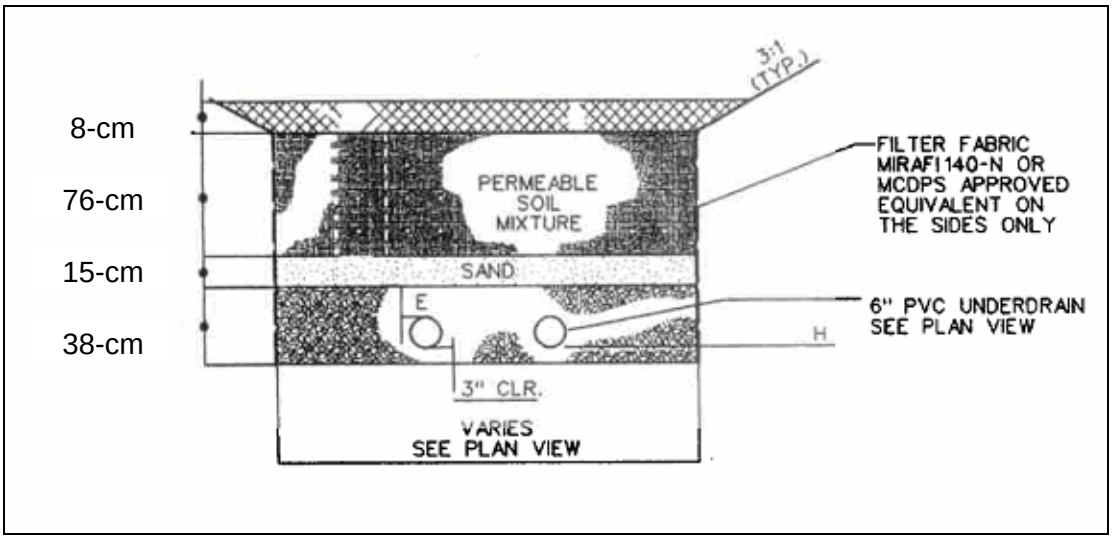

Figure 2.4 Cross-section of proposed media depths and organization. The 15cm underdrain is shown in the bottom, gravel layer.

A study done in 2007 found the cell media to consist of a sandy clay loam with a pH of 7.7 and an organic matter content of 12.2%. According to the study the cell media was 54% sand, 26% silt, and 20% clay (Li 2007). While it is difficult to tell how close these values are to the blueprint specifications, the media is within typical bioretention values (Davis 2008; Passeport et al. 2009). From these measurements a porosity of 42% was estimated by adding the weighted-average porosities of each media type (sand, silt, and clay) (Fetter 2001). The overall media distributions are compiled in Table 2.1.

Table 2.1 Media distributions and porosity for Sligo-Dennis bioretention cell.

Media Type	Average Porosity % (Fetter 2001)	Fraction in Cell
Sand	40	0.54
Silt	42.5	0.26
Clay	46.5	0.20

Figure 2.5 shows the cell after installation in 2005. Specific vegetation types and quantities were planted according to the cell blueprints. The vegetation planted

was fairly mature to better ensure survival and optimal effectiveness. Figure 2.6 shows the cell after 5 years, in June, 2010; the plants have grown and filled the cell since installation in 2005.

Figure 2.5 Picture of cell after installation in 2006 (Davis 2008).

Figure 2.6 Picture of cell taken in June, 2010.

Shade, ornamental, and evergreen trees were all planted in the cell initially. A number of shrubs, ornamental grasses and perennials were also planted. A list of all vegetation initially planted in the cell is shown in Table 2.2. From 2005 to present, the vegetation has grown substantially. No hydric vegetation has overtaken the cell, suggesting that the cell is not consistently oversaturated. Lack of hydric conditions

also implies the cell is draining normally and not ponding excessively due to clogging or compression of the media (Asleson et al. 2009). Periodic observations of the cell during and after storm events confirm that ponding only occurs in larger storms and water levels in the cell decline according to the overall, saturated infiltration rate of the cell. This decrease in ponding height was continuous. From these observations, the cell seems to be performing according to its design.

PLANT LIST

Qty	Key	Botanical Name	Common Name
		Shade Trees	
7	AR	Acer rubrum 'October Glory'	Red Maple
0	NS	Nyssa sylvatica	Black Gum
3	QP	Quercus palustris	Pin Oak
1	TA	Tilia americana	Basswood
		Ornamental Trees	
0	AA	Amelanchier arborea	Downy Serviceberry
0	CC	Cercis canadensis	Redbud
2	CV	Chioanthus virginicus	White Fringetree
		Evergreen Trees	
13	PS	Pinus strobus	White Pine
6	TC	Tsuga canadensis	Canadian Hemlock
		Shrubs	
27	AP	Aesculus parviflora	Bottlebrush Buckeye
22	CO	Cephalanthus occidentalis	Buttonbush
33	IG	Ilex glabra "Shamrock"	Inkberry
3	KL	Kalmia latifolia "Otsbo Red"	Mountainlaurel
3	LB	Lindera benzoin	Spicebush
6	VC	Vaccinium corymbosum	Highbush Blueberry
24	VD	Viburnum dentatum	Arrowwood Viburnum
		Ornamental Grasses	
~~345~~455	AV	Andropogon virginicus	Broomsedge
702	PV	Panicum virgatum	Switchgrass
442	SP	Scirpus pungens	Three Square Bullrush
		Perennials	
~~96~~120	IV	Iris versicolor	Blue Flag
385	LC	Lobelia cardinalis	Cardinal Flower

Table 2.2 List of all vegetation planted in cell as well as size, source, and establishment before planting (blueprints).

2.1.2 Cell Drainage Area and Curve Number Estimates

A number of storms were observed to determine the drainage area and flow patterns both in the parking lot and the bioretention cell. The drainage area was initially estimated to be 0.45 ha. However, after observation, a new estimate of 0.37 ha was made, excluding part of the curbed, exiting driveway at the left side of Figure 2.2. Runoff was not found to travel over the curbs of this area into the cell. Both the initial and observed drainage areas are shown in Figure 2.7, where a grey outline depicts the new, estimated drainage area. Part of the driveway and grassy areas south of it were not included in this new estimate.

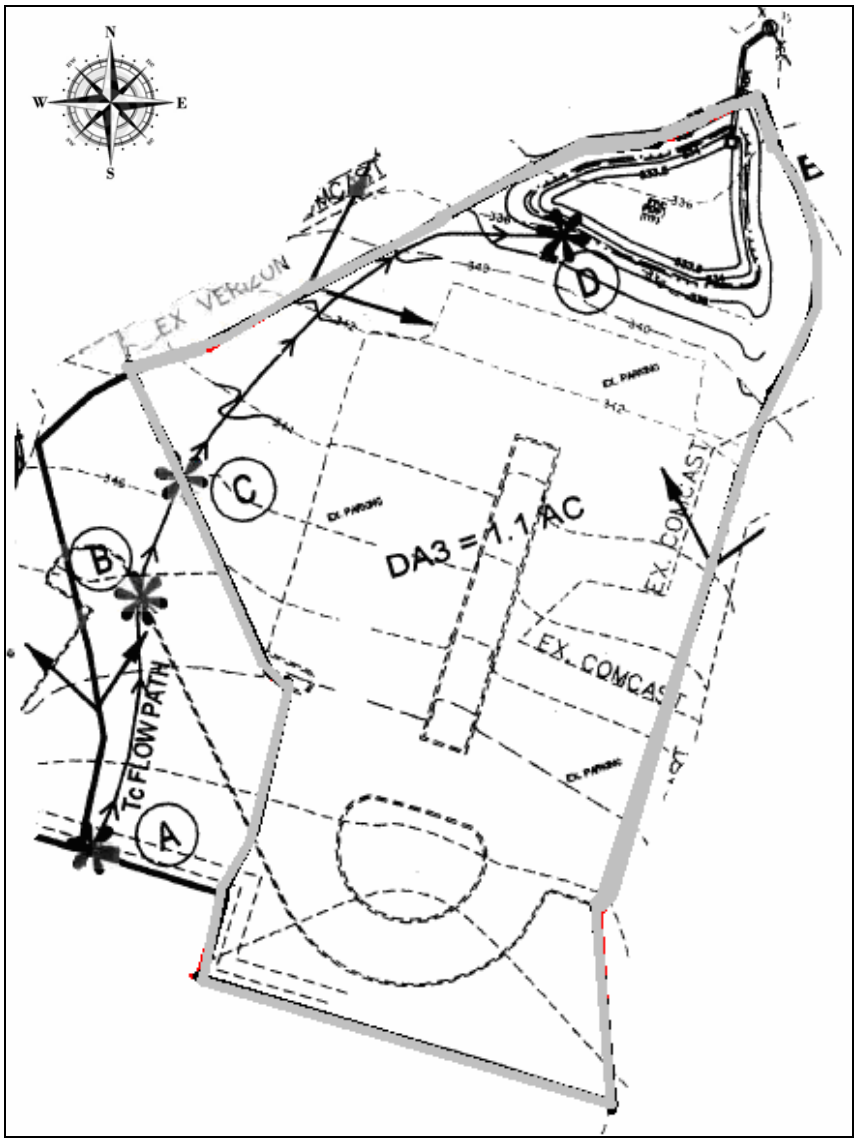

Figure 2.7 Original, proposed drainage area in black line. Revision outlined in grey. This revision removes the driveway from the drainage area and more closely represents the drainage observed at the site during storm events (blueprints).

The drainage area includes grassy areas in the parking lot that contribute a total of 0.15 ha or 41% of the entire drainage area. The remaining 59% of the drainage area is impervious. According to the blueprints for the cell, soil types C and D cover the drainage area. Because the exact areas encompassed by each soil type are not specified, soil C and a curve number of 74 was used for the grassy areas in the

curve number calculations. A weighted curve number of 88 was found for the drainage area using the weighted CN equation (McCuen 2005).

$$CN_w = CN_p(1 - f) + f(98) \quad (2\text{-}1)$$

In this equation, f is the fraction of imperviousness and CN_p is the curve number of the pervious portion (in this case the grass). With a resulting CN_w of 88, the drainage area is close to completely impervious (represented by a CN of 98), meaning a majority of rainfall that reaches the parking lot will run off into the cell.

In order to judge the performance of the cell, curve number estimates were also used to predict the behavior of three different land uses given the same drainage area. Woods B, woods C, and pavement areas were simulated given the rainfall distribution of the current data set. Runoff depths from each area were estimated using the SCS Rainfall-Runoff Equation (McCuen 2005):

$$Q = \frac{(P - 0.2S)^2}{P + 0.8S} \quad (2\text{-}2)$$

Where: Q = runoff depth (cm)
P = rainfall depth (cm)
S = potential maximum soil moisture retention (cm)

S is a function of the CN and was found using the following equation:

$$S = \frac{1000}{CN} - 10 \quad (2\text{-}3)$$

Runoff depths were determined for land uses woods B, woods C, and pavement using this method for all recorded storm events and compared to the outflow depth from the cell.

Two methods were used in comparing cell performance with the CN derived land uses. The first method assessed the overall runoff mitigation of the Sligo-Dennis

site, meaning all runoff depths were based on the site drainage area and rainfall depth. For this method, the outflow depth was calculated as follows:

$$Q_{OUT(1)} = \frac{V_{OUT}}{DA} \tag{2-4}$$

In this equation Q_{OUT} represents cell outflow depth over the drainage area, V_{OUT} represents outflow volume (L), and DA is the drainage area of the Sligo-Dennis site. For final analysis all runoff depths were divided by the corresponding rainfall depth to make values dimensionless:

$$R_{OUT(1)} = \frac{Q_{OUT}}{Q_R} \tag{2-5}$$

where R_{OUT} represents the dimensionless ratio of outflow depth over rainfall depth for a given storm event.

Method two evaluated the bioretention cell separate from the Sligo-Dennis site, comparing all runoff values with cell inflow depth and assuming 100% of all water from a storm event entered the cell. This method quantified cell performance based on how much water actually entered the cell rather than how much water fell on the site. This was an important distinction because only an average of 35% of all rainfall actually entered the cell as inflow. Outflow depth was calculated accordingly:

$$Q_{OUT(2)} = P\left(\frac{V_{OUT}}{V_{IN}}\right) \tag{2-6}$$

In this equation Q_{OUT} represents outflow depth over the drainage area, V_{OUT} represents outflow volume (L), V_{IN} represents inflow volume (L), and P is the rainfall depth. The inflow depth was calculated by dividing the inflow volume by the

drainage area for each storm event. The outflow runoff depths, along with those found for Pavement, Woods B, and Woods C were divided by the corresponding inflow depth in order to make the data points dimensionless, and then ranked and plotted in an exceedance plot; outflow is used as an example:

$$R_{OUT(2)} = \frac{Q_{OUT}}{Q_{IN}} \tag{2-7}$$

where $R_{OUT(2)}$ represents the dimensionless ratio of outflow depth over inflow depth for a given storm event.

Table 2.3 Summary table of the CN and S values for each land use. The Sligo-Dennis Parking Lot CN represents the value derived based on the percent pervious and impervious (Equation 2-1). Other CN values were found from literature reports (McCuen 2005).

Land Use	Curve Number	S (cm)	I_a (cm)
Sligo-Dennis Parking Lot	88	3.45	0.69
Pavement	98	0.508	0.10
Woods C	73	9.40	1.88
Woods B	60	16.9	3.38

Curve Numbers were estimated for the cell as well as the Sligo-Dennis drainage area using both overall averages and the least squares method. The CN and S values used for each land use are compiled in Table 2.3. Average CN values were calculated using the inflow and outflow runoff depths found from both method one and method two. Equation 2-2 was rearranged in order to solve for corresponding *S* values for each outflow runoff depth for both Method one and Method two:

$$S = 5\left[P + 2Q - \sqrt{4Q^2 + 5PQ}\right] \tag{2-8}$$

$$CN = \frac{1000}{S + 10} \tag{2-9}$$

Each *S* value was used to find a corresponding CN using Equation 2-9, which was found by rearranging Equation 2-3. An average of the calculated CN's for each storm event was then taken and assumed to be the overall CN.

Runoff ratios (as calculated in Equations 2-5 and 2-7) were also used in a least squares analysis of the cell and Sligo-Dennis drainage area Curve Numbers. For each land use analyzed, the difference was found between the land use runoff depth over rainfall depth (or inflow depth when considering the cell as separate land use) and the runoff depth over rainfall depth (or inflow depth) of a given Curve Number for each storm event. Differences from all storms were squared and then summed. The CN yielding the smallest sum was found to be the closest match. Curve Numbers from both methods were then plotted with the corresponding land use. The closest fit was used as the final estimated CN for a given land use.

2.1.3 Cell Monitoring and Sampling Protocol

Two monitoring stations were incorporated into the bioretention cell. The first station recorded the inflow level at the flume and the rainfall, while the second recorded the outflow water level through the underdrain. Water levels were measured using Teledyne ISCO 730 Bubbler Modules located in each monitor. The rain depth was measured using an ISCO 674 0.25-mm tipping rain bucket gauge. A 15-cm Thel-Mar plug in weir was placed in the mouth of the underdrain to monitor flow. Because the exact dimensions of the weir were known, outflow flowrate could be

calculated from the monitored water levels. Similarly, the 23-cm Parshall Flume dimensions where the inflow bubbler was placed were known, and therefore allowed for the calculation of inflow flowrate. Data were downloaded periodically from each station onto a laptop using the program *Flowlink 4.12*. *Flowlink* data were exported into Excel in which all analyses were done. The installed flume was used to measure inflow level. Hydrologic data collection for this project began in May 2008. Because power was available at the site, continuous monitoring of rainfall and flows was done.

A bubbler gage attached to the flume measured the water height H in ft. at a specified location in the flume. The *Flowlink* software provided conversion equations from level to flow for both the inflow flume and the outflow weir. Eqn. 2-8 from *Flowlink* was used to convert inflow level to flow:

$$Q_{IN} = 87H^{1.5} \quad (2\text{-}10)$$

Q = volumetric flow rate (L/s)

Equation 2-9 was used to convert from outflow water level to flowrate in the underdrain, Q_{out}:

$$Q_{out} = 101H^{2.6} \quad (2\text{-}11)$$

Both stations were also equipped with ISCO 6712FR Refrigerated Samplers, which collected water samples during storms to evaluate for water quality. Sampling began July 23, 2009. Flow-weighted samples were taken from storms to attain representative data over the course of a storm event. For all storms, 10mL of water was pulled into the sample bottle for every 10L of inflow passing through the flume and 10mL was pulled out for every 1L of outflow. Large, glass, sample bottles (10L

and 20L) made such sampling possible. The different water quality tests performed and methods used are discussed in the Water Quality section of this chapter.

2.1.4 Monitoring Chronology

Hydrologic monitoring of the site for this project began in May 2008. Data from April 2006 through June 2007 were also acquired from a previous project (Li and Davis 2009). The data for six storm events from April 2009 through the beginning of June 2009 were lost due to the displacement of the outflow weir and power outages in both the inflow and outflow monitors. Heavy rainfall during this period may have created high flowrates in the outflow underdrain, which could have pushed the weir out of the pipe and onto the bottom of the manhole, where it was found. Rain also leaked into the monitors, causing them to short circuit. Secure coverings over the outlets in both monitors were put in place to prevent future power outages.

Four other storms with outflow were also excluded from the data set due to obvious, incorrect readings from the outflow weir. These failures were due to movement of the weir as well as the bubbler line in the pipe, causing it to become unlevel and giving unrealistic readings. Snow events were excluded from the data set due to absence of rainfall depth and the complications snow melt had on the data.

In response to the number of weir problems, the bubbler line was replaced with a longer line, allowing the weir to be placed further into the underdrain, away from outside interference. The bubbler tubing was also taped securely to the weir to avoid displacement from heavy outflows. The weir itself was also expanded to fit as

snugly as possible in the underdrain. These changes improved the weir's reliability and durability.

2.1.5 Water Quality Sampling

Total Phosphorous (TP) and Total Suspended Solids (TSS) tests were completed on samples from selected storms beginning July 23, 2009. Total Kjedahl Nitrogen (TKN), and nitrate tests were also run on all selected samples beginning in November 2009. These samples were taken to the lab within 24 hours of the contributing storm event and either analyzed immediately or acidified according to Standard Methods protocol and refrigerated at 4°C until analysis. Before retrieval, samples were kept refrigerated at 4°C in the 6712FR Refrigerator Samplers on site.

Tests were performed at the University of Maryland Environmental Engineering Laboratory. Sample bottles were shaken thoroughly before water was taken to ensure fully representative results. Gravel particles, however, were excluded in samples due to their heavy weight, which increased TSS values dramatically.

The Persulfate Digestion and Ascorbic Acid (4500-P E) Methods were followed according to Standard Methods for testing for TP. The Standard Methods 2450D procedure was followed in performing TSS testing. TKN values were measured using Standard Method 4500-N-org-B, which consists of The Macro-Kjedahl Method and 4500-NH_3. Nitrate levels were measured using the Ion Chromatography Method 4110. Table 2.4 summarizes the methods and Minimum Detection Limits (MDL) for each pollutant tested for.

Table 2.4. Methods and Minimum Detection Limits summarized for all laboratory tests done at the Environmental Engineering Lab of the University of Maryland.

Pollutant	Minimum Detection Limit (mg/L)	Methods
Total Phosphorous	0.01	Persulfate Digestion and Ascorbic Acid (4500-P E) Methods
Nitrate-N	0.2	Ion Chromatography Method 4110
Total Kjedahl Nitrogen	1	Standard Method 4500-N-org-B
Total Suspended Solids (TSS)	1	Standard Method 2450D

Gloves were worn at all times in the lab and when handling samples. All glassware used, with the exception of volumetric flasks, were subject to a cleaning series, which included rinsing and scrubbing with soapy tap water, a series of two deionized water dips, an overnight 0.1 N HNO_3 acid soak, and finally a series of three deionized water dips. While the use of 0.1 N HNO_3 for cleaning was of concern when testing for nitrate in samples, results did not show interference. Volumetric flasks were soaked in deionized water overnight and then transferred to a 0.1 N HNO_3 acid soak the next day and let to sit overnight. After soaking in acid, volumetric flasks were also subject to the final series of three deionized water dips.

Sample bottles in the field were exchanged with a clean bottle at least every 3 days to prevent contamination. Dirty bottles were rinsed with DI water and then filled with 0.1 N H_2SO_4 and left to sit capped for no less than 24 hours. Two sets of sample bottles were used and acid was transferred from the clean bottles to the dirty bottles using a funnel. The clean, empty bottles were then rinsed with DI water again, capped, and transferred to the site where they were placed in the monitors. This

method ensured that there was almost always a clean set of sampler bottles ready to go into the monitors.

Blanks with deionized water were always prepared when testing for total phosphorous, nitrate, and TKN. These blanks served as a methods check. If results yielded significant (greater than the minimum detection limit) concentrations of a given constituent in the blank, the test was redone. Care was also taken to ensure resulting concentrations for all tests were within the concentration range of a given test. Samples exceeding the concentration range of a given test were diluted until within range. In the case of phosphorous testing, different length (1 cm or 5 cm) cuvettes were used depending on the sample concentrations.

Nitrate testing involved a specific order of sample inputs into the ion chromatograph. Blanks filled with deionized water were always placed before and after all samples to clean the tubing from any previous tests as well as to ensure the validity of following tests. Samples and a standard were then entered between the blank vials in order of increasing, predicted nitrate concentrations. This ranking was used to reduce cross-contamination between samples. If the initial concentration order was incorrect, the test was run again in the correct order as a check.

Standards were made for phosphorous concentration ranges of 0.15-0.80 mg/L (1 cm) and of 0.01-0.25 mg/L (5 cm). A cuvette rinsed and filled with deionized water was inserted as a blank prior to testing the samples. Because the spectrophotometer measurements remained fairly constant over the course of the study, standards were only used when a second blank cuvette (rinsed and filled with

deionized water) was recorded to be ±0.05 Absorbance Units (AU) in relation to the first blank.

2.1.6 Data Processing and Analysis

An individual storm event was defined as any rainfall that was preceded and followed by a dry period of at least 6 hours. All but one storm were analyzed under this assumption. On January 25, 2010 a 0.20 cm storm event occurred a little over 8 hours after a larger, 1.22 cm storm. Outflow occurred through the duration of both storm events, making it difficult to separate the event outflows. Because the second storm event's rainfall depth was significantly below the cell storage capacity (to be discussed), no outflow would have been produced by this storm alone. In order to avoid misleading results, the storms were combined into one storm event with a total rainfall depth of 1.42 cm.

The monitoring devices measured in two-minute increments. To make the data more manageable, the points were consolidated into four-minute increments. Consecutive rainfall levels were added together because the two-minute values represented the cumulative depth of rain that had fallen in 2-minutes. The inflow and outflow levels, however, were average flow values within two-minute increments. Therefore, consecutive two-minute flowrate values were averaged to get four-minute values. All plots and other values were computed using these four-minute increment values.

To estimate the inflow and outflow volumes, the recorded flowrates were integrated with respect to time. The volume is the time integral of the flow:

$$V = \int Q(t)dt = \Sigma Q(t)\Delta t \quad (2\text{-}12)$$

More specifically, the trapezoidal method was used to estimate this integration:

$$V = \int Q(t)dt = \sum \Delta t \left[\frac{Q(t_1) + Q(t_2)}{2} \right] \quad (2\text{-}13)$$

Where $Q(t_1)$ and $Q(t_2)$ are flowrates from consecutive, two minute time intervals. Once all flowrates and volumes were tabulated, hydrographs and flow-duration curves were constructed for each storm event. Cumulative flow-duration curves were also made for each month and for all storm events. These curves were made by ranking all four-minute inflow and outflow flowrate values separately from highest to lowest. The ranked values were then plotted against time, resulting in an inflow and an outflow flow-duration curve.

Each storm was put into one of four categories based on its behavior throughout the bioretention cell. The four categories were (1) The recorded outflow was less than that of the inflow, (2) No recorded outflow, (3) No recorded inflow or outflow, and (4) The recorded outflow was greater than that of the inflow. No storms in the data set were described by category four.

Hydrographs and flow-duration curves were used to analyze each storm event. A hydrograph follows the rainfall, inflow and outflow throughout the duration of a storm. These graphs help show lag-time between the inflow and outflow as well as overall volume, flow values and the duration of the inflow and outflow. Hydrographs also helped validate data and to distinguish between consecutive storms.

Exceedance plots were used to compare the rainfall distributions and f(v) ratios (representing the ratio of cell outflow volume over cell inflow volume) of data

from the current study and that from Li (2007), and to evaluate cell volumetric performance compared with other land uses.

Data were ranked from highest to lowest for each land use, assigning the highest value a rank of "1" and the lowest "n" assuming a sample size of "n." Corresponding non-exceedance probabilities and Z-values were then calculated for each value based on its rank. The non-exceedance probability, *p*, was calculated from:

$$p = \frac{i - 3/8}{(n + 1/4)} \tag{2-14}$$

where *i* is the *i*th smallest number among a sample size *n* (Cunnane 1978). Corresponding Z-values were then calculated from these probabilities assuming a normal distribution. The data for were plotted against their corresponding Z-values on a log-normal scale, resulting in a linear trend. This linear behavior of the data implies a log-normal distribution, which is characteristic of previous parameters used for stormwater approximation (Van Buren et al. 1997).

In order to determine if linear regressions derived from the current data set and from the previous data set (Li 2007) were statistically the same, the Chi-Squared test was used with the corresponding correlation coefficients from the respective regression lines, which were generated in excel. The following equations were used in this method (Iman 1997):

$$Z_i = \frac{1}{2}\ln\left(\frac{1 + r_i}{1 - r_i}\right) \tag{2-15}$$

$$\chi^2 = \frac{(Z_1 - Z_2)^2 (n_1 - 3)(n_2 - 3)}{n_1 + n_2 - 6} \tag{2-16}$$

Where r_i represents the respective correlation coefficient and n represents the respective sample size. Once χ^2 values were obtained, they were compared to values in the Chi-Square Distribution Table (Ayyub and McCuen 2003) with a υ=1. If the computed values corresponded to a $p<0.05$, the H_o: $p_1 = p_2$ is rejected and the two regression lines are assumed to be statistically different.

Both the Paired Student's t Test and the Wilcoxon Signed-Rank Test were used to determine the statistical significance of the recorded water quality data. Within these methods, all storm events producing no outflow were recorded to have zero effluent concentrations. All values found to be below the detection limit were estimated to have a concentration of half the detection limit value. Once all values were established, the difference between the log of the influent and effluent EMC values for each pollutant and each storm event were calculated.

$$C_{influent} - C_{effluent} = \Delta C \tag{2-17}$$

An average ΔC_{avg} was then calculated for each pollutant and a corresponding "t" value was found:

$$t = \frac{\Delta C_{avg} - \mu}{S/\sqrt{n}} \tag{2-18}$$

Where n, S, and μ are the sample size, standard deviation, and population average respectively. In this case, a normal distribution was assumed and null μ was set to zero, representing no change between the influent and effluent EMC values. An α of 5% was chosen for this study and the degrees of freedom $\nu = n-1$ were assumed. Two hypotheses were then presented:

$$H_o: \mu_{\Delta C} = 0$$

$$H_A: \mu_{\Delta C} > 0$$

Where $\mu_{\Delta C}$ is the mean value of ΔC. Therefore, if the resulting "t" values were greater than $t_{\alpha=0.05}$ (found in a *t* distribution table) then the null hypothesis H_o can be rejected and H_A accepted, meaning the cell removed a significant amount of the pollutant.

The Wilcoxon signed ranks test was also used as a non-parametric test for the data. It does not require the population to be normally distributed and therefore served as an alternate analysis to the Paired Student's t Test, which requires a normal distribution. The Wilcoxon signed ranks test requires only that the data be paired and that the pair difference is continuous, independent, and is representative of the population. The test statistic T is found as follows (Mendenhall and Sincich 2007; McCuen 1985; Li 2007):

1. Take the absolute value of ΔC_n for each data pair.
2. Rank the resulting ΔC_n values from highest to lowest.
3. Assign the appropriate sign to the rank corresponding to each ΔC_n value.
4. Sum the positive ΔC_n values, S_p and negative ΔC_n values, S_n, separately.

The test statistic, *T* is equal to the lesser of the absolute value of S_p and S_n. If this *T* is less than the $T_{\alpha=0.05}$, the nul hypothesis H_o can be rejected and H_A accepted, again meaning the cell significantly removed that pollutant.

Overall Event Mean Concentrations (EMC's) and pollutant mass loads were also calculated for each sampled constituent. In order to calculate the overall EMC, all pollutant concentrations were multiplied by the respective inflow or outflow volumes, resulting in a total pollutant mass for a given storm event. These masses as well as all inflow and outflow volumes were summed over all samples. The summed

pollutant mass was then divided by the summed corresponding volume in order to determine the overall EMC. Pollutant mass loads were then calculated using the following equation (Davis and McCuen 2005):

$$L_{IN} = \frac{PC_F R_V C}{100} \quad (2\text{-}19)$$

Where P = the average annual rainfall [1,067 mm/year for Maryland; Maryland Department of the Environment (MDE) 2000]; C_F = factor that corrects for completely captured storm events, a value = 0.9 was used for impervious area (Davis and McCuen 2005) was used; R_V = runoff coefficient for drainage area (0.9); and C = overall input pollutant EMC (mg/L). The resulting L_{IN} is in kg/ha-year. Values for L_{OUT} were found similarly:

$$L_{OUT} = \frac{PC}{100}\left(\frac{V_{OUT}}{V_{IN}}\right) \quad (2\text{-}20)$$

These outflow values also accounted for volume reduction as shown by the ratio of cell outflow and inflow volumes (V_{OUT}/V_{IN}).

2.1.7 Metrics used for Analysis

Individual storm event data were also compiled with all storm events to analyze the overall performance of the cell over the course of the study. A number of metrics were established for evaluating the hydrologic performance of the cell. Volumetric and flow-duration reductions were evaluated in order to compare the cell's performance with post-development as well as pre-development. The fraction, f(v) was established as a metric for volumetric performance:

$$f(v)=V_{out}/V_{in} \quad (2\text{-}21)$$

f(v) represents the ratio of the volume of outflow over the volume of inflow. By comparing the resulting f(v) from a range of storm sizes, trends in cell performance could be observed.

One main goal of the current study was to establish a metric for peak flow-duration rather than solely peak-flow reduction. The overall cell inflow and outflow flow-duration curves (Figure 2.8) were compared with that of a forested stream, Pond Branch. This plot, along with a number of comparison hydrographs between the cell and Pond Branch, helped to compare the hydrologic regime of the cell with actual pre-development values. While a defined threshold, peak-flow duration was not established, a difference in the general hydrology of the two sites was observed and analyzed. Therefore, hydrologic regime, including runoff volume, flow-rate, and flow-duration was established as a crucial metric by which to assess bioretention cells.

2.2 Oregon Ridge Analysis

2.2.1 Oregon Ridge Data Acquisition

Data acquired from the USGS was used to compare the performance of the Sligo-Dennis bioretention cell with that of a completely forested stream, Pond Branch. Current data were downloaded from http://waterdata.usgs.gov/md/nwis/nwisman?site_no=01583570; older data were supplied by Jon Dillow of the USGS. This stream is located in Oregon Ridge Park, which is 3.7 km west of Cockeysville, MD and about 72 km northeast of the cell

(Figure 2.8). Oregon Ridge Park, shown in Figure 2.9, is comprised of 422 ha of primarily forested land. The Pond Branch stream specifically has a drainage area of about 31 ha, which accounts for about 18% of the total Oregon Ridge Park. This site is almost two orders of magnitude greater than the cell drainage area of 0.37 ha.

While streamflow data were taken from the Pond Branch stream near the south of the park, rain data was obtained from a rain gage about 1.2 km north of the flow gage. The relative locations of the gages are shown in Figure 2.9.

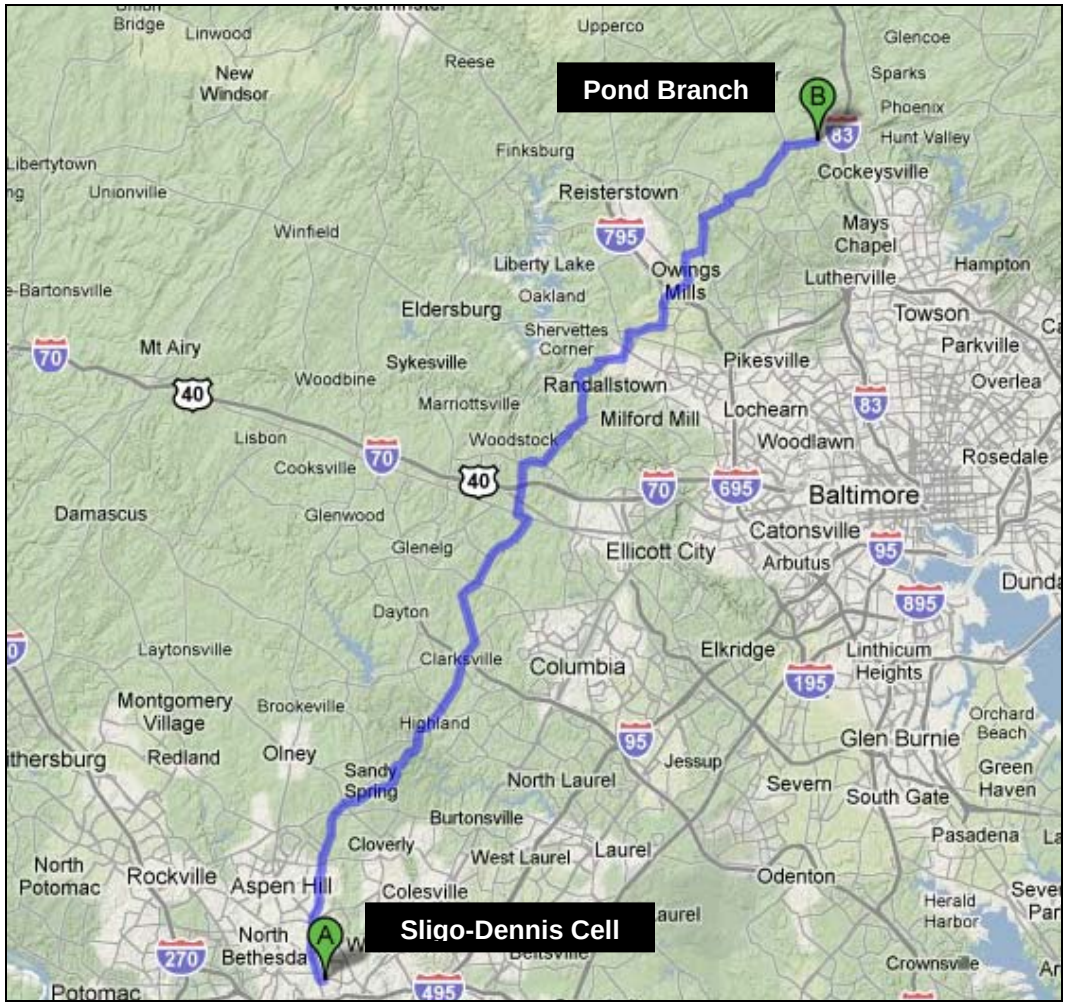

Figure 2.8 The Sligo-Dennis cell, located near Washington, DC, is at the bottom of the map. The Pond Branch Stream is 3.7 km west of Cockeysville, MD and 72 km northeast of the cell (www.googlemaps.com).

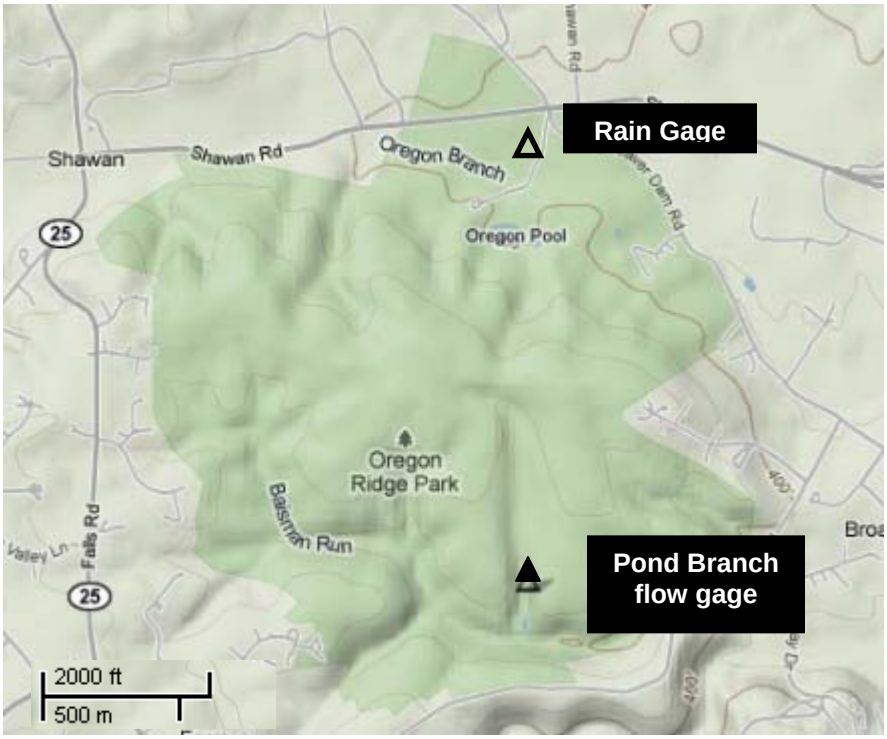

Figure 2.9 Map of forested site to be used for comparison to bioretention site. The green area outlines Oregon Ridge Park and the solid triangle represents where the Pond Branch stream gage is located. The outlined triangle in the north of the park represents the rain gage used. Green represents forested area (USGS).

Streamflow from Pond Branch has been monitored by USGS since April 15, 1998 using a Sutron 8400 electronic stage recorder equipped with a USGS 5-cm x 44-cm galvanized crest-stage gage, which is placed to next an aluminum weir plate placed across the cross-section of the stream. This monitoring set-up is shown in Figure 2.10. Water level values were collected at 15min intervals by this stage recorder and analyzed and converted into flow data by USGS. Flow data from May 2008 through May 2010 were obtained from USGS and used in comparison analysis of the Sligo-Dennis bioretention cell performance.

Figure 2.10 Flowrate monitoring setup at Pond Branch. The aluminum weir plate is shown at the bottom of the picture and the Sutron 8400 electronic stage recorder is upstream of the weir on the right (USGS).

A Qualimetrics 6110-A Tipping Bucket Rain Gage was used by USGS to record rain data from Oregon Ridge. Continuous data have been recorded starting in September 2008. Data were also collected before this date, however, records were not continuous. The Center for Urban Environmental Research and Education at the University of Maryland Baltimore County analyzes these data, correcting for any gage malfunctions or snow events. Data from May 2008 through May 2010 were obtained through both USGS and The Center for Urban Environmental Research and Education.

Streamflow and rain gage data were both used in creating stream hydrographs, which were compared with hydrographs from the cell from the same storm event. Because storms generally reached the cell a few hours before the Oregon Ridge gages, the time scale was shifted accordingly. In order to align the Oregon Ridge and

Sligo-Dennis cell hydrographs, the rainfall recorded at the cell was first shifted to match the timing of the Oregon Ridge rainfall. The cell outflow and inflow were then shifted by the same amount.

2.2.2 Oregon Ridge Data Analysis

The streamflow data from May 2008 through May 2010 were also organized into a flow-duration curve and plotted with the cumulative flow-duration curves for the inflow and outflow from the cell. These plots were then used to assess cell performance as a comparison to pre-development hydrologic values.

In order to compare the stream and cell data, both data sets were normalized by dividing by their respective drainage area. Therefore, while all Pond Branch flows were divided by 31 ha, all cell inflow and outflow values were divided by 0.39 ha. In addition to normalizing with drainage area, baseflow was also removed from the Pond Branch flow using the constant slope method in hydrograph comparisons (McCuen 2005). In order to estimate the baseflow, the stream flowrates were graphed against time during the storm event. A line was then drawn from the start of the storm event t_1 (characterized by the last constant flow value before the storm) to the inflection point of the downward curve of the hydrograph t_2. A slope s was found from this line and used to find the baseflow q_b at each time interval between the points.

$$q_b = q_1 + s(t - t_1) \tag{2-22}$$

where the value q_1 represents the initial flowrate at time t_1. Before time t_1 and after time t_2 baseflow q_b is equal to q. Figure 2.11 illustrates this method graphically.

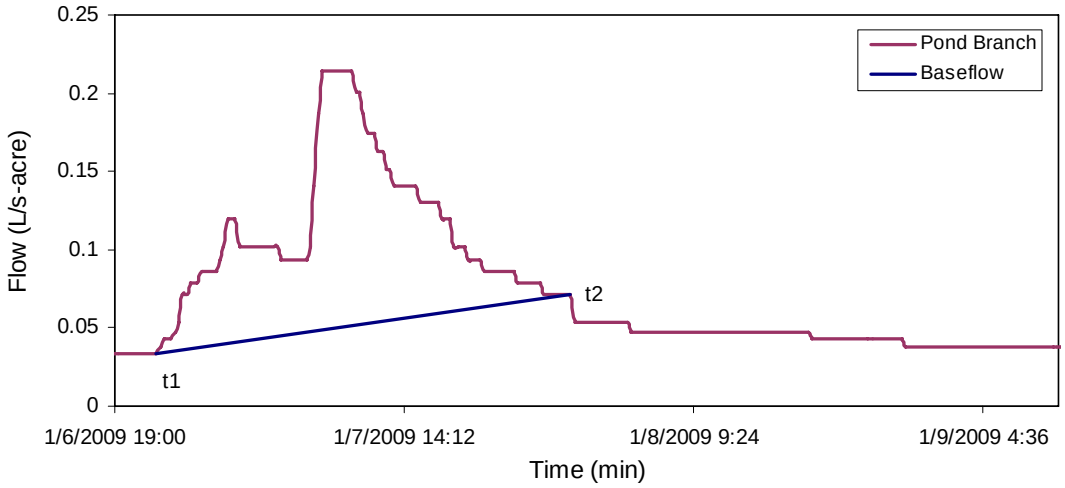

Figure 2.11 Baseflow removal using the constant slope method (McCuen 2005).

In order to remove baseflow for the overall flow-duration curve, the mode flowrate value for the Pond Branch data was determined to be the baseflow and subtracted from all flow values. This mode was found to be 0.057 L/s-ha, which was the lowest, constant flow between storm events. Flows less than 0.057 L/s-ha were set to zero.

Streamflow volumes were also computed for both individual storms and for the duration of the study. The integral of the streamflow data was estimated with the trapezoidal method, as was done for the cell inflow and outflow volumes in Equation 2-9.

Chapter 3: Results and Discussion: Hydrologic and Water Quality Performance

3.1 Rainfall Trends and Distribution

3.1.1 Rainfall Distribution

A total of 197 storm events were recorded from May 2008 through April 2010. All 52 events producing only 0.0254-cm (corresponding to one tip of the tipping rain bucket gage) were removed from the data set. Condensation of moisture in the air, or equipment malfunctions may have caused some of these small events and were therefore, not counted as storms. After removing all 0.0254cm events, a total of 145 storm events were analyzed in the current study. For comparison data from 56 storm events from April 2006 to July 2007 were also used to track the cell's performance over time (Li 2007).

Rainfall depth, duration, and frequency were analyzed in order to normalize the cell's performance compared to other cells. While the cell only produced outflow in about 20% of the storm events recorded, a high percentage of those storms were smaller storm events (< 1.27 cm). Therefore, in order for the hydrologic data from this cell to be useful, the rainfall events that contributed to these data must be taken into account. While there is some variation, both data sets show similar trends to that of the average Maryland rainfall distributions. All three data set distributions are shown in Table 3.1, which is a Depth-Duration Table of Maryland storm events.

Table 3.1 Depth-Duration Table Summary of rainfall distribution based on rainfall depth and event duration. Each box contains the fractions of storms of that given depth and duration at the top. In the bottom left of each box, the total number of storms of that category is given. In the bottom right, all storms completely contained (producing no outflow from the bioretention cell) are given. Darkly shaded boxes represent storm categories that were completely contained by the cell. Lighter shaded boxes represent categories that were partially contained and white boxes represent categories not completely contained at all by the cell. Current Data is labeled as CD, previous data (Li 2007) are labeled as PD, and Maryland Averages (Kreeb and McCuen 2003) are labeled as MD.

Event Duration		Rainfall Depth (cm)					
		0.0254-0.254	0.255-0.635	0.636-1.27	1.28-2.54	> 2.54	Sum
0-2 hr	CD	0.214 31, 31	0.048 7, 7	0.021 3, 3	0.014 2, 0	0 0, 0	0.297 43, 41
	PD	0.175 10, 10	0 0, 0	0.018 1, 0	0.018 1, 0	0 0, 0	0.211 10, 12
	MD	0.2857	0.214	0.0167	0.0043	0.0008	0.3289
2-3 hr	CD	0.014 2, 2	0.034 5, 5	0.014 2, 2	0.014 2, 0	0 0, 0	0.0795 11, 9
	PD	0.070 4, 4	0 0, 0	0.018 1, 1	0.018 1, 0	0 0, 0	0.105 6, 5
	MD	0.0164	0.0257	0.221	0.0089	0.0025	0.0756
3-4 hr	CD	0.028 4, 4	0.014 2, 2	0.007 1, 1	0 0, 0	0 0, 0	0.0483 7, 7
	PD	0.018 1, 1	0.035 2, 2	0.018 1, 1	0.035 2, 1	0.018 1, 0	0.123 7, 5
	MD	0.0085	0.0223	0.0198	0.0083	0.0038	0.0627
4-7 hr	CD	0.069 10, 10	0.062 9, 9	0.028 4, 2	0.021 3, 0	0 0, 0	0.179 26, 21
	PD	0.018 1, 1	0.018 1, 1	0.053 3, 2	0 0, 0	0.035 2, 0	0.123 7, 4
	MD	0.0099	0.351	0.475	0.0221	0.0087	0.1233
7-13 hr	CD	0.021 3, 3	0.048 7, 7	0.083 12, 12	0.083 11, 3	0.028 4, 0	0.255 37, 25
	PD	0.018 1, 1	0 0, 0	0.070 4, 4	0.053 3, 1	0.035 2, 0	0.175 10, 6
	MD	0.0058	0.0337	0.0629	0.0528	0.0266	0.1818
13-24 hr	CD	0.007 1, 1	0.014 2, 2	0.021 3, 3	0.021 4, 3	0.028 4, 0	0.0966 14, 9
	PD	0 0, 0	0.018 1, 1	0 0, 0	0.105 6, 1	0.105 6, 0	0.228 13, 2
	MD	0.0024	0.007	0.0397	0.0611	0.0515	0.1617
>24 hr	CD	0 0, 0	0 0, 0	0.007 1, 1	0.007 1, 0	0.034 5, 0	0.0483 7, 1
	PD	0 0, 0	0 0, 0	0 0, 0	0 0, 0	0.035 2, 0	0.035 2, 0
	MD	0	0.0009	0.0043	0.0172	0.0435	0.0659
Sum	CD	0.352 51, 51	0.221 32, 32	0.179 26, 24	0.159 23, 6	0.090 13, 0	1.0 145, 113
	PD	0.298 17, 17	0.070 4, 4	0.175 10, 8	0.228 13, 3	0.228 13, 0	1.0 57, 32
	MD	0.3287	0.1461	0.213	0.1747	0.1374	1

Both the current and previous data sets were within 10% of the Maryland average distributions for the summed rainfall depth categories (shown in the bottom row of Table 3.1). Both the current and previous data sets differed significantly from the Maryland averages in medium storms (0.255 -0.635 cm). The current data set demonstrated 7.5% more medium storm events, while the previous data set (Li 2007) observed 7.6% less medium storm events. The previous data set also recorded 9.1% more large storms (>2.54 cm).

Storm events producing >2.54 cm (large storms) accounted for about 14% of all storm events according to Maryland averages. Larger storm events accounted for 9% of the current data set and 23% of the previous study data set. Therefore the Maryland average for large storms is about 1.5 times more than the current study and about half that noted in the previous study. Both data sets were very close to the Maryland averages in all other rainfall depth categories. Figure 3.1 shows this comparison in graphical form.

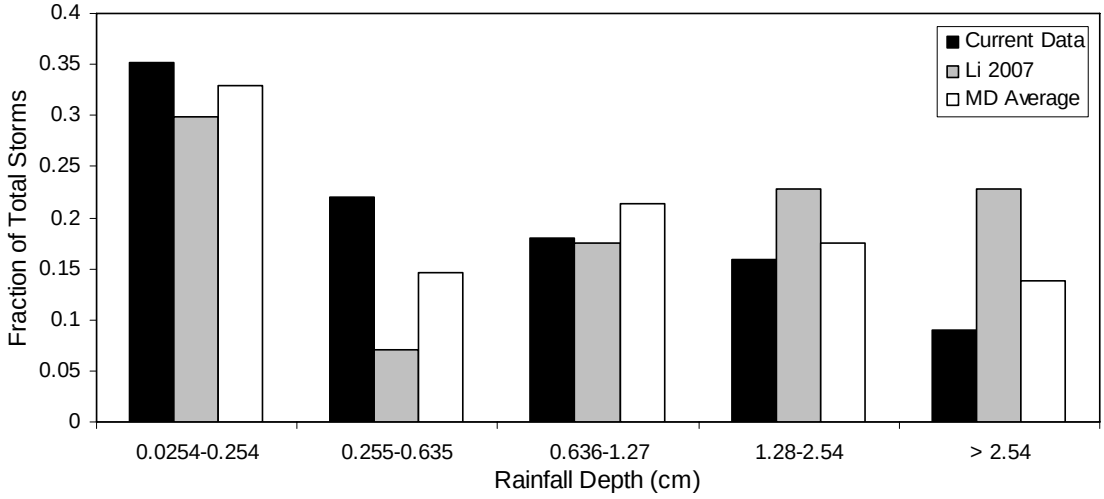

Figure 3.1 Comparison of overall rainfall distributions based on event rainfall depth for bioretention studies (MD average from Kreeb and McCuen 2003).

Looking at the sum column in Table 3.1, the storm distributions for the current and previous data sets are all within 15% of the Maryland average according to event duration. These values are also shown graphically in Figure 3.2. The current data set showed the greatest deviation from the Maryland average distribution in event durations of 7-13 hrs and 13-24 hrs with respective differences of 7.3% and -6.5%. The previous data set shows the greatest variance in 0-2 hr storm events, with a percentage of 21%, which is 12% less than the Maryland average value of 33%.

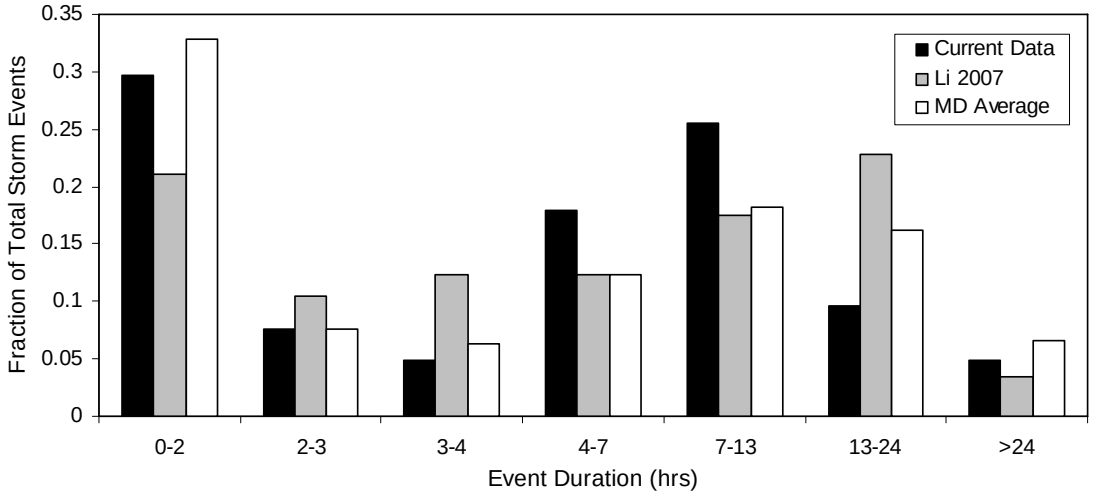

Figure 3.2 Comparison of overall rainfall distributions based on event duration for bioretention studies and Maryland average values (Kreeb and McCuen 2003). The most notable difference is between storms with a duration of 0-2-hr.

Overall, both data sets follow the general trend of the Maryland average distribution, and are both within 15% of the average values of all storm distributions. They also agree with each other within 22% for each storm category; the largest difference occurring in storm events with depths of 0.255-0.635 cm. The current data set had a high percentage (22.1%) of these storm events, while the previous data set only had 7%. All other storm categories were within 15% of each other. Therefore,

over the course of both studies, a general rainfall distribution characteristic of the Maryland average was observed at the site.

Data from the previous study had a higher percentage of larger storms (>1.27 cm), while 75% of the rainfall events recorded in the current study produced ≤1.27 cm of rainfall. This difference in distributions is shown graphically in Figure 3.3. About 50% of the storm events recorded in the previous study and 30% of those recorded in the current study exceeded 1 cm. While the previous data (Li 2007) set is more negatively skewed and weighted towards larger storms, both studies show similar rainfall distributions. Because similar rainfall trends were seen over the course of both studies, overall cell performance should be comparable between the studies.

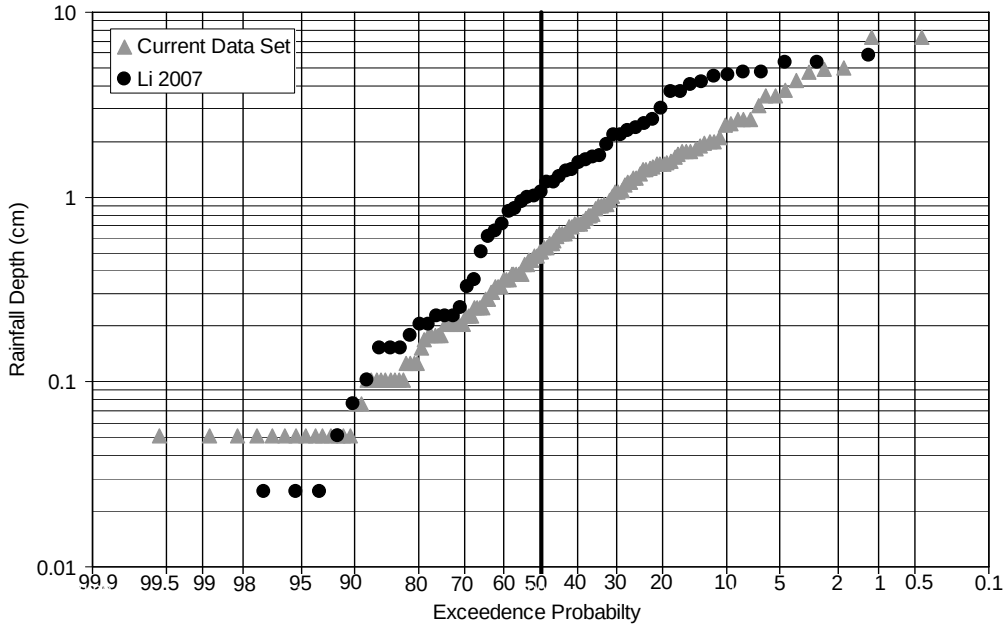

Figure 3.3 Exceedance plot of the rainfall distribution over the course of two studies on the Sligo-Dennis bioretention cell.

While 145 storm events were used to evaluate the overall rainfall distribution for the current study, 21 of these storm events were consumed by the initial

abstraction of the parking lot. These storm events were excluded from the bioretention cell analysis because they did not reach the cell. With these events removed, the current study observed 130 storm events actually entering the bioretention cell, 26% of which were small storm events. This percentage deviates further from the Maryland average of 33% small storms than the initial value of 35%, which included non-inflowing storm events. The parking lot itself completely captured about 7% of all storm events at the site. Therefore, while the site experienced rainfall representative of the Maryland average distribution, storm events actually entering the cell had fewer small storms (0.0254-0.254 cm).

3.1.2 Rainfall Trends

All 145 recorded storms were used in the rainfall analysis of the current study. Figure 3.4 illustrates how rainfall events showed a trend of increasing rainfall depth with increasing rainfall duration in the current and previous studies. Rainfall depth increases with increasing storm duration in both data sets with a similar trend. The current data plot (Figure 3.4a) shows a greater percentage of storm events producing ≤2 cm of rainfall than the previous data plot (Figure 3.4b).

The previous data (Li 2007), however, observed a greater number of more intense storm events with depths ≥2 cm and durations ≤1 day. The current data set also had a number of storm events ≥1 day, of which the previous data set had none. Overall, the two data sets show similar rainfall trends, however, the previous data set observed shorter storm events, producing more rainfall while the current data set saw

a greater number of longer, smaller storm events. This difference in intensity of storms may affect cell performance, as to be discussed.

(a)

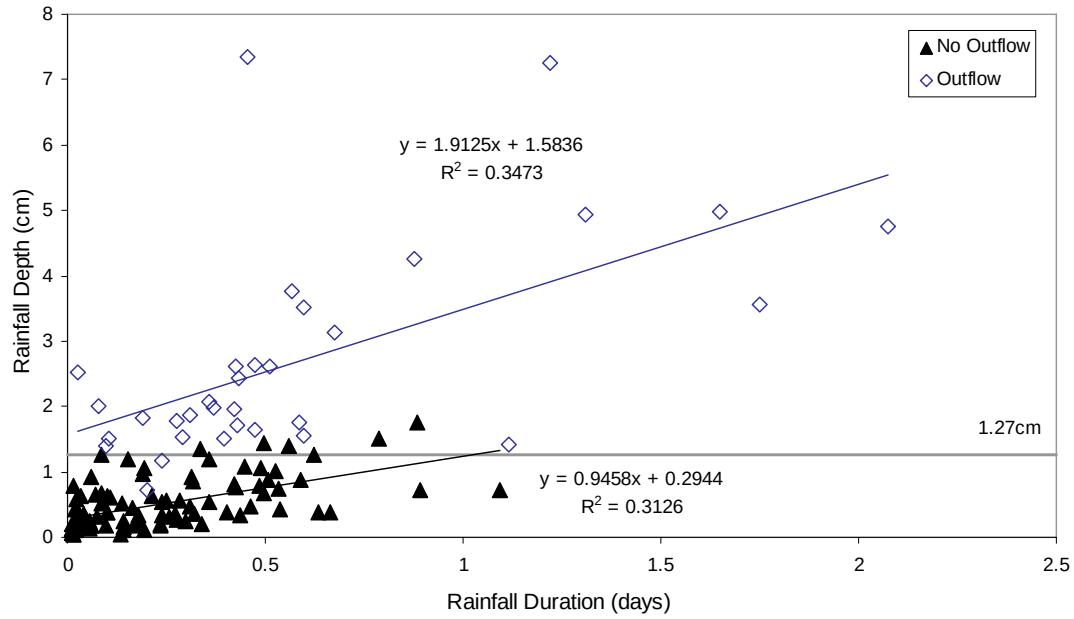

(b)

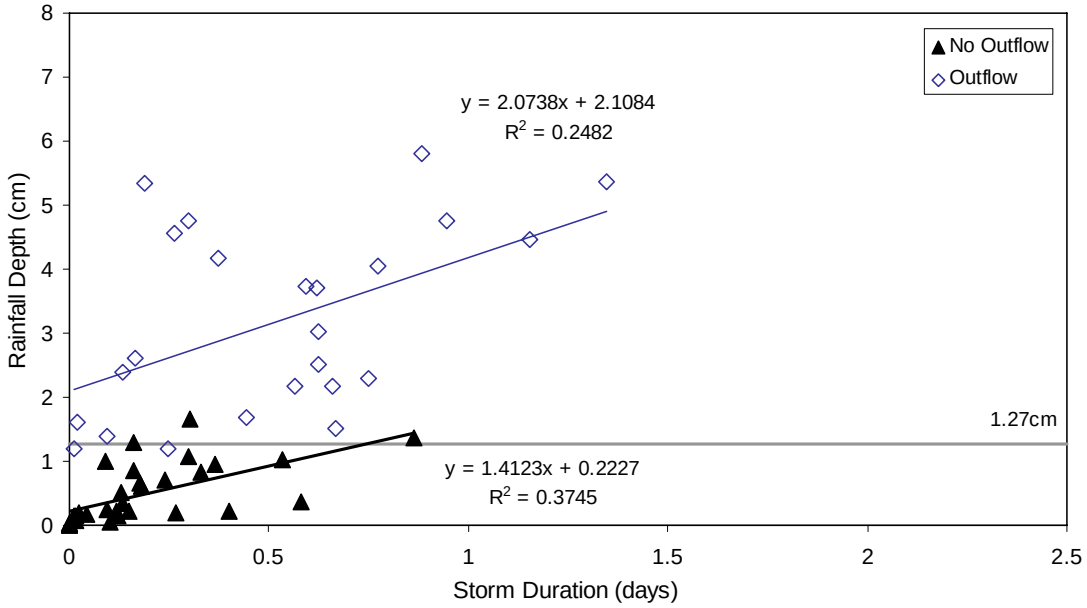

Figure 3.4 Rainfall depth versus duration for (a) the current study and (b) the previous data set (Li 2007). A threshold of about 1.27cm of rainfall is seen in both data sets, distinguishing inflowing and outflow storm events. All storm events follow the trend of increased rainfall depth with increased duration.

Figure 3.5 shows the respective average storm intensity vs. storm duration plots of the current (a) and previous (b) data sets. As seen in Figure 3.5, the previous data set contains more storm events with storm intensities ≥0.5 cm/hr. Despite this difference, both data sets followed the same trend of high intensity, short storms and lower intensity, long storms. Neither data sets observed intensities ≥0.5 cm/hr in storm events with durations ≥0.5 days. Similarly, a maximum intensity around 4.5 cm/hr was observed in both data sets. Both storm events had a duration off ≤1 hr.

(a)

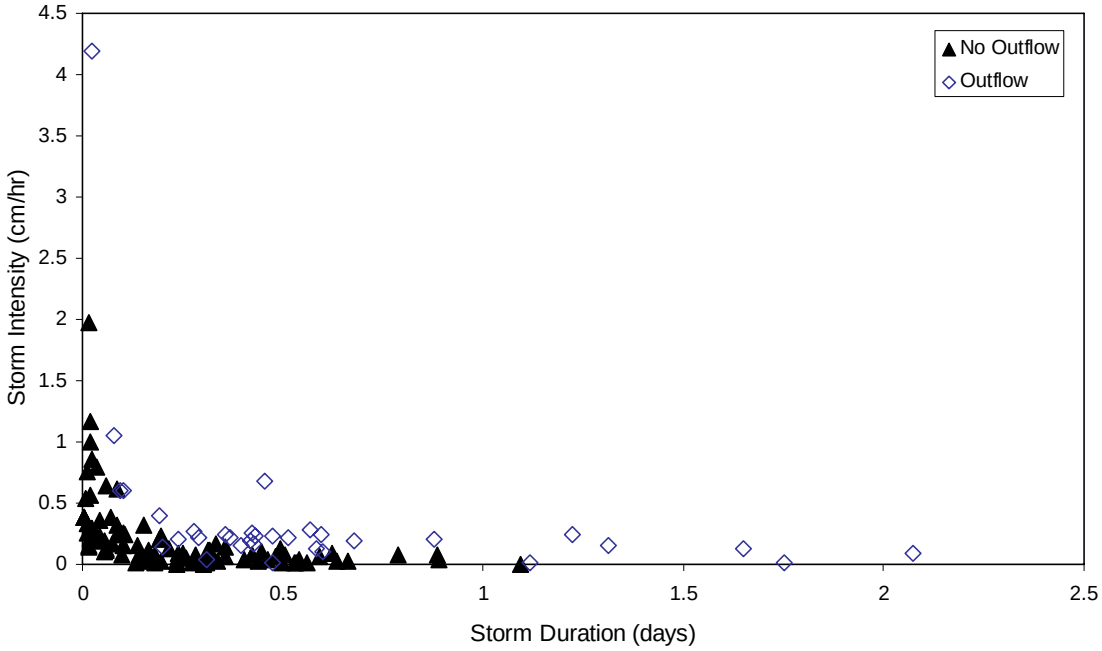

(b)

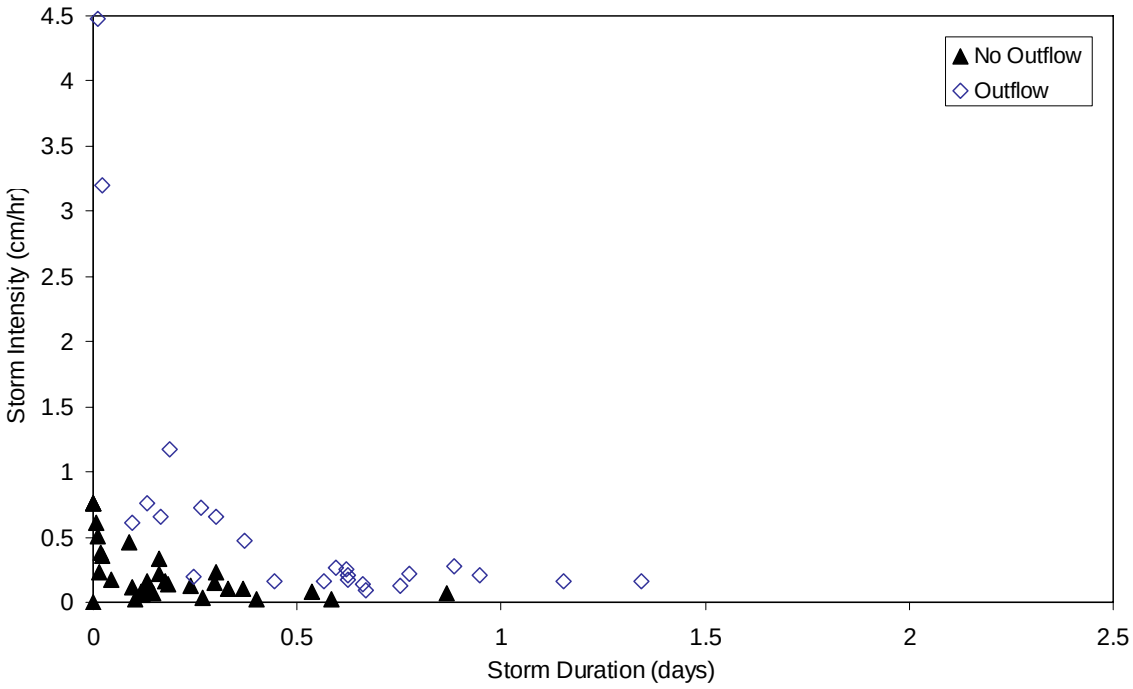

Figure 3.5 Storm intensity vis-à-vis duration for (a) the current data set and (b) the previous data set (Li 2007). Storms producing outflow either have low intensity and high duration or higher intensity and low duration than storms that do not produce outflow.

3.2 Cell Inflow

The recorded runoff inflow volumes were plotted against the projected inflow volumes calculated from the rainfall depths and drainage area. Strong linear relationships were seen in both the current and previous data sets (Li 2007), as presented in Figure 3.6. The projected inflow volumes represent the actual volume of water created by the total rainfall of a given storm event over the drainage area. Conversely, the runoff inflow or cell inflow represents the actual volume of water observed to enter the cell during a given storm event. Plotting these volumes against the inflow volumes for each event shows how much of the rainfall entered the cell and how much was mitigated by the drainage area. The following equation, with an r^2=0.953 was derived from the current data set:

$$V_{IN} = 0.437V_{INp} - 1830 \quad (3\text{-}1)$$

where V_{IN} represents the observed inflow volume in liters and V_{INp} represents the calculated inflow volume in liters from the observed rainfall depth and total drainage area. A similar relationship was observed in the previous data with an r^2=0.852:

$$V_{IN} = 0.401V_{INp} - 1557 \quad (3\text{-}2)$$

The actual inflow volume was related linearly to the projected inflow volumes in both data sets. Initial abstraction and losses to surrounding areas accounted for a large fraction of rainfall in smaller storm events. This effect, however, was lessened in larger storm due to the larger volume of water entering the site. Using Equation 3-1, a storm event producing 15,000 L of rainfall creates about 4,800 L of inflow to the cell or 32% of the original water volume. With the same equation, a larger storm producing 80,000 L of rainfall allows 33,000 L of runoff to enter the cell, which

accounts for 41% of the total rainfall volume. An initial abstraction of 0.69 cm was estimated for the cell (Table 2-2), which corresponds to a volume of 25,700 L mitigated by the drainage area every storm event. The site mitigates significantly more than this initial abstraction in storms producing >80,000 L of rainfall. Therefore, the surrounding grassy areas around the site may mitigate runoff in larger storms, accounting for this increased relative abstraction.

This relationship is important in comparing this cell's performance with bioretention cells in other studies. The same rainfall depth may produce different inflow volumes in different cells based on their drainage area characteristics. Therefore, the relative inflow volume, in addition to rainfall depth, is needed to assess the performance of a bioretention cell.

The cell drainage area was initially estimated to have a curve number of 88 based on relative land use fractions, with about 59% impervious and 41% grassed. This 41% grassed area accounted for a majority of the initial abstraction of the drainage area, mitigating about 60% of the rainfall before it entered the cell based on the slope of 0.0437 shown in Equation 3-1. Using the least squares and CN methods, the site was also later estimated to have a CN of 96. These determinations will be discussed further later in this section.

(a)

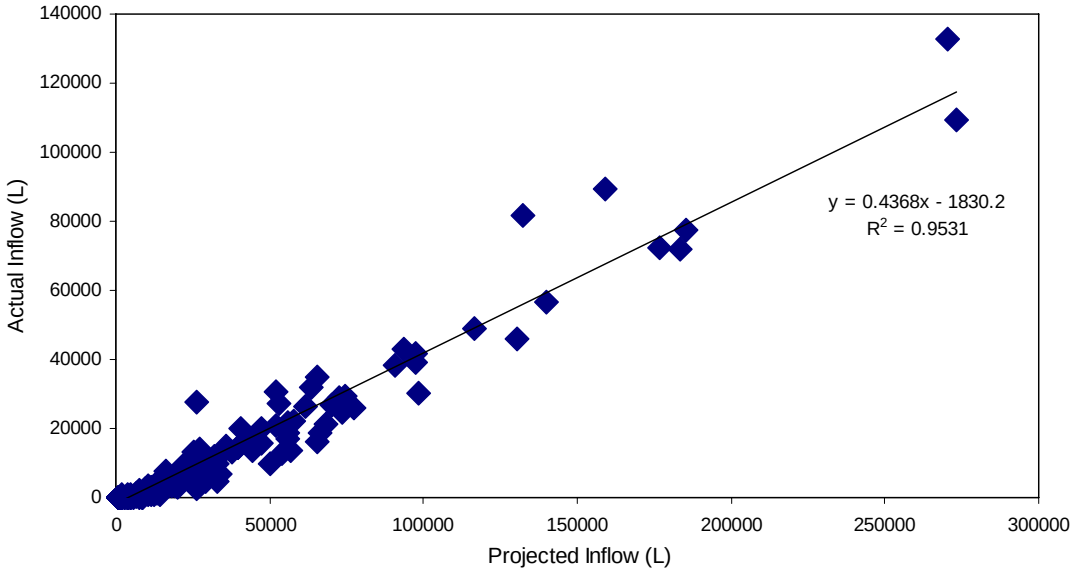

(b)

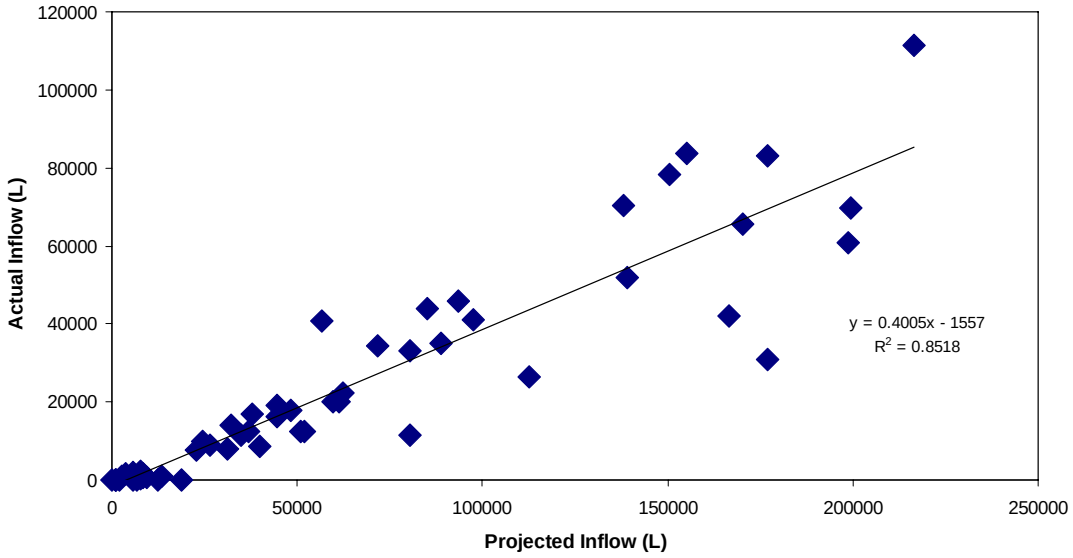

Figure 3.6 Relationship between actual inflow volume and the projected inflow volume based on the corresponding rainfall depth of a given storm event for (a) the current data set and (b) the previous data set (Li 2007). A strong, linear correlation is observed in both data sets. Projected inflow calculated as the volume of water produced over the drainage area from rainfall.

A linear relationship was observed between the recorded inflow volume and rainfall depth values for both study data sets. In this case, a linear relationship

implies that the cell inflow is directly dependant on rainfall depth. The corresponding equation for the current data set shows:

$$V_{IN} = 16264P - 1830 \quad (3\text{-}3)$$

V_{IN} represents the inflow volume (L) and P represents rainfall depth (cm). An $r^2 = 0.95$ was found for this relationship, which shows a strong correlation between the inflow volume and rainfall depth. This relationship helped to validate the collected data and to occasionally predict inflow values based on given rainfall depths. The rain gage was clogged between June 17 and June 26, 2007, and this relationship was used to estimate the corresponding storm rainfall depths based on inflow volume. This relationship is presented in Figure 3.7a.

The previous data set (Li 2007) shows a similar trend of inflow volume as a function of rainfall depth:

$$V_{IN} = 14915P - 1557 \quad (3\text{-}4)$$

With an $r^2 = 0.852$, there was much more scatter in the previous data set (Li 2007). The same general trend was found as in the current data set as shown in Figure 3.7b. Therefore rainfall depth and inflow volumes maintained the same, linear relationship over the course of both studies. Because the rainfall distributions during both studies were similar, the cell mitigated similar inflow volume distributions as well. Cell performance, as a result, appears to be similar in both studies.

(a)

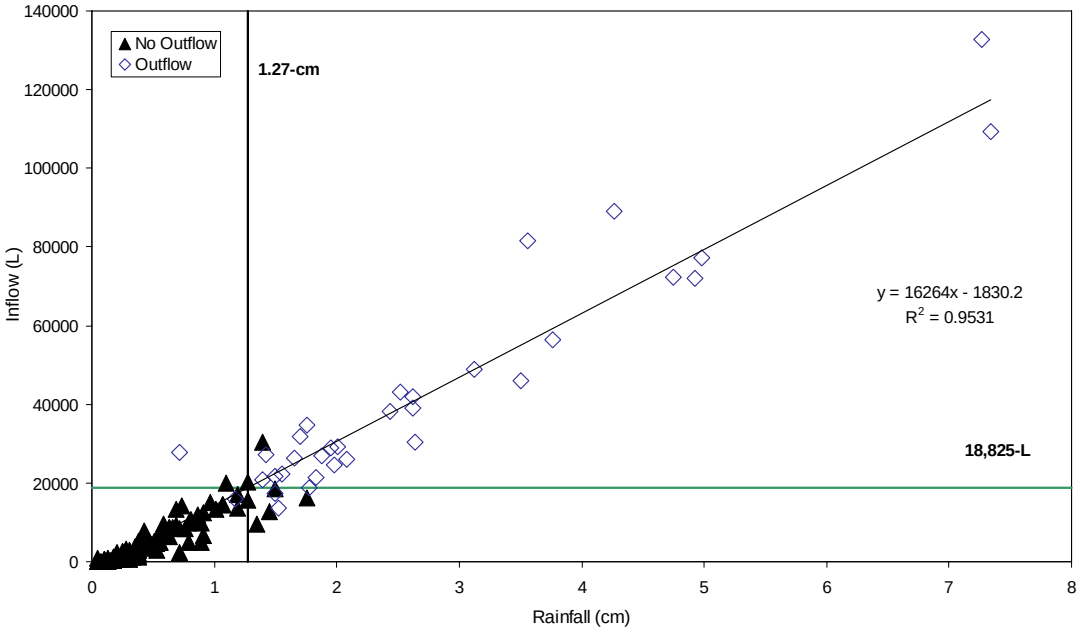

(b)

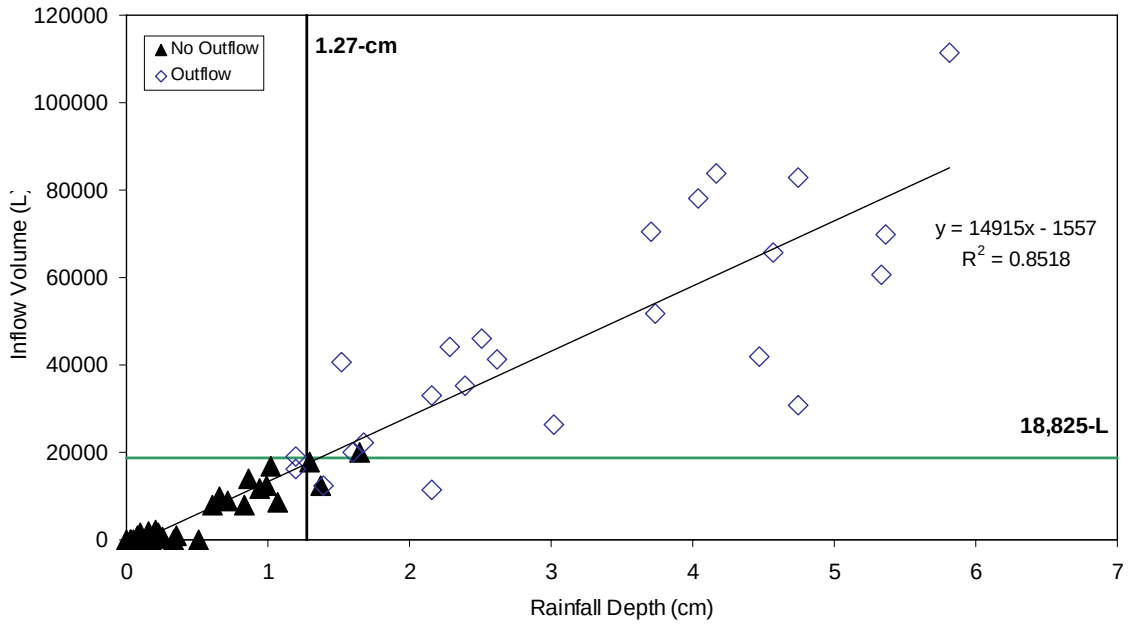

Figure 3.7 Inflow volume as a function of rainfall depth for (a) current data set, and (b) previous data set (Li 2007). Inflow entering the cell from the parking lot is linearly related to the rainfall depth. Each point represents a storm event. The storm events producing no outflow were separated into a quadrant by the corresponding, maximum storage values of 1.27 cm and 18,825 L.

Based on the chi-square test for two correlation coefficients, Equations 3-1 and 3-2 are not statistically the same. By the same methods, Equations 3-3 and 3-4 are statistically different as well (Iman 1977). Both regression pairs showed $p<0.001$, meaning there is only a 0.1% chance that deviations between the regressions is due to chance. While these equations show that the current data and previous data (Li 2007) regressions are different, hydrologic analysis found the two data sets to be the same. Curve numbers for both data sets were estimated using both the least squares method and averaged CN values from each storm event. According to the least squares method, the Sligo-Dennis site inflow fit best to a CN = 96 for both studies. Because this CN value matched the data better than the initially estimated value of 88 obtained through analysis of the drainage area, a CN of 96 was assigned to the Sligo-Dennis site. Therefore, the drainage area served by the cell behaved the same hydrologically in the previous study (Li 2007) and in the current study, and data can be compared between the studies.

3.3 Flowrate and Rainfall Depth

Because the time of concentration for the drainage area of the cell is very short (<5 min as noted by comparing rainfall and inflow) and water from the area was observed to be transferred in sheet flow to the cell, inlet inflow rates are very sensitive to rainfall intensities. As will be shown in Subsection 3.4.1, inflow peaks occur almost simultaneously with rainfall peaks. While no overall trend was observed between 4 min peak rainfall depths and 4 min peak inflow rates, Figure 3.8 shows the relationship between 4 min peak inflow value and rainfall depth.

Two general trends are suggested by the data. One trend shows high peak inflow values corresponding to smaller rainfall depths. The second trend shows lower peak flows with larger rainfall depths. These two trends, shown in Figure 3.8, may be functions of rainfall intensity. The first trend may represent storm events with higher rainfall intensities, while the second represents storms with lower rainfall intensities. The two outflowing storm events with rainfall depths <1.27 cm (the estimated storage depth of the cell to be discussed in Section 3.5) had 4 min peak flow values >15 L/s. Of four completely captured storm events producing >1.27 cm, three had peak flow values <10 L/s, suggesting that storm intensity affects the storage capacity of the cell.

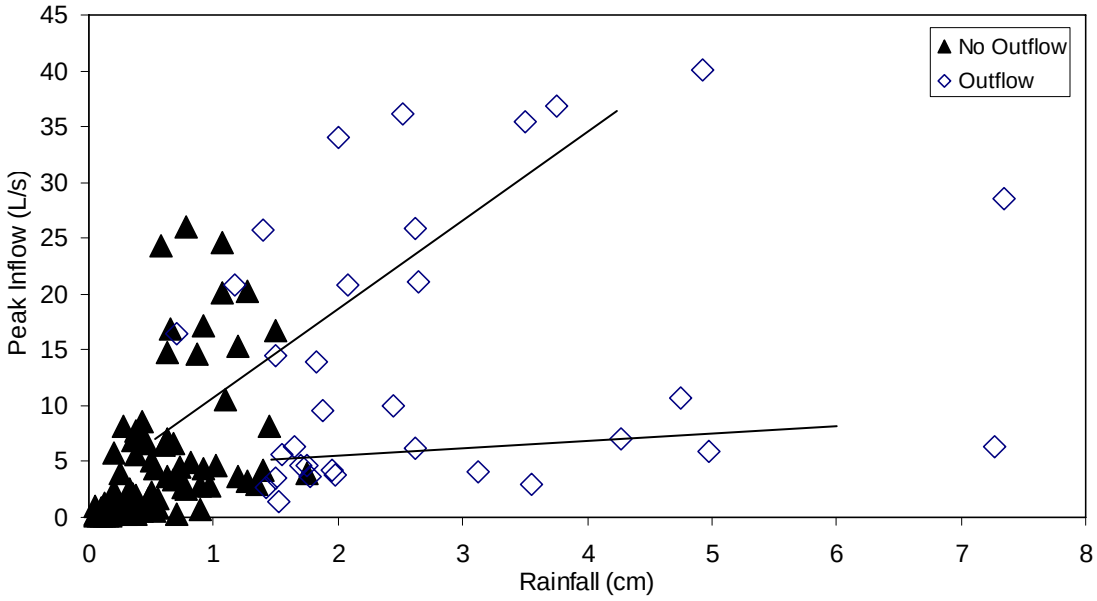

Figure 3.8 Two main types of storms are characterized by different intensities. Storms with greater peak inflow values tend to have lower rainfall depths, indicating smaller, more intense events. Larger storms tend to have lower peak inflow values, indicating long, steady storm events assuming larger storms are generally longer.

Cell outflow is less sensitive to rainfall intensities than inflow. As a result, the outflow curve shown in Figure 3.11, is much smoother than the flashy inflow curve.

Outflow occurs only once the volumetric storage capacity of the cell is met. Once the cell is saturated, outflow was assumed to follow saturated flow according to Darcy's Law (Fetter 2001):

$$Q = kA\left(\frac{L+h}{L}\right) \tag{3-5}$$

Where: Q = infiltration rate (L/s)
L = length of path of water, or media height (0.9 m)
h = height of pooling water above media (m)
A = footprint area of cell (102 m^2)
k = media saturated hydraulic conductivity (m/s)

As shown by Darcy's Law, ponding height increases with increasing outflow rate. Therefore, given the cell storage capacity is met, the outflow becomes a function of rainfall intensity, which can increase ponding. However, due to the lengthened pathway of the media, the effect is much smaller than that seen in the inflow rates.

Because outflow rate is directly related to ponding depth, it is dependent on how much water enters the cell and at what rate. Therefore, as rainfall depth increases, the outflow rate should increase as increasing ponding occurs. A weak linear relationship between peak outflow and rainfall depth is shown in Figure 3.9, with an r^2=0.473.

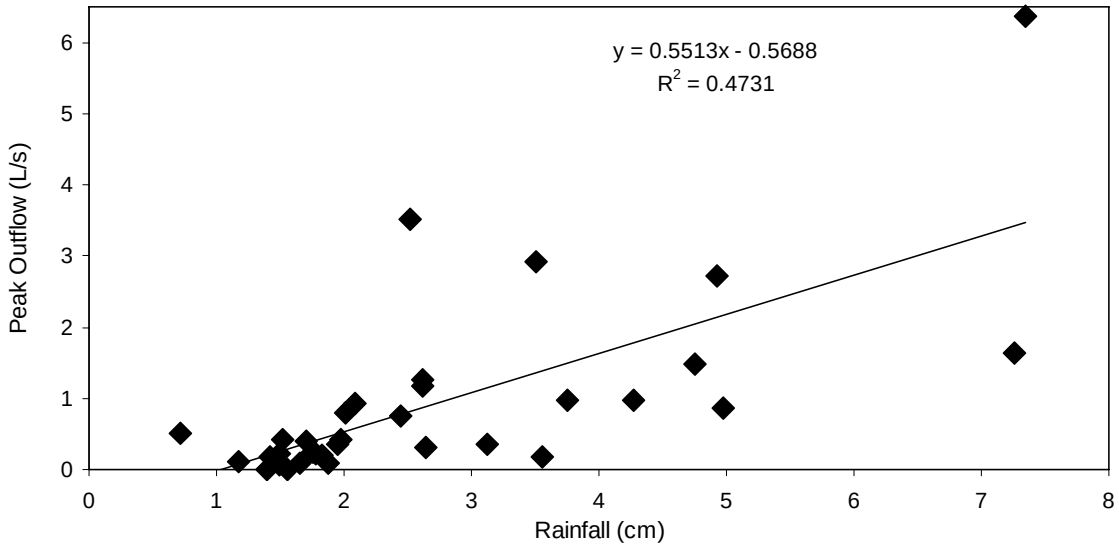

Figure 3.9 A weak linear relationship was found between peak outflow values and event rainfall depth. Increased rainfall depth should increase ponding on the cell surface, possibly increasing the outflow flowrate.

This is a weak correlation because many other factors contribute to outflow rate such as rainfall intensity (how fast water enters the cell and contributes to ponding) and the rainfall duration. A 4-cm storm lasting 0.50-days may result in much greater outflow rates than a 4-cm storm lasting 1day because the 0.50 day storm would deliver the same amount of water to the cell in half the time, increasing the ponding depth more quickly. Figure 3.10 shows a weak (r^2=0.311), linear relationship between the peak outflow and peak inflow rates. Peak outflow rates increase gradually with increasing peak inflow values according to the following equation:

$$Q_{OP} = 0.0599Q_{IP} + 0.0703 \quad (3\text{-}6)$$

where Q_{OP} represents the peak, 4-min outflow rate and Q_{IP} represents the corresponding peak 4-min inflow rate for a given storm event. While peak outflow values show a stronger correlation with rainfall depth (Figure 3.9), Figure 3.10

suggests that peak inflow values also control outflow rates. The slope of 0.0599 in Equation 3-6 represents a peak flow reduction of about 94% from cell inflow to cell outflow. The intercept of 0.0703 may represent a minimum outflow rate before ponding occurs, directly after the cell storage capacity has been met.

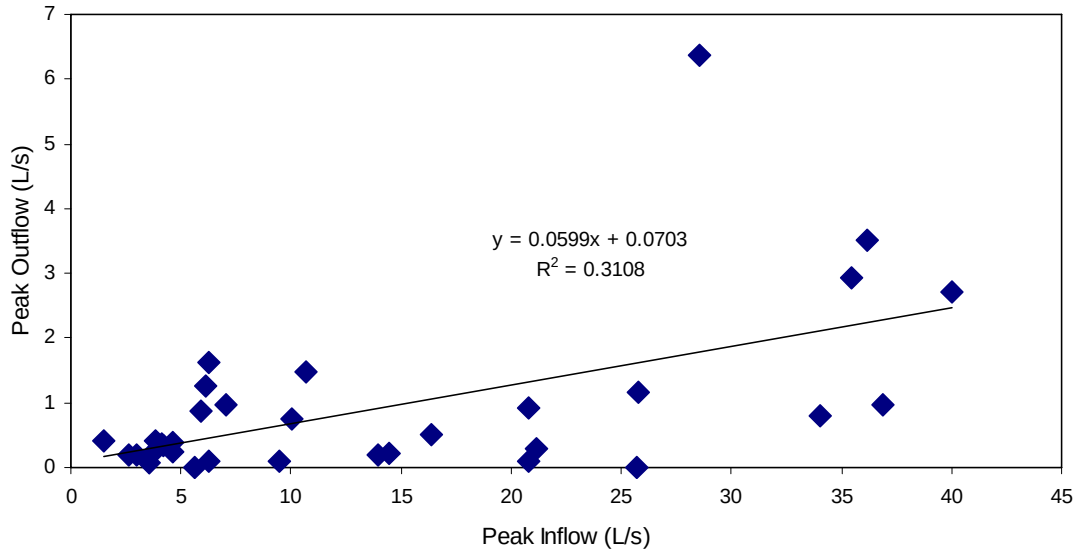

Figure 3.10 Linear relationship between the peak outflow and peak inflow values based on 4 min data increments.

3.4 Bioretention Cell Performance

3.4.1 Individual Storm Results

Hydrographs and flow-duration curves were constructed using values from all recorded storm events to determine relationships and trends based on the behavior of the cell in different storms. By finding such relationships, the cell could be better understood and its behavior better predicted. Understanding how the cell behaves is crucial to designing cells based on desired performance.

Figure 3.11 and Figure 3.12 were taken from a large storm event that occurred on 5/11/2008, which had a rainfall depth of 7.26 cm (2.86 in.). This storm represents one of the larger rainfall events that hit the cell during the course of the current study. Figure 3.11 shows the hydrograph of the storm. The inflow and rainfall curves show the same shape and trends. When the rainfall peaks, the inflow peaks as well, and when the rainfall levels off, inflow also levels off. This sensitivity of the inflow to rainfall shows that runoff from the drainage area has a very small time of concentration and is attenuated very little before it reaches the cell. Additional rainfall brings more runoff into the flume. For a high intensity rain, the runoff will flow into the flume at a higher rate, which is reflected in the inflow values.

A lag time of 2.57 hrs is shown between the start of inflow and the initial cell outflow. The outflow volume is significantly less than the inflow volume, found by comparing to the area under the outflow curve. The volumes of the inflow and outflow were 1.33×10^6 and 7.21×10^5 L, respectively. The volume of incoming water was almost double that of the water that exited the cell. The peak flowrates for the inflow and outflow were 6.26 and 1.63 L/s, respectively. These results show both flow rate and volume reductions in outflowing water. The bioretention cell reduces the "flashiness" of the urban hydrograph, allowing less erosion and sedimentation downstream (Walsh 2005).

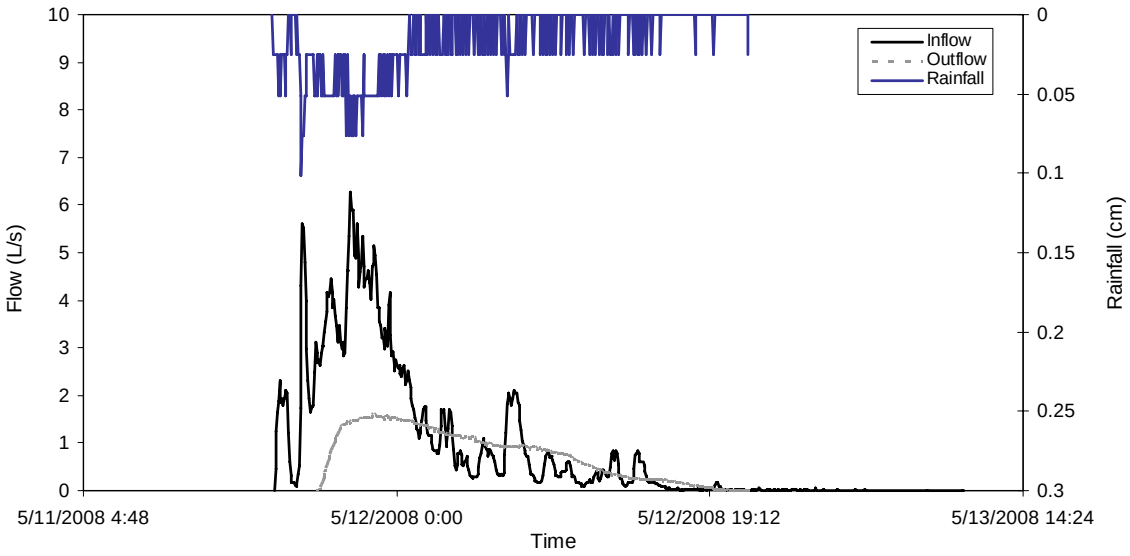

Figure 3.11 Hygrograph for 7.26 cm storm event occurring on 5/11/2008 at Sligo-Dennis bioretention cell.

Figure 3.12 shows the flow-duration plot of the 5/11/08 storm based on the hydrograph of Figure 3.11. This plot was developed by ranking all of the inflow and outflow values in order of greatest to smallest over the course of the entire storm. As discussed, the peak inflow was 6.26 L/s and the outflow peak was 1.63 L/s. The inflow curve has a steep slope, dropping from 6.26 L/s down to 1L/s in 600 min. The outflow curve is more gradual, going from 1.6 L/s down to 1 L/s in the same 600 min period, indicating less variation in outflow rates. This reduction in flow fluctuation is due to the stronger dependence of peak outflow values on rainfall depth as opposed to rainfall intensity shown in Figures 3.9 and 3.10. Because outflow rate is a function of saturated infiltration, the effect of rainfall intensity is dampened, making outflow rates more constant than inflow rates, which react directly to rainfall intensities.

In addition to peak flowrate of runoff discharge entering natural waters, the duration of flow is also important. Even if peak flowrates are reduced, if they are maintained for long periods of time they may still cause erosion downstream.

Conversely, if flowrate duration is reduced, leaving peak flowrate values higher, downstream ecosystems may also be negatively affected. The exact affect, however, depends on the receiving ecosystem and pre-development conditions. Flow-duration curves show all flow values and how long they were maintained. By comparing the flow-duration curves of the inflowing and outflowing water, a better assessment of how the cell mitigates flows is made.

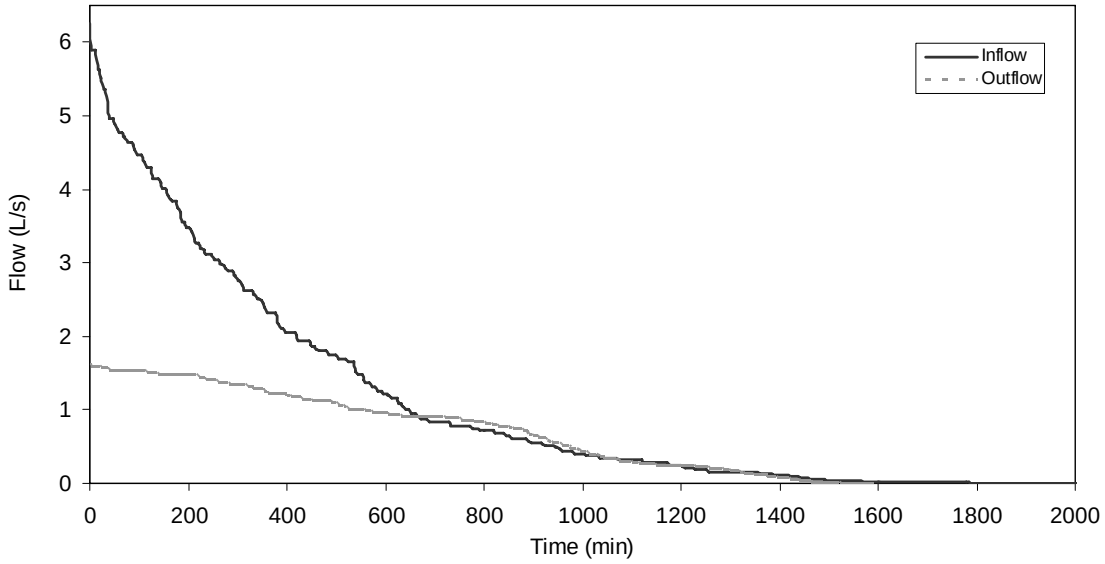

Figure 3.12 Flow-Duration curve for 5/11/2008 Storm.

3.4.2 Overall Flow-Duration

Cell flow performance was evaluated over the entire course of the current study. Flow-duration curves from each storm (127 total) were combined and all flow data were ranked to make both monthly and overall plots. The overall flow-duration curve represents all four-minute increment flowrate values from all recorded storm events ranked from greatest to smallest for both inflow and outflow. Figure 3.13 shows the overall flow-duration curve for the cell for the two years of the study. The

maximum inflow was 40 L/s while the maximum bioretention outflow value was 6.8 L/s, which is almost six times less than the inflow maximum.

The respective durations of the outflow and inflow curves were about 20,000 min and 39,000 min. Water inflowed into the cell for almost twice as long as it outflowed from the cell, reducing the overall site flow-duration by half. Therefore, the cell mitigated almost 20,000 min out of 39,000 min of inflow into the cell. Volume reduction is also evident by comparing the relative areas under each curve. A total of 2040 m^3 of water inflowed into the cell, while 423 m^3 was discharged from the cell. Therefore, outflow accounted for 10.5% of all inflow, reducing the overall runoff volume of the site by almost 90% over the course of the 127 storm events analyzed.

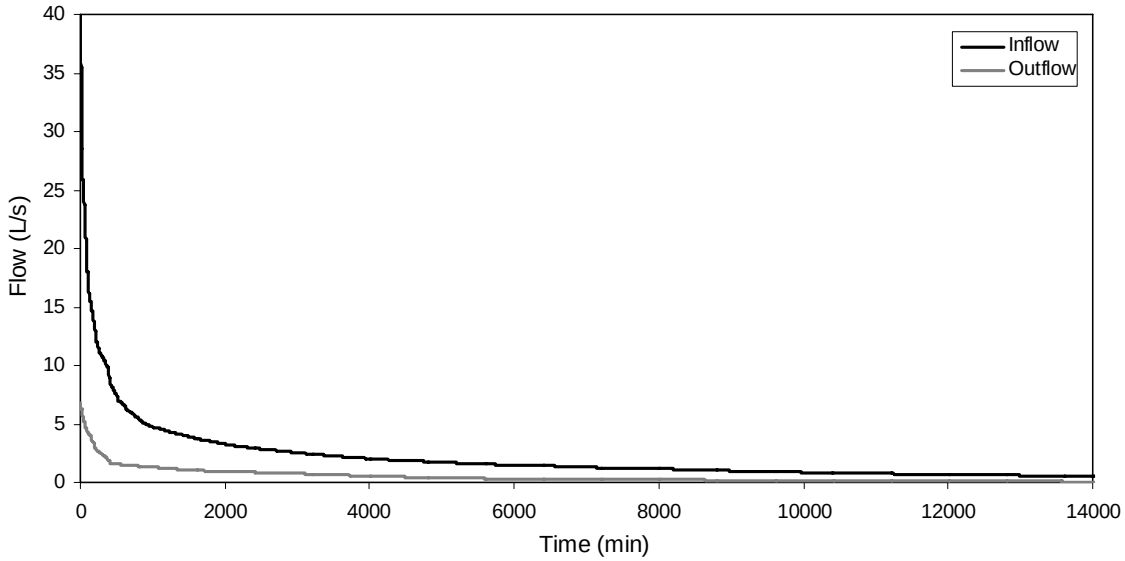

Figure 3.13 .Overall Flow-Duration Curve for Sligo-Dennis bioretention cell of all 127 storm events recorded over 2 years.

The inflow curve steeply declines until it reaches a flow of about 6 L/s after 620 min, after which the curve becomes much more gradual. The initial drop in the

outflow curve begins to slow at about 2.6 L/s , which occurs after 264 min. While both the inflow and outflow curves have steep, initial drops in flowrates, the outflow curve drop is more gradual and shorter. Inflowing water, therefore is moving more quickly, for longer periods of time than outflowing water from the cell.

Figure 3.14 provides a close up view of the overall flow-duration curve shown in Figure 3.13, better illustrating the difference in the initial slopes of the inflow and outflow curves. The difference between corresponding inflow and outflow values is also plotted, which follows the trend of the inflow curve closely, showing greater dependence on the inflow values. The shape of the difference curve illustrates the relative smallness of the outflow rates as compared to the inflow rates. The differences in slope between the curves are also more pronounced in Figure 3.14. While the inflow curve almost follows the form of exponential decay, the outflow curve is more constant, falling very slowly, implying that the outflow values have less variability. This difference may be a function of the increased flow path provided for runoff from the cell. With a longer flow path, the cell produces outflow rates that depend more on ponding depth rather than rainfall intensity, like cell inflow. Because ponding depth changes much more slowly than rainfall intensity, outflow rates reflect this dampening affect. As a result, the steeper inflow curve represents flashier flows, while the more gradual outflow curve represents more stable flows.

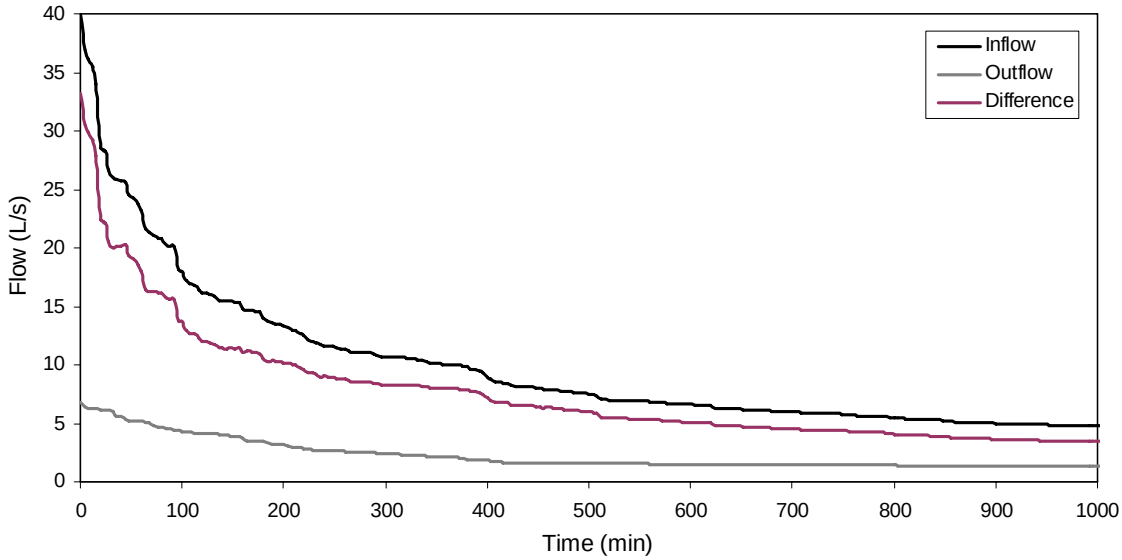

Figure 3.14 Zoomed-in view of overall flow-duration curve for all storm events analyzed of the course of the 2 year current study. The difference between corresponding inflow and outflow values is also plotted.

Bioretention has reduced peak flow, flow-duration, and flow volume significantly in the current study. Because runoff must first fill up the cell, and infiltrate down through the media in order to produce outflow, the affect of rainfall intensity is greatly dampened. As shown in Section 3.3, outflow rates are directly dependent on ponding depth rather than only rainfall intensity like the inflow rates. As ponding depth decreases, so should the outflow rates.

3.5 Overall Hydrologic Performance

3.5.1 Overall Trends

Over the course of the current study, runoff from 127 storms entered the cell, 33 of which produced outflow, leaving 94 storm events, about 74% of all events being completely captured by the cell. According to the rainfall analysis done in

Section 3.1, these events are representative of the average Maryland rainfall distribution (Kreeb and McCuen 2003). Therefore, the cell performance observed in the current study should represent how a cell placed in Maryland would behave. This 74% is significantly greater than results from one study done at the University of Maryland, which found 18% of 49 storm events were completely captured by the lined cells being monitored (Davis 2008), showing the difference in performance between lined and unlined (Sligo-Dennis) cells. Unlined cells like the Sligo-Dennis cell perform significantly better than lined cells. A study done in North Carolina showed overall outflow volume over the course of one year to be less than 50% of all runoff entering the cell over the same time period (Hunt et al. 2006). The Sligo-Dennis site produced an overall outflow volume of less than 20% of all recorded inflow volume over the course of the two year study. This increased runoff volume reduction in the Sligo-Dennis cell may be due to a difference in rainfall distributions or a different drainage area: cell ratio.

Out of the 127 storm events, cell peak inflow was reduced by an average of 92% for all outflowing storms, with a minimum reduction of 72% occurring during the 4/11/2009 storm event. Storm duration did not seem to affect peak flow reduction. These reductions are slightly higher than those found in a study done by Davis (2008), which found a peak reduction range of 44-63%.

3.5.2 Cell Performance Based on Rainfall Trends

The current and previous (Li 2007) data sets have similar rainfall distributions, and therefore exhibit the same hydrologic cell behavior. The cell

captured the same size storms (≤1.27 cm) in both data sets. In the current study, storms that produced less than or equal to 1.27 cm of rainfall comprised about 75% (Table 3.1) of recorded storms and the cell completely captured 74% of all storms. Similarly in the previous study, the cell completely captured about 57% of all storms and 54% of all storms produced ≤1.27 cm of rainfall (Li 2007). Therefore, from a volumetric perspective, the cell performed the same in both studies, unchanged with time, providing storage capacity of about 1.27 cm of rainfall.

As shown in Figure 3.4, storm events producing outflow were caused by greater rainfall depths. The completely captured storms are separated by the outflowing storms by the threshold of about 1.27 cm of rainfall. Both data sets followed this threshold. The cell produced outflow after about 1.27 cm of rainfall regardless of storm duration. Because events producing more rain often have longer durations, many of the outflowing events also occur during longer storm events.

Rainfall intensity also characterizes a storm event. As shown in Figure 3.4, storms producing outflow tended to have lower intensities and longer durations than storm events that were completely captured by the cell, corresponding to larger rainfall depths. Events producing outflow with shorter durations had slightly higher intensities and, therefore, greater rainfall depths than events of the same duration that did not produce outflow. In both cases, outflow is more likely caused by a greater rainfall depth rather than by a high storm intensity. As a result, a threshold intensity was not found to distinguish completely captured storms from outflowing events. This trend is due to the runoff storage and infiltration provided by the cell. Outflow

is buffered by this storage, and is only produced after 1.27 cm of rainfall has entered the cell.

Using 1.27 cm as the maximum storm size captured by the cell, the linear relationship shown in Figure 3.7 and Equation 3-3 can be used to determine the corresponding inflow entering the cell. For the current data set, a value of 18,800 L marks the maximum inflow volume the cell will hold before producing outflow, or the storage capacity of the cell. Figure 3.7a was divided into quadrants by lines corresponding to a rainfall depth of 1.27 cm and the calculated inflow storage volume of 18,800 L, which represented the cell's maximum storage.

Storms in the upper left and lower right quadrants deviated from the linear relationship used to relate rainfall depth to inflow volume in Equation 3-3. Data in the upper left quadrant represent rainfall depths <1.27 cm that produce >18,800 L of inflow. Data points in the lower right quadrant represent the opposite, rainfall events with depths >1.27 cm producing <18,800 L of inflow.

The lower left quadrant represents all storm events with a rainfall depth ≤1.27 cm and an inflow volume ≤18,800 L. All but one of these storm events produced no outflow. The storm producing outflow in this quadrant had a rainfall depth of 1.17 cm and an inflow volume of 15,990 L. This storm occurred on 6/20/2009, with an antecedent dry time of 1.79 days prior to a 3.76 cm rainfall event. The air temperature recorded at a gage located at BWI this day was 57°F (www.wunderground.com).

The upper right quadrant represents all storm events with rainfall depths >1.27 cm and inflow volumes >18,800 cm. Almost all storm events in this quadrant produced outflow. One completely captured storm event is in this quadrant, with a

rainfall depth of 1.40 cm and an inflow volume of 30,400 L. This storm took place on 11/30/2009 and had an antecedent dry period of 2.87 days prior to a storm event producing 0.559 cm of rainfall. The air temperature at BWI was 52°F on this day.

These discrepancies may be due to antecedent dry period and the rainfall depth of previous storms. While the non-conforming outflowing event had an antecedent dry time of 1.79 days, the large non-outflowing event had an antecedent dry time of 2.34 days. Therefore, water in the cell had more time to infiltrate and to undergo evapotranspiration before the storm event that completely captured more than the predicted storage capacity. The respective storm sizes of the antecedent storms for the completely captured and outflowing storm events were 0.559 cm and 3.76 cm, respectively. Prior to the outflowing storm event, the cell had surpassed the storage capacity of 1.27 cm and had produced outflow. Therefore, the cell was saturated from this storm event, leaving less room for storage for the 6/20/2009 storm event. The 0.559-cm storm did not meet the storage capacity of the cell and did not saturate the cell, leaving more room to capture the 11/30/2009 storm.

As shown by these discrepancies, cell behavior is a function of more than simply the rainfall depth of a given storm event. While distinguishable trends were not found, antecedent dry time, antecedent storm size, and air temperature may all play a role in how much runoff a cell can mitigate during a specific storm event. However, assuming these forcing functions are small compared to rainfall depth, the estimated storage capacity of 18,800 L is representative of the data, excluding only 2 out of 127 storm events.

The previous data set also followed this storage trend. Assuming 1.27 cm to be the maximum captured rainfall depth, a storage capacity of 17,390 L is predicted by Equation 3-4, which is within 7.6% of the 18,800 L predicted by the current data. The relationship between rainfall depth and inflow volume is consistent between the current and previous studies, showing an average cell storage capacity of about 18,100 L.

The same quadrant of 18,800 L of inflow volume and 1.27 cm of rainfall is drawn in Figure 3.7b as was drawn for the current data in Figure 3.7a. This quadrant contains all but one completely captured storm event as well as one outflow-producing event. Because there is more scatter in these data, the storage capacity is not as clear as it is in the current data (Figure 3.7a). Different storm intensities, antecedent dry periods, and other cell conditions may have also played a role in how storm events with similar rainfall depths produced different responses by the cell. Both data sets showed similar inflow storage values. However, because the current data set showed less scatter and were comprised of more than twice as many storm events, the 18,800 L inflow value is assumed to be the storage capacity of the cell.

3.5.3 Relating Inflow and Outflow Volumes

Cell storage capacity can directly be observed in the relationship between inflow and outflow volumes. Figure 3.15 shows this relationship in the current data set, where each point represents a single rainfall event. Outflow did not occur until about 20,000 L of inflow is introduced to the cell, after which a linear relationship between inflow and outflow volume is observed. While the volumes follow a similar

trend as the rainfall-inflow curves shown in Figure 3.7, outflow begins around 22,000 L of inflow rather than 18,800L as estimated by the quadrants drawn in Figure 3.7. The following equation represents the linear relationship between the inflow and outflow volumes for storm events producing outflow:

$$V_{OUT} = 0.59V_{IN} - 12{,}886 \quad (3\text{-}7)$$

where V_{OUT} represents outflow volume (L) and V_{IN} represents inflow volume (L). This relationship was made using all storm events that produced outflow and had an r^2 of 0.918, which shows a strong correlation between inflow and outflow in storm events that produced outflow. If V_{OUT} is set to zero, an inflow value of 21,840 L is calculated from this relationship, which represents the storage capacity of the cell in this linear relationship. From Equation 3-7, cell outflow volume is 60% of cell inflow volume. An intercept of 12,886 L is subtracted from this percentage, so with larger storm events, cell outflow approaches 60% of the cell inflow volume. As shown by the data, most storm events produced outflow volumes closer to 20% of the inflow volume.

After about 22,000 L of runoff has entered the cell, outflow is a function of inflow according to the linear relationship shown in Equation 3-7. The relative outflow volume for a given storm event increases with increasing inflow volume. A storm event producing 40,000 L of inflow, for example, produces 9,800 L of outflow according to Equation 3-7, which accounts for 25% of the inflow volume. A storm event producing 30,000 L of inflow produces 4,300 L of outflow, which is only 14% of the inflow volume. Therefore, the ratio of outflow volume to inflow volume (f(v))

increases with increasing inflow volume. This trend will be discussed further in Section 3.5.4.

(a)

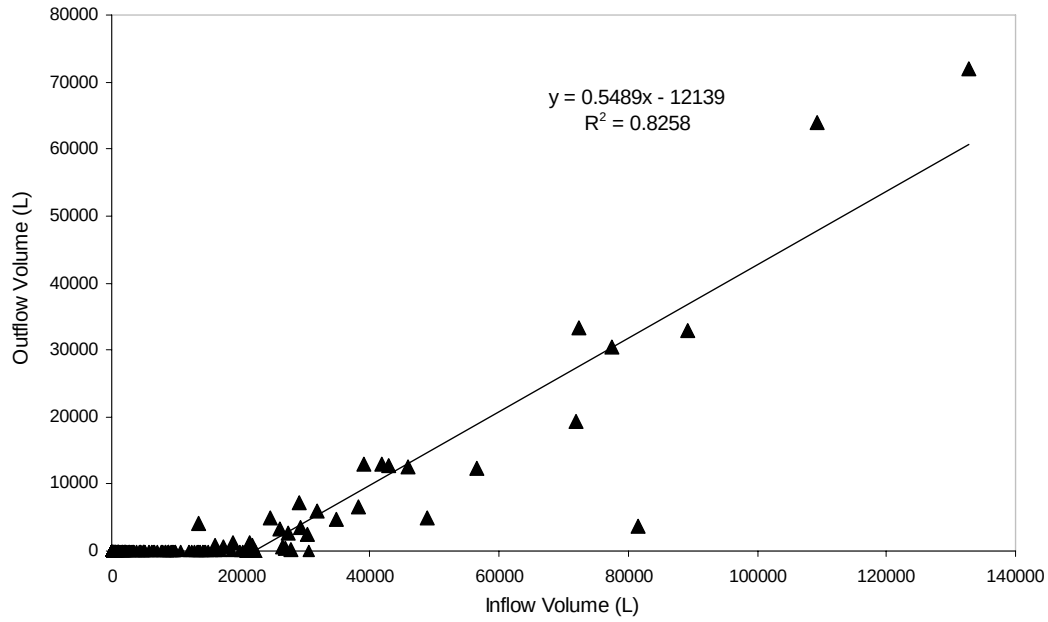

(b)

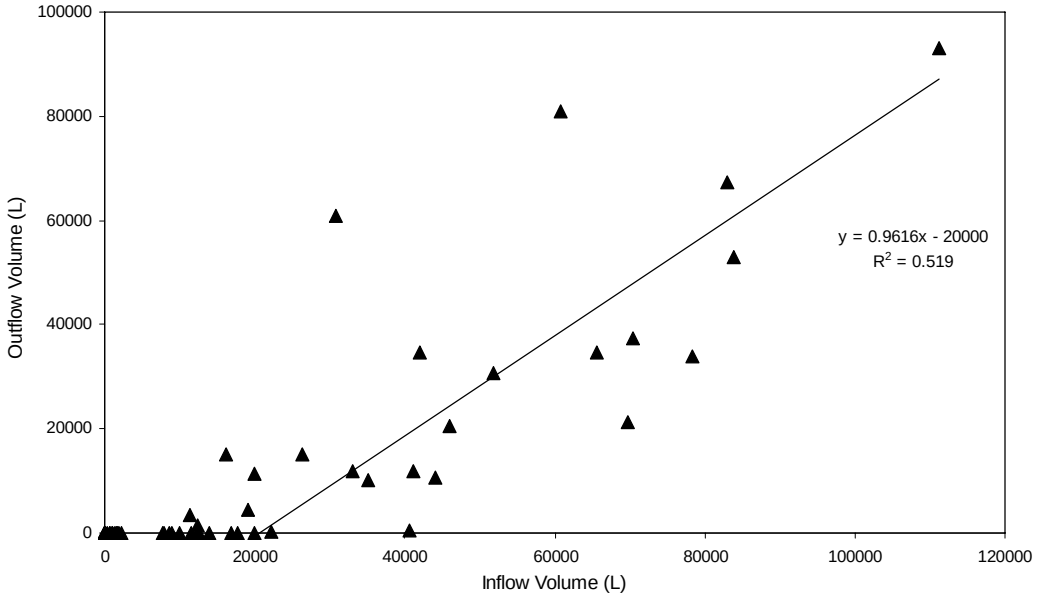

Figure 3.15 The relationship between inflow and outflow bioretention runoff volume in (a) current data set and (b) previous data set (Li 2007). Storages of about 22,000 L, and 21,000 L are observed in the current and previous data sets respectively.

The same volume relationship is observed in the previous data set (Li 2007). Because there is more scatter in the data, the trend is less evident. However, as shown in Figure 3.15b, outflowing storm events begin to occur after about 21,000 L of inflow has entered the cell. Once outflow begins, the following linear relationship reflects the inflow-outflow processes:

$$V_{OUT} = 0.75V_{IN} - 7267.7 \quad (3\text{-}8)$$

Due to the scatter, this relationship has an $r^2 = 0.578$, which shows a much weaker correlation between outflow volume and inflow volume than that found using the current data, which has an $r^2 = 0.918$. A storage capacity of only 9,690 L is found by setting V_{OUT} to zero in this equation, which is much lower than the estimate of 22,000 L. However, after setting the intercept to -20,000 L of outflow, a storage capacity of about 21,000 L is calculated:

$$V_{OUT} = 0.96V_{IN} - 20000 \quad (3\text{-}9)$$

This relationship has an $r^2 = 0.519$, which represents only a slightly weaker correlation and is represented in Figure 3.15b. While the r^2 value is lower than that of the original trendline, this linear relationship better illustrates the cell storage capacity. Completely captured events occur up until about 20,000 L of inflow. Shifting the trendline reflects this cell storage despite the scatter of the data, resulting in an inflow storage volume of around 21,000 L, which is close to the determined storage capacity of 18,800 L.

While Equations 3-8 and 3-9 are statistically different according to the chi-square test (Iman 1977), both data sets were found to behave hydrologically similarly. Using the least squares method, a CN=79 for the current data and a CN=80 for the previous data (Li 2007) were found to fit best to each data set. Therefore, the Sligo-Dennis performed essentially the same hydrologically in both studies, over a total duration of almost 5 years.

Because the 18,800 L inflow storage volume corresponds directly to the rainfall depth (1.27 cm) at which outflow began for both the current and previous data sets (Table 3.1), this value is considered as the most accurate estimate of the cell storage capacity in terms of inflow volume. The volume trends shown in Figure 3.15 represent a more indirect relationship between rainfall depth, inflow volume, and outflow volume caused by the more variable relationship between inflow volume and outflow volume versus that between rainfall depth and inflow volume. All storage estimates were within 3,200 L of each other, making them statistically the same. Therefore, the relationships between rainfall depth and inflow volume, and between inflow and outflow volumes consistently predict a similar storage capacity value despite data scatter.

The determined cell storage capacity of 18,800 L or 18.8 m^3 makes up 20% of the total cell volume of 91.8 m^3 as calculated in Chapter 2. A porosity of 42% was Calculated in chapter 2 using the observed media make-up by a study done by Li (2007). The cell storage capacity accounts for almost half of the total estimated porosity of the cell. This percentage represents the maximum saturation, or field capacity for the cell. At this point, all available pores in the media are filled with

water and any additional water added to the system would cause outflow from the underdrain. This available storage value may also represent the difference between a media's field capacity and wilting point water content. Further research is needed to test this idea. However, knowing how to determine the storage capacity of a cell based on its media and proposed volume could greatly improve the predictability of bioretention effectiveness. With a storage capacity estimate, bioretention cells could be better designed to capture a given volume of inflow.

3.5.4 Relating Inflow and Outflow through f(v)

Building on the linear relationship between outflow and inflow volumes, a plot was made of f(v) as a function of rainfall depth for the current data set, where f(v) is the ratio of the outflow volume over the inflow volume for a given storm event. A fairly linear relationship between the f(v) of storm events producing outflow and corresponding rainfall depths was observed in this plot (Figure 3.16). This relationship has good correlation, with an r^2=0.672. The following equation shows this relationship:

$$f(v) = 0.0813P - 0.0345 \quad (3\text{-}10)$$

P represents the respective rainfall depth (cm) for a given storm event. Plugging 1.27 cm into this equation yields an f(v) of 0.069, which corresponds to an outflow volume of 1,294 L assuming an inflow of 18,800 L. Ideally, this outflow volume would be 0 because 18,800 L represents the storage capacity of the cell. No outflow should occur until >18,800 L of inflow has entered the cell. However, due to scatter in the data, the relationships between rainfall depth, inflow volume, and outflow volume do not

all perfectly match the storage capacity of 1.27 cm rainfall. There are too many variables that affect how the cell will behave in any given storm event. The corresponding inflow and outflow volumes will not always be the same for a specific rainfall depth. This outflow volume of 1,294 L is very small, showing while the regressions are not perfect, they still represent the general trend of the data.

The ratio of outflow volume over inflow volume increases as rainfall depth increases. Therefore the cell's effectiveness decreases as rainfall depth increases.

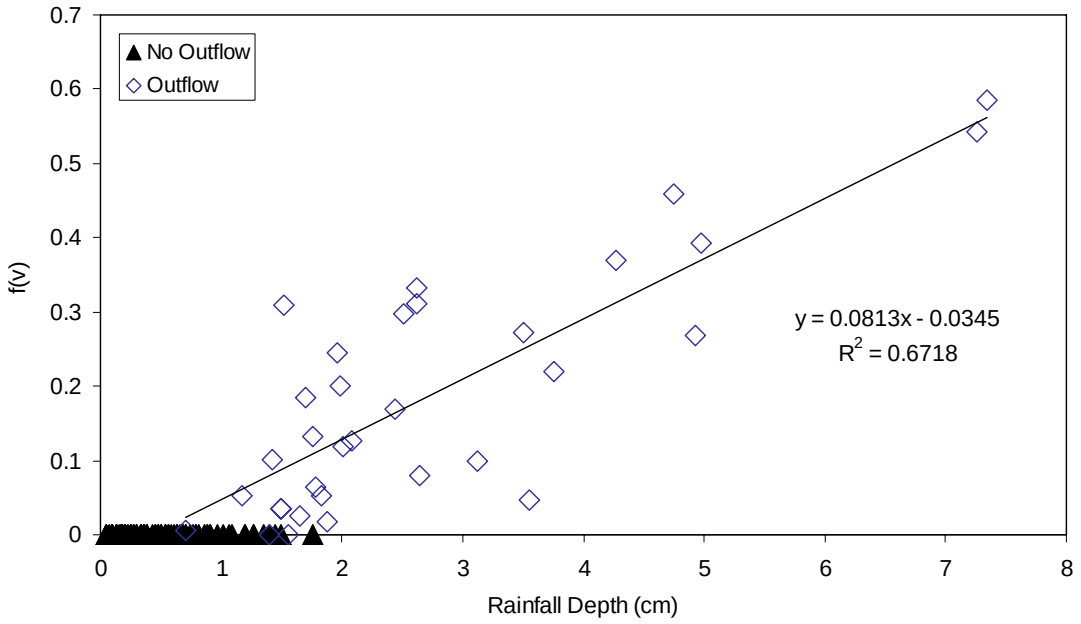

Figure 3.16 The linear relationship between the outflow to inflow volume ratio (f(v)) and rainfall depth. As rainfall depth increases, proportionally more outflow is produced relative to the inflow volume.

Of the 33 storms that produced outflow, the average f(v) was 0.19, meaning less than 20% of all runoff entering the cell, left the cell as outflow. The maximum f(v) value was 0.59, which occurred during a 9/6/2008 hurricane producing 7.34 cm of rainfall; the largest storm event recorded during the study. These values are

consistent with other studies done on similar cells, showing a range of f(v) values of 0.18-0.23 (Davis 2008). Another study done in North Carolina reported all outflow volumes were less than 50% of the inflow volumes in unlined bioretention cells over the course of a year (Hunt et al. 2006). With the exception of two large storm events, the current data agreed with this finding.

3.5.5 Curve Number Estimation

Cell performance was also compared to the Curve Number derived land uses, Woods B (CN=60), Woods C (CN=73), and Pavement (CN=98) with the same drainage area. Runoff depth values for each land use were calculated using the SCS Rainfall-Runoff Equation (Equation 2-2) as derived in Table 2.2. Two methods were used to analyze cell performance. The first method assessed the overall Sligo-Dennis site performance by basing all runoff values on rainfall depth. Equations 2.4 and 2.5 were used in method one. The second method evaluated the cell as a separate land use by defining all runoff depth based on cell inflow depths. Equations 2.6 and 2.7 were used in method two.

Because the Sligo-Dennis drainage area provided some initial abstraction, the overall site performance was better than the cell performance alone. Figures 3.17 and 3.18 show the how the site compares with Woods B, Woods C, and Pavement land uses. A CN = 79 was calculated by averaging the CN's from individual storm events and a CN=75 was fit to the data using the least squares method for the Sligo-Dennis site. Scatter in smaller, outflowing storm events as well as the dependence of CN on

storm size were sources of the disagreement in the CN's. Because CN=79 was found to fit the outflow data best, it was chosen as the estimated CN for the cell.

Figure 3.18 shows how closely the plot of CN=79 follows that of the bioretention outflow. Only about 25% of storm events produced runoff ratios exceeding zero for both curves. The CN=79, however, does describe a land use with greater runoff in larger storm events. The cell outflow had a maximum runoff depth/rainfall depth ratio of 0.27 while the CN=79 had a maximum of 0.38.

The CN-derived Pavement and the cell inflow produced similar runoff depths. The pavement values were slightly higher than those of the cell inflow because the drainage area was measured to be 41% grassed. While the Sligo-Dennis parking lot was observed to have a CN of 88, least squares analysis estimated a CN=96 for the site as shown in Figure 3.18. This difference may be due to the routing of curbs, which kept most runoff on the parking lot, guiding it towards the cell.

However, with the exception of one storm event that produced more inflow than rainfall, the maximum inflow depth/rainfall depth ratios were around 0.60, which is 30% less than the maximum ratios around 0.90 for the pavement land use (CN=98). Figure 3.17 shows this trend. The CN=96 had a maximum inflow/rainfall ratio of 0.85 and mitigated about 20% of all storm events due to initial abstraction. Conversely, the Sligo-Dennis site was found to mitigate less than 5% of the 127 storm events analyzed. Because of its lower initial abstraction and lower inflow/rainfall ratios, the site performance does not fit a CN well. In order to best assess the cell's performance, it was estimated to have a CN=96.

Therefore, overall, the cell reduced the Sligo-Dennis site from a CN=96 to a CN=79, performing almost as well as the Woods C land use, which had a CN=73. Therefore, from a volumetric perspective, the site is similar to a Woods C drainage area of the same size.

A little more than 15% of all storms produced outflow in land use Woods C, as opposed to 25% in the cell. As shown in Figure 3.17, the storage capacity of the site was around 1.27 cm of rainfall and that of the Woods C land use was about 1.75 cm. After an exceedance of 5%, the cell outflow and Woods C curves show similar runoff/rainfall ratios, suggesting both land uses control water volume in a similar manner after volumetric storage capacity is met. Figure 3.18 shows how both exceedance curves have the same general shape, shifted 10% apart due to differing storage capacities. This trend is also seen in Figure 3.17, where the cell outflow and Wood C follow each other very closely from storm events producing ≥2 cm. Intensity may also play a role in the large runoff/rainfall ratios in the cell from rainfall depths 1.5-2.5 cm. As shown in Figure 3.5, storm intensity can affect how much outflow the cell produces. Because the CN-derived land uses were based on rainfall depth alone, intensity does not affect their performance. Therefore, the overall site performance may be closer to Woods C than CN's predict.

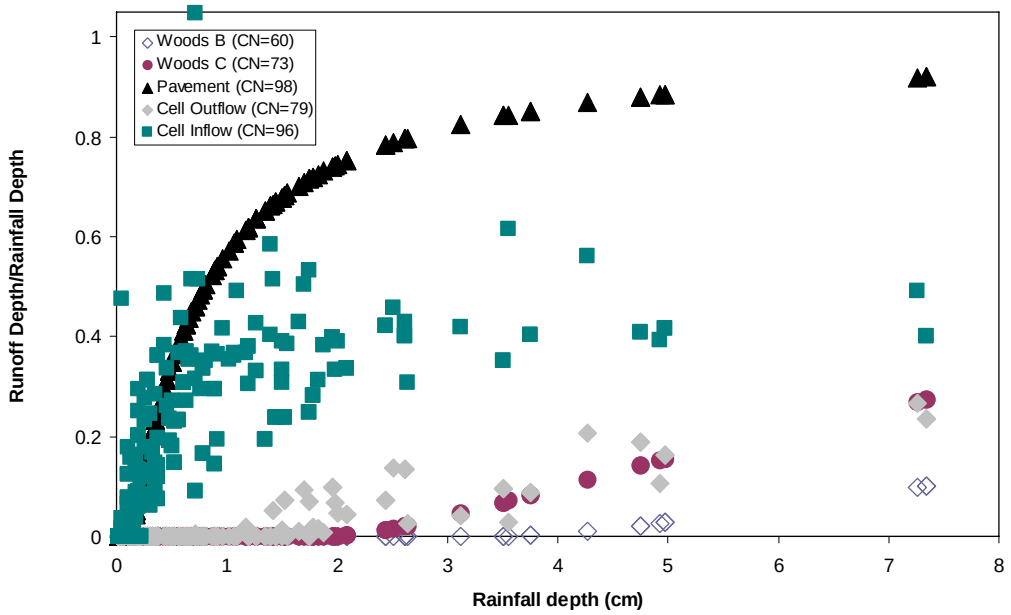

Figure 3.17. Runoff depth/rainfall depth versus rainfall depth for cell outflow, woods B, woods C, and Pavement land uses. All CN-derived land use runoff depths were calculated using Equations 2-2 and 2-3, with rainfall depth as P. The cell inflow and outflow depths were determined by dividing the respective volumes by the drainage area.

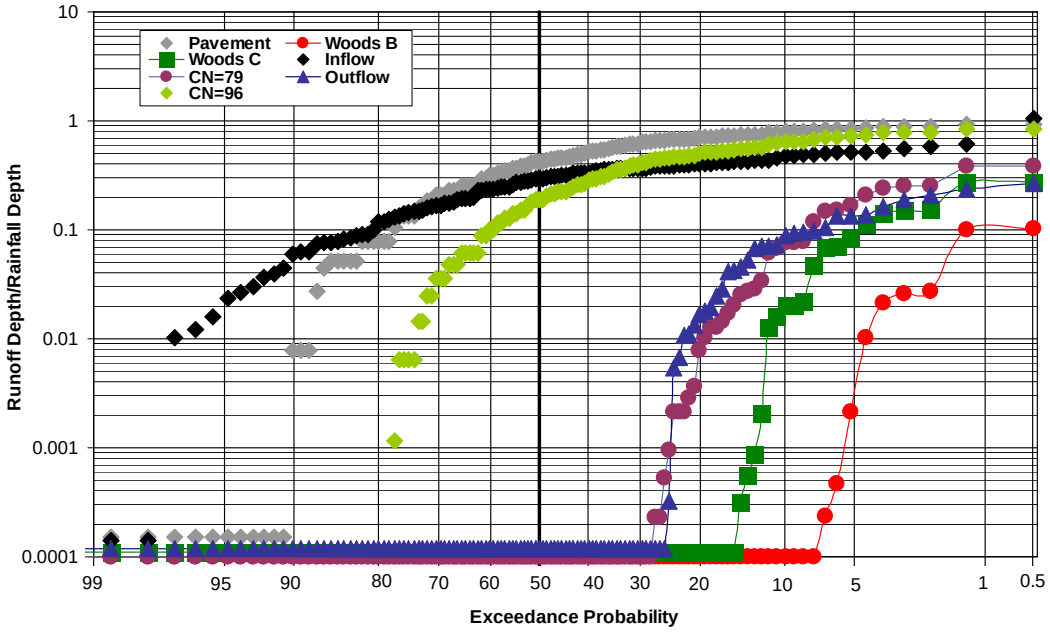

Figure 3.18 Exceedance plot of ratio of runoff depth over rainfall depth comparing cell inflow, the cell outflow, pavement, Woods C, and Woods B. The cell outflow produces slightly higher runoff depths than Woods C with the same drainage area. All runoff/rainfall ratios ≤0.0001 were set to 0.0001.

These CN runoff depths were also used to determine relative storage capacities for each land use. Using the storage capacity of 20% of the total cell volume, relative bioretention cell volumes were estimated for each land use based on the maximum storm size completely captured by each. Table 3.2 summarizes these values for Sligo-Dennis, overall site performance. Therefore, in order for the Sligo-Dennis site to mitigate the same volume of runoff as a Woods C land use with the same drainage area, a 150 m^3 cell would be required. Assuming a depth of 0.9 m (the same as the current cell), a Woods C cell would take up an area of 167 m^2, or about 4.5% of the total drainage area, which is within the typical cell/drainage area ratio range of 3-5% (Davis 2008). In order to control the same volume of water as Woods B, a cell volume of 276 m^3 and an area of 307 m^2 would be required, representing 8.3% of the total Sligo-Dennis drainage area. Given a similar drainage area, a typical bioretention cell should perform volumetrically close to land use Woods C.

Table 3.2 The bioretention cell volumes required in order to capture the same size storm events as Woods C and Woods B. For example, because a plot of Woods B with the same drainage area as the cell would completely contain all storms with rainfall depths ≤ 3.51 cm, a cell volume of 276 m^3 would be required to mimic this performance.

	Maximum Rainfall Depth producing no Outflow		**Corresponding Inflow Volume**		**Required Cell Volume**	**Cell to Drainage Area Ratio**
	cm	in	L	m^3	m^3	%
Cell	1.27	0.50	18,800	18.8	94.1	2.81
Woods C	1.96	0.77	30,000	30.0	150	4.48
Woods B	3.51	1.38	55,300	55.3	276	8.24
Pavement	0.127	0.05	235	0.2	1	0.04

Method two assessed cell performance separate from the site, which will allow its results to be applied to different drainage areas and to be compared with similar bioretention cells regardless of drainage area characteristics. Figures 3.19 and 3.20 show the resulting plots. These plots represent the cell's performance if all rain entering the drainage area entered the cell. The cell reduces the inflow from a CN=100 to a CN=92, which is not close to Woods B (CN=60) or Woods C (CN=73). About 70% of all storm events produced no outflow from the cell compared with 0% for CN=100, 95% for Woods C, and almost 99% for Woods B. As shown in Figures 3.19 and 3.20, the cell produces significantly less runoff than a comparable drainage area with 100% imperviousness, but significantly more runoff than Woods B and Wood C land uses.

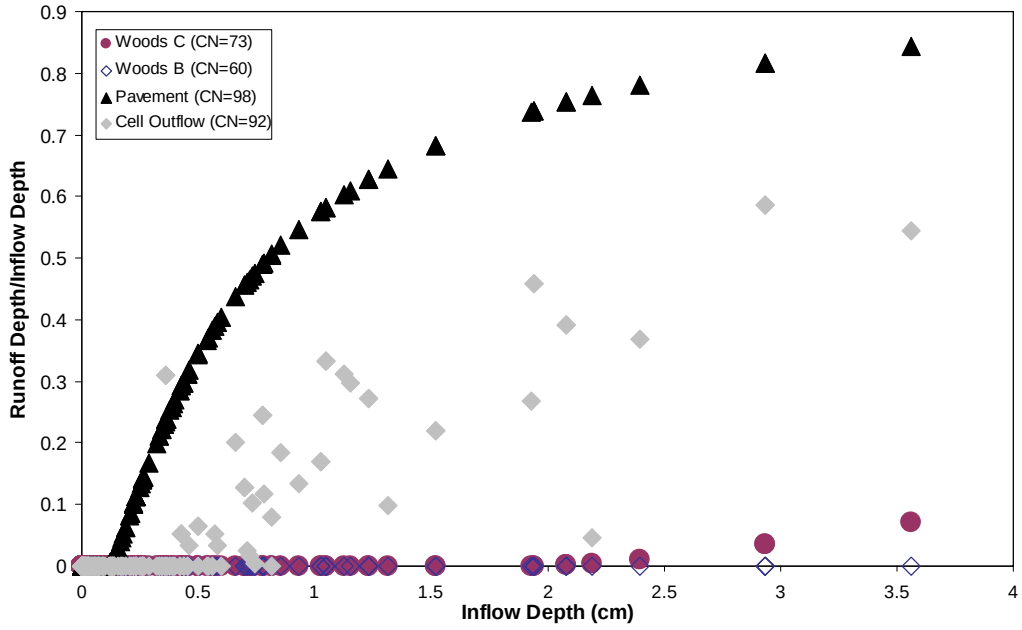

Figure 3.19 Runoff Depth/Inflow Depth versus Inflow Depth. CN-derived runoff depths were calculated using Equations 2.2 and 2.3 with cell inflow depth as P. The cell outflow curve was found by dividing the corresponding outflow volume by the inflow volume for each storm event.

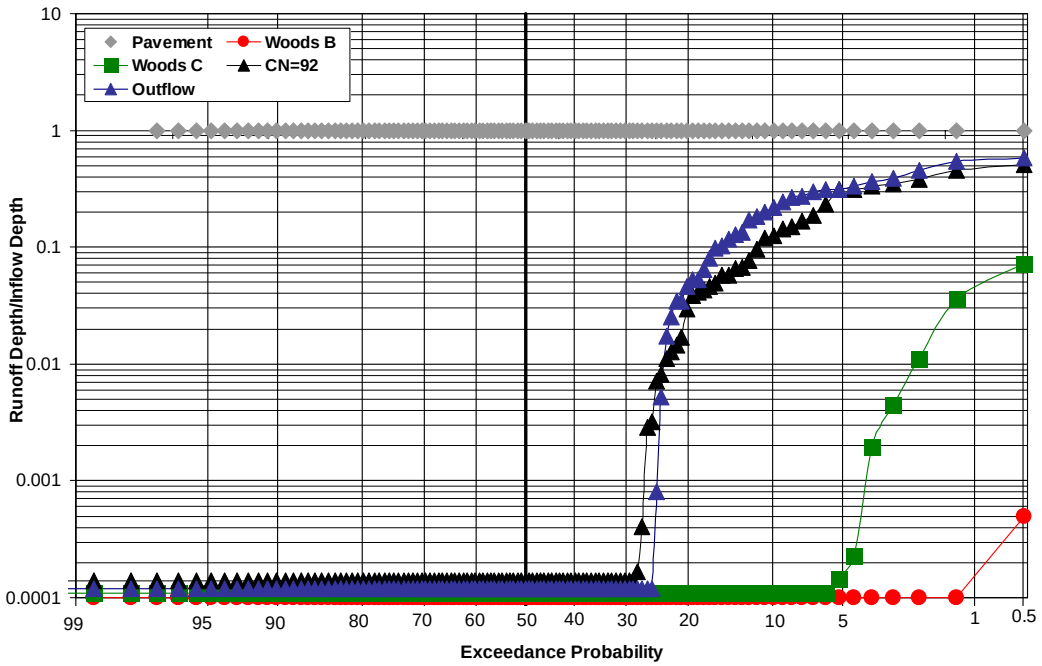

Figure 3.20 Exceedance plot derived from treating the bioretention cell as a separate land use. The cell was estimated to have a CN = 92. All runoff/inflow ratios ≤0.0001 were set equal to 0.0001.

The resulting required cell volumes based inflow depths are compiled in Table 3.3. Similar to the inflow and outflow volume relationship shown in Figure 3.15a, a storage capacity of about 21,000 Lwas found for the current cell, corresponding to 0.561 cm of inflow over the drainage area. Assuming storage accounts for 20% of the total volume of the cell, a volume of 104 m^3 was estimated from this inflow depth, which is slightly greater than the actual volume of 91.8 m^3. Because cell performance is affected by antecedent dry time, storm intensity, as well as temperature, there was not a singular inflow depth at which outflow began (Figure 3.19). While the 0.561 cm of inflow depth was found to produce the smallest outflow/inflow depth ratio, some storm events producing less inflow also produced more outflow. However, a depth of 0.561cm was chosen to be the cell inflow storage because it included all outflowing events.

In comparison, a cell volume of 359 m^3 would be required to control the same volume of water as Woods C, which corresponds to a cell with an area of 400 m^2 and a depth of 0.9 m, taking up 10.7% of the total Sligo-Dennis drainage area. As opposed to the volumes found in Table 3.2, this volume represents the cell size required assuming all rainfall from a storm event enters the cell. Therefore, a 359 m^3 cell placed in a 100% impervious, 0.37 ha drainage area would perform the same volumetrically as an area of Woods C.

Table 3.3 The bioretention cell volumes required in order to capture the same size storm events as Woods C and Woods B based on inflow depth values.

	Maximum Rainfall Depth producing no Outflow		**Corresponding Inflow Volume**		**Required Cell Volume**	**Cell to Drainage Area Ratio**
	cm	in	L	m^3	m^3	%
Cell	0.561	0.22	20,900	20.9	104	3.12
Woods C	1.93	0.76	71,900	71.9	359	10.7
Woods B	3.56	1.40	133,000	133	663	19.8
Pavement	---	---	---	---	---	---

3.6 Comparing Bioretention Performance with Forested Stream Data

3.6.1 Comparison Hydrographs

In order to compare cell performance with that of the Pond Branch forested site on an individual storm basis, comparison hydrographs were complied of storm events that occurred at both sites with similar rainfall depths. Because of the distance between the sites, these comparisons do not represent completely congruent storm events. Rainfall data for the Pond Branch stream was measured by a USGS rain gauge in Oregon Ridge Park about 1.2 km north of the flow gage. Four storm events

were analyzed using comparison hydrographs to evaluate the cell's relative performance. Both the least squares method and CN methods were used to estimate an overall CN of 76 for the Pond Branch site, which represents volumetric performance between that of the Sligo Dennis site (CN=79) and that of woods C (CN=73).

Figure 3.21 shows the comparison hydrograph of a moderate-sized storm event occurring on 9/26/2009 that produced 3.25 cm of rainfall at Pond Branch and 3.12 cm at the cell. The total outflow volume at the cell (13,100 L/ha) was slightly higher than the Pond Branch flow volume of 10,400 L/ha. In this case, the cell performs slightly worse than the Pond Branch stream volumetrically in this storm event. Both the cell outflow (13,100 L/ha) and Pond Branch (10,400 L/ha) produced an order of magnitude less runoff than the cell inflow, which produced 132,000 L/ha of runoff (Table 3.5).

However, the cell outflow had much higher normalized flowrates (the normalized peak flow was over twice that of the Pond Branch peak flow) and maintained these higher flowrates for longer. From 12:00AM on 9/27/2009 to 3:36AM on the same day, the cell outflow rates are almost double those of Pond Branch.

Over this time period, the cell outflow rates ranged from around 0.5 to 0.95 L/s-ha, while Pond Branch values ranged from 0.20 to 0.43 L/s-ha. Pond Branch flows lasted almost twice as long, taking 8.5 hrs to peak, but quickly dropped after this peak. The cell outflow, reached its peak after about 1 hr, maintaining flowrates almost double those of Pond Branch for almost 4 hrs before leveling out to flowrates

>0.5 L/s-ha. The Pond Branch flow also lasted for a little under 18 hrs, which is almost twice the 9 hr duration of cell outflow. These results are summarized in Table 3.4. This difference in flow-duration and distribution show that although the cell outflow and Pond Branch flow are similar volumetrically, the cell does not mitigate flow as well as the selected pre-developed area.

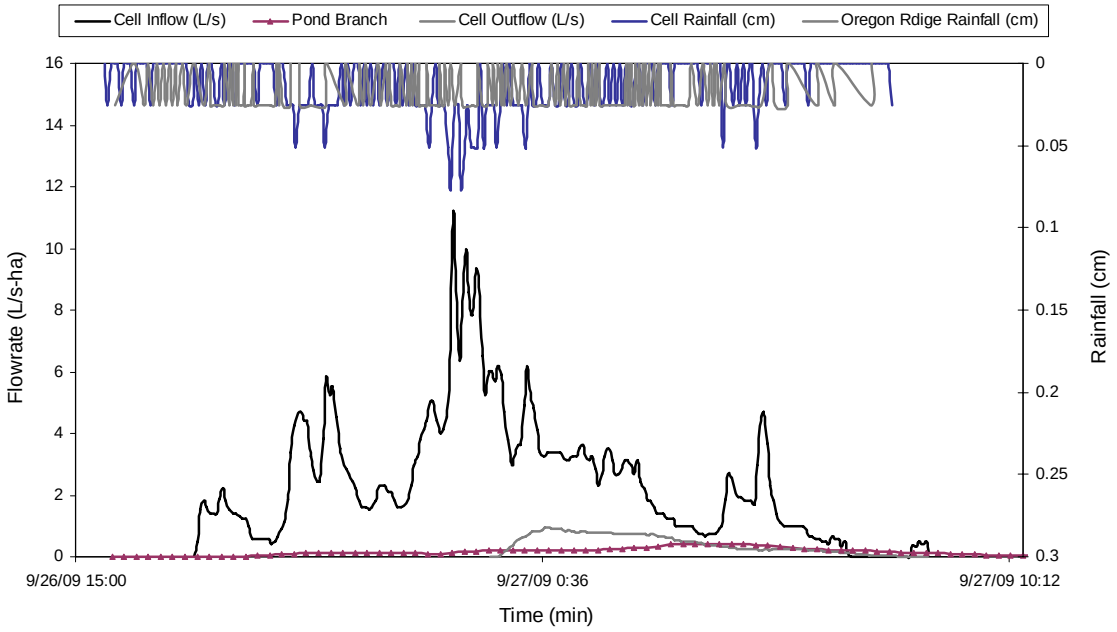

Figure 3.21 Hydrograph comparing a 9/26/2009 storm event occurring at the cell (3.12 cm) and at forested Pond Branch site (3.25 cm).

Table 3.4 Summary Table of comparison hydrographs from 9/26/2009 storm event. The bioretention cell performed similarly volumetrically to the Pond Branch stream. The cell peak flow is over twice that of Pond Branch. The Pond Branch flow lasts almost twice as long as the cell outflow.

	Rainfall (cm)	Volume (L/ha)	Peak Flow (L/s-ha)	Flow Duration (hr:min)	Time to Peak (hrs)
Cell Inflow	3.12	132,000	11.2	15:08	5:20
Cell Outflow	3.12	13,100	0.95	9:00	1:08
Pond Branch	3.25	10,400	0.43	17:45	8:30

Figure 3.22 shows the resulting hydrograph from a 5/15/2008 storm event producing 1.68 cm of rainfall at Pond Branch and 1.98 cm of rainfall at the cell. While the cell saw about 0.3 cm more rainfall, in this case it produced a disproportionately large volume of outflow compared to Pond Branch. The cell outflow volume was 13,400 L/ha and the Pond Branch flow volume was 3,700 L/ha, almost four times less than that of the cell outflow. The peak flowrate of Pond Branch (0.16 L/s-ha) was about seven times less than the cell outflow peak of 1.13 L/s-ha. Pond Branch flow duration and time to peak were also much longer than the cell outflow. Table 3.5 summarizes the results from this storm event.

The cell performed worse volumetrically as well as with respect to flow-duration in this storm event. With a rainfall depth of 1.98 cm at the Sligo-Dennis site, this storm exceeded the cell storage capacity of 1.27 cm by 0.71 cm, creating a corresponding outflow volume of 13,400 L/ha. Because the Pond Branch drainage area is forested and provides more infiltration as well as interception (King et al 2010), it may have a larger storage capacity, only producing significant flow after a rainfall depth >1.27 cm and around storm events with rainfall depths ~1.7 cm. However, because forested streams are complex ecosystems, their hydrology may not be as simply modeled as that of the Sligo-Dennis bioretention cell. Pond Branch may mitigate water differently than the cell, making it difficult to define a Pond Branch storage capacity.

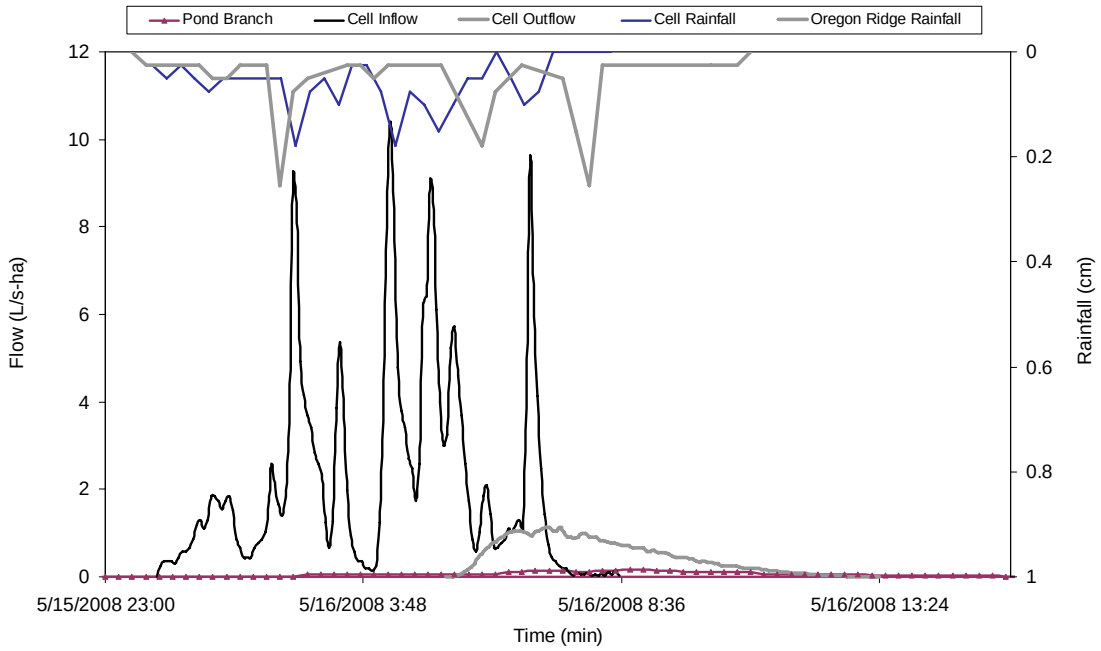

Figure 3.22 Comparison hydrograph for a 5/15/2008 storm event, which produced 1.68 cm of rain at Pond Branch and 1.98 cm at the bioretention cell.

Table 3.5 Summary table for the comparison hydrograph from 5/15/2008 storm event. The cell produced almost four times more outflow than the Pond Branch Stream and had a peak flow rate seven times greater than that of Pond Branch. The Pond Branch flow also lasted over twice as long as the cell outflow.

	Rainfall (cm)	Volume (L/ha)	Peak Flow (L/s-ha)	Flow Duration (hrs)	Time to Peak (hrs)
Cell Inflow	1.98	66,500	10.4	8:36	4:20
Cell Outflow	1.98	13,400	1.13	8:04	1:52
Pond Branch	1.68	3,700	0.16	19:30	6:45

Figure 3.23 and Table 3.7 summarize the resulting hydrograph from a 12/15/2008 storm event. The rainfall patterns affecting each site were different. The storm event at Pond Branch was longer and had lower rainfall peaks. Therefore, higher flowrates should be expected at the cell. However, because the rainfall depths are similar, the overall volume of water entering each site should be comparable per hectare. The cell received 1.95 cm of rainfall, producing about 19,000 L/ha of

outflow. Pond Branch received 1.80 cm of rainfall and produced about 4,400 L/ha of flow, about four times less than that of the cell. These volumetric results are similar to those found in the 5/15/2008 storm event.

While the cell outflow peak flowrate (0.94 L/s-ha) is almost four times that of the Pond Branch stream (0.25 L/s-ha), the cell's flow duration and time to peak are very close to those for the stream, as shown in Table 3.6. Therefore in this storm, the cell flow-duration and peak flow values were comparable to those of Pond Branch. The cell however, performed much worse volumetrically. Again this large discrepancy between the cell outflow and Pond Branch flow volumes may be due to different relative storage capacities.

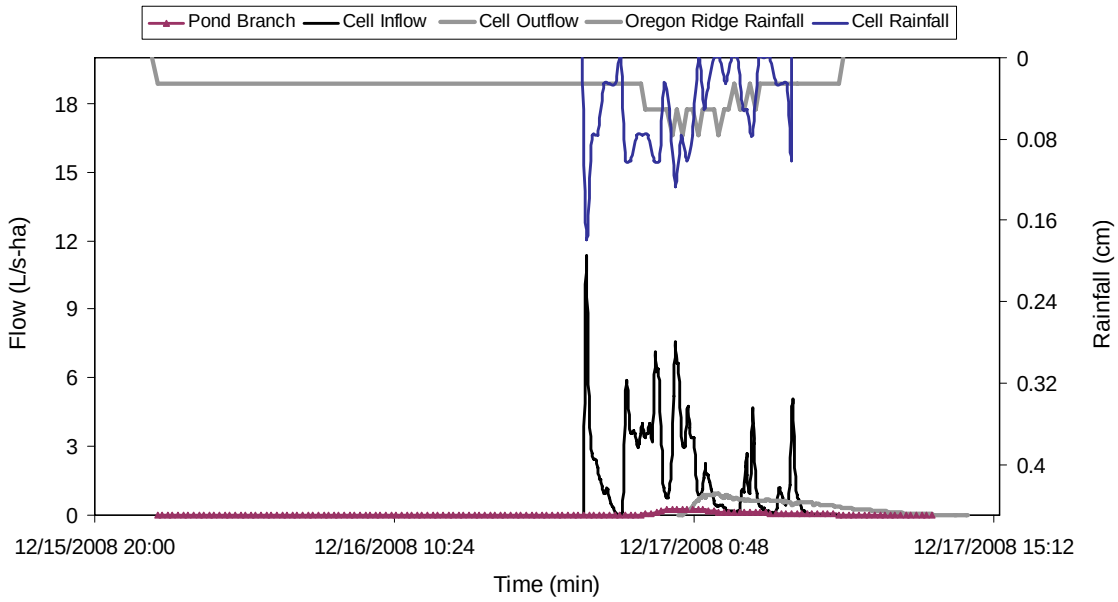

Figure 3.23 Comparison hydrograph of a 12/15/2008 storm event. The cell received 1.95 cm of rainfall, producing about 19,000 L/ha of outflow. Pond Branch received 1.80 cm of rainfall and produced about 4,400 L/ha of flow.

Table 3.6 Summary table for comparison hydrograph for 12/15/2008 storm event

	Rainfall (cm)	Volume (L/ha)	Peak Flow (L/s-ha)	Flow Duration (hrs)	Time to Peak (hrs)
Cell Inflow	1.96	78,400	11.4	12:16	0:08
Cell Outflow	1.96	19,200	0.94	13:56	1:48
Pond Branch	1.83	4,400	0.25	14:15	2:00

.

Finally, Figure 3.24 and Table 3.7 show the results for a 3/26/2009 storm event producing 0.889 cm of rainfall at both the cell and Pond Branch. This event did not produce outflow from the cell because it did not meet the cell's storage capacity of 1.27 cm. The Pond Branch stream, did however produce flow, summing to 1,300 L/s-ha.

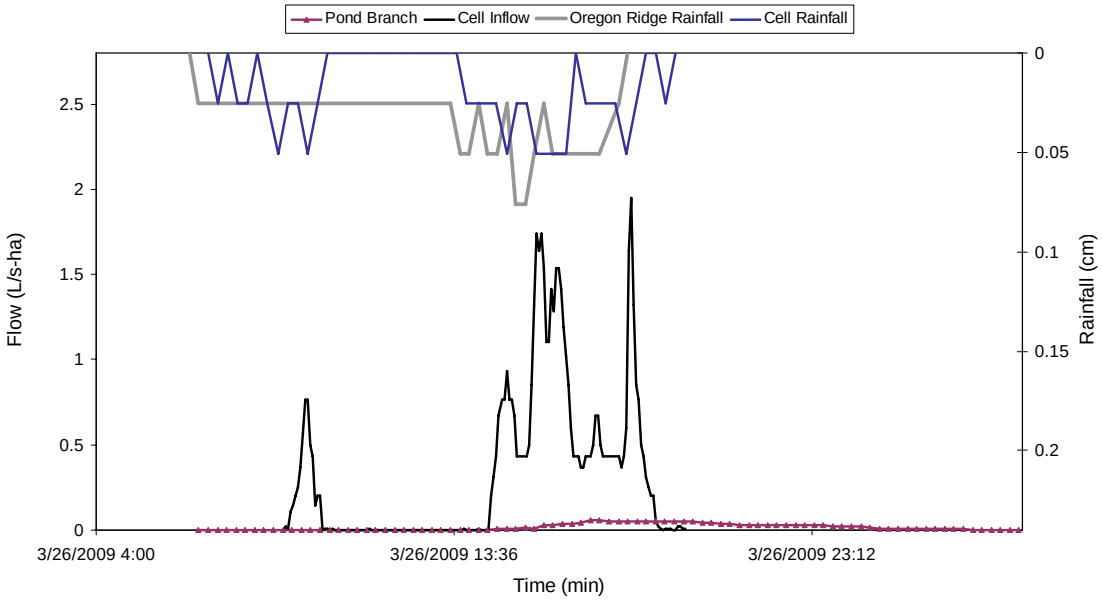

Figure 3.24 Comparison hydrograph of a 3/26/2009 storm event producing 0.889 cm. Pond Branch produced 1313 L/ha of flow. The cell produced no outflow.

Table 3.7 Summary table of 3/26/2009 comparison hydrograph. No outflow occurred from the cell.

	Rainfall (cm)	Volume (L/ha)	Peak Flow (L/s-ha)	Flow Duration (hr)	Time to Peak (hrs)
Cell Inflow	0.89	13,000	1.95	10:48	9:20
Cell Outflow	0.89	---	---	---	---
Pond Branch	0.89	1,300	0.06	14:15	2:45

The 3/26/2009 hydrograph suggests that while the cell produces outflow after a given storage capacity, Pond Branch and forested streams do not have the same kind of thresholds. Therefore, Pond Branch produced flow in all analyzed storm events. These flows all had long durations, typically ≥14 hrs. Time to peak was usually significantly greater than that of cell outflow. The cell also maintained higher relative flowrates for longer than Pond Branch, suggesting that runoff does not only infiltrate down to the stream as it does in the cell. High flow rates are mitigated more quickly in Pond Branch, which may be due to a number of factors including a greater time of concentration due to the larger drainage area and channel meanders.

3.6.2 Comparing Cell and Pond Branch Volumetric Trends

Because the Pond Branch stream did not have a clear storage capacity, a Curve Number could not be fit to the data. While CN land uses produce no runoff until a given initial abstraction is met after which runoff related linearly to rainfall depth, runoff was produced in every storm analyzed at Pond Branch. Two such storm events were completely captured by the Sligo-Dennis cell, each producing <5,000 L/ha of flow. The fact that Pond Branch is a stream rather than simply a wooded area may explain this lack of initial abstraction at the site. While baseflow was estimated

and removed from all storm events, infiltration in the Pond Branch drainage area may also feed stream flow. Therefore even though the forested area provides greater infiltration and mitigation of runoff, Pond Branch will always produce flow.

Despite this continuous flow, Pond Branch performed better both volumetrically and with respect to flowrate than both the cell inflow and cell outflow. Figure 3.25 plots the relationship between flow volume and rainfall depth for each area, all of which show strong linear correlations. Both the cell outflow and Pond Branch slopes, which are respectively 26,700 and 4,450 L/ha-cm are smaller than the cell inflow (45,100 L/ha-cm). The cell outflow regression represents only storm events producing outflow.

The cell outflow slope is six times that of Pond Branch, predicting much larger flow volumes after about 2 cm of rainfall. According to the regression lines (Figure 3.25) the cell outflow and Pond Branch sites produce 11,500 L and 5,460 L of flow, respectively, after 2 cm of rainfall. This trend matches the results found in the comparison hydrographs in Figures 3.22 and 3.23, which represent storm events producing slightly less than 2 cm of rainfall. However, a number of actual storm events with rainfall depths between 3 and 4 cm produced similar flow volumes in the cell and Pond Branch. The regression lines predict a cell outflow volume of 38,300 L and a Pond Branch flow volume of 9,910 L from a 3 cm rainfall depth. Conversely, the 9/26/2009 comparison hydrograph (Figure 3.21) shows similar volumetric performance for both sites, resulting in a cell outflow volume of 13,100 L from a 3.12 cm rainfall, and a Pond Branch flow volume of 10,400 L from a 3.25 cm rainfall.

Because of scatter as well as limited data points for Pond Branch, these regression lines are not fully representative of all storm events. Based on both individual storm events and the overall volume trends shown in Figure 3.25, it was estimated that the cell outflow volumes match those of the Pond Branch data closely for rainfall depths <2 cm. After this point, the difference in slopes is more significant. Environmental factors such as antecedent dry time, temperature, and rainfall intensity may also play a role in how the cell performs compared to Pond Branch in larger storm events.

Differences in cell outflow and Pond Branch flow volumes in the storm events producing around 2 cm of rainfall may be due to scatter in the cell outflow data, and individual storm characteristics rather than differing storage capacities. The cell outflow also may be more sensitive to rainfall intensity than Pond Branch due to less infiltration. The cell, therefore, performs worse volumetrically compared to the Pond Branch stream with increasing storm size.

An estimated baseflow of 0.057L/s-ha was also subtracted from all Pond Branch flow values in order to better compare performance. Despite removing this estimated baseflow, Pond Branch flows were not limited to during and directly after storm events. Baseflow may have changed from storm to storm, making it difficult to remove. The Pond Branch drainage area (31 ha) was also almost an order of magnitude greater than that of the Sligo-Dennis cell (0.37 ha). This large drainage area may have contributed to a greater time of concentration and may have made the overall hydrologic behavior of the Pond Branch site very different from that of the

curbed and controlled Sligo-Dennis site. All flows were divided by their respective drainage areas in order to normalize the values, making the units L/s-ha.

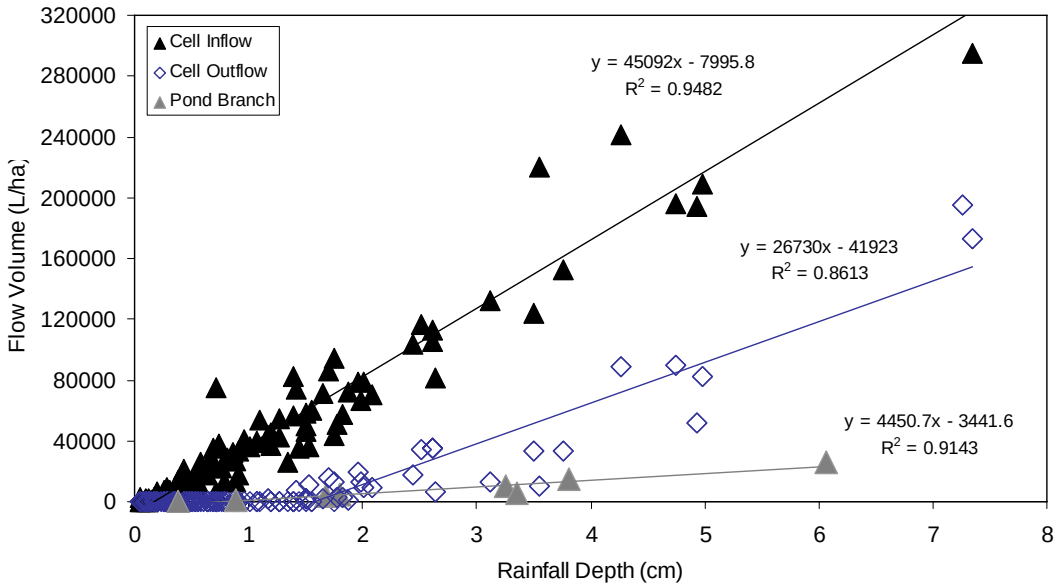

Figure 3.25. Relationship between flow volume and rainfall depth for cell inflow, cell outflow, and rainfall depth.

3.6.3 Comparison Flow-Duration Curves

A flow-duration curve comparing cell inflow, cell outflow, and forested stream flow was compiled using continuous flow data from May 2008 through April 2010. Flow data from the cell for all storm events over the course of the current study were recorded and compiled into 4-min increments. USGS provided continuous flow data in 15-min increments from Pond Branch Stream.

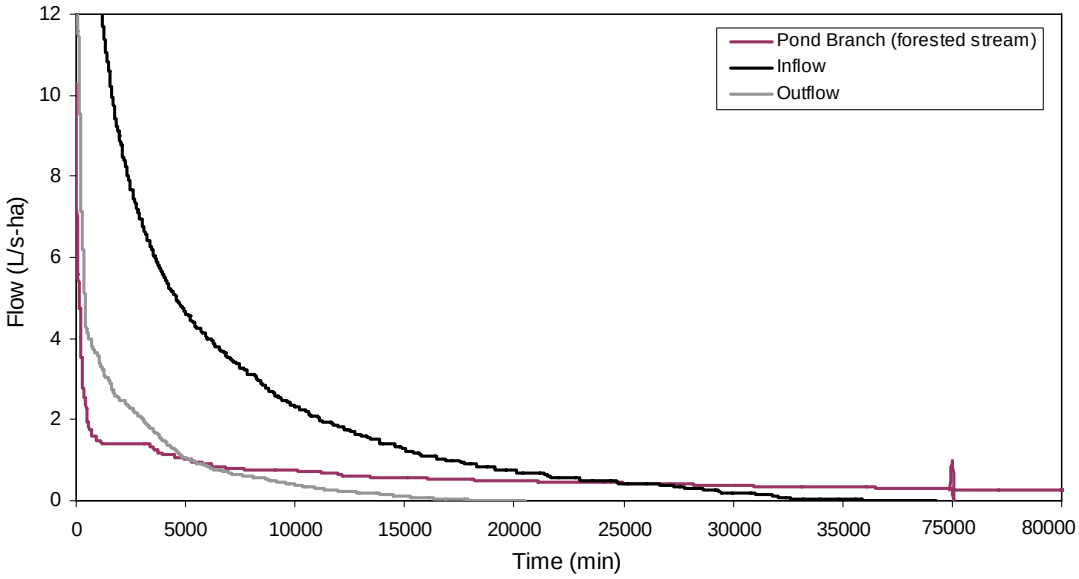

Figure 3.26 Flow-duration curves for the Sligo-Dennis cell inflow, the Sligo-Dennis cell outflow, and the Pond Branch Stream. The cell inflow, cell outflow, and Pond Branch flows had respective durations of 39,232 min, 20,460 min, and about 1,000,000 min resulting from 2 years of monitoring.

Because of the continuous flow, the Pond Branch stream data set does not represent an exact pre-development goal for the Sligo-Dennis site. The cumulative flow-duration plot is shown in Figure 3.26. With an estimated baseflow removed, the cumulative duration of flow for the Pond Branch data was still over 1,000,000 min over the course of the two year study, which is still much longer than the respective bioretention inflow and outflow durations of 39,232 min and 20,460 min.

While Pond Branch flow data were fairly continuous, the bioretention data represent flows solely during or after storm events. Flowrates were zero all other times; there was no continuous flow from the cell between rainfall events unless events were very close together. The maximum flowrate for inflow from the health center is about 108 L/s-ha, for outflow about 18.4 L/s-ha, and for Pond Branch about 10.3 L/s-ha. The inflow maximum is almost ten times that of Pond Branch,

demonstrating the impact of development, and the outflow maximum value is almost double that of Pond Branch.

These large differences between cell outflow and Pond Branch peak flows may be due to increased infiltration and mitigation in the forested Pond Branch drainage area (King et al. 2010). While the cell reduced the overall peak flow of the site by 83%, the cell's peak flow of 18.4 L/s-ha is still almost twice that of the selected pre-development values. While Section 3.5.5 shows that the Sligo-Dennis site is close to the volumetric performance of pre-development, Figure 3.26 shows the cell has not quite reached pre-development flow values.

The bioretention outflow graph appears to descend slightly faster than the inflow curve. Outflow values are also consistently below inflow values, indicating that inflow rate and exposure duration are being reduced by the cell. The inflow curve exceeds the Pond Branch maximum from time 0-1280 min. The outflow curve exceeds the maximum Pond Branch value from time 0-116 min. This reduction, however, does not reach the pre-development values represented by the Pond Branch curve. Storm events of the same size are producing more high flowrates (>1.5 L/s-ha) in the cell than in the Pond Branch stream.

All three curves were initially very steep. However, the Pond Branch curve had much shorter, steeper decline, indicating it had fairly constant flow rates over the course of the study. The Pond Branch curve began to steady out after a duration of 930 min, falling to a flowrate of 1.5 L/s-ha. After this point, the Pond Branch curve is very gradual, taking about 1,000,000 min to finally reach 0 L/s-ha. The cell inflow

and outflow curves only reach flowrates of 13.6 L/s and 3.6 L/s-ha, respectively, after the same 930 min.

While the cell inflow and outflow curves have similar shapes, the outflow curve does not quite follow the exponential decay form of the inflow, but rather has three stages, each with decreasing steepness, falling down to more constant flowrates more quickly. The first stage begins at time zero with a flowrate of 18.4 L/s-ha and quickly declines to a flowrate of 4.24 L/s-ha after 460 min. After 460 min, the outflow curve falls to about 0.20 L/s-ha at a time of 13,000 min, after which the curve steadily declines to 0 over 7,000 min.

At about 4,900 min, the cell outflow curve intersects and dips below the Pond Branch curve at a flowrate around 1.1 L/s-ha. After this point, the outflow curve continues to decrease a steeper slope than the Pond Branch, reaching 0 L/s-ha after about 15,100 min. The Pond Branch curve reaches 0 L/s-ha after 995,000 min with a much more gradual decline in flowrate. As shown in Section 3.6.1, Pond Branch flow for individual storm events consistently lasted for >14 hrs, contributing to its large overall flow-duration. Cell outflow duration was less consistent and often shorter than that of Pond Branch, changing from storm to storm.

A zoomed-in graph of the cell outflow and Pond Branch flow-duration curves better shows the comparison between the two in Figure 3.27. Both curves have a similar shape. The greatest difference between the curves exists between 460 and about 3000 min. During this time, the Pond Branch reaches a steady decline in flowrate after 930 min. The cell outflow flowrates conversely remain higher (above 1.5 L/s-ha) for longer. Therefore, Pond Branch may mitigate larger, more intense

storm events better than the cell, resulting in lower peak flows and fewer high flows overall.

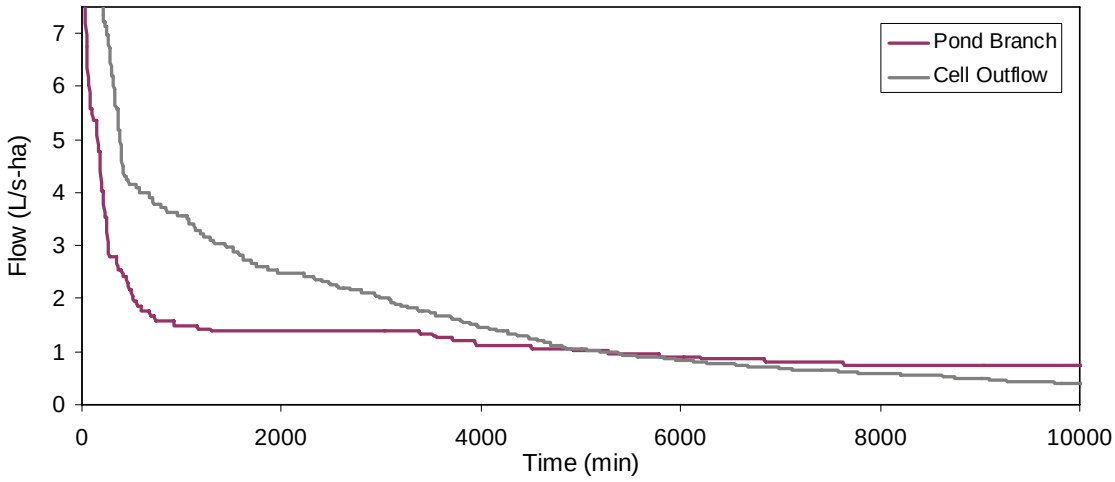

Figure 3.27 Flow-duration curve of cell outflow and Pond Branch flow up to a duration of 10,000 min. While both curves have similar shapes, the cell outflow curve maintains higher flows for a longer duration.

While the bioretention cell has produced much lower flowrates in outflow, these flowrates are still significantly higher than the Pond Branch flowrates. The outflow falls under the maximum Pond Branch values 11 times faster than the cell inflow.

The storm events causing the maximum flowrate values for each system were also analyzed. The maximum flowrate for Pond Branch occurred on 9/27/2008 around 4 pm, which was recorded as a 9.07 cm storm in Baltimore on the 27th and 0.762 cm on the 26th.

The maximum peak values for the bioretention inflow and outflow did not occur in the same storm events. The max inflow value (108 L/s-ha) occurred during a 5/8/08 storm which lasted 1.31 days with a rainfall depth of 12.5 cm. This intensity also correlated to a 4-min rainfall depth of 0.533 cm, which was the maximum 4-min

rainfall depth over the course of the study. The hydrograph from this storm event is shown in Figure 3.28. The inflow rate is very sensitive to rainfall intensity. As shown in Subsection 3.6.1 the inflow and rainfall curves follow each other very closely.

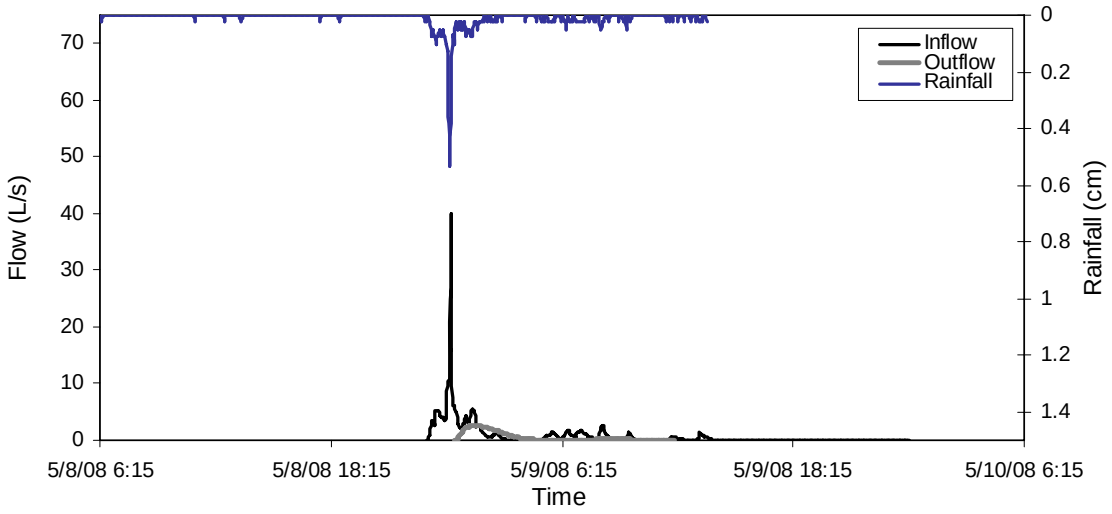

Figure 3.28 The peak inflow rate at the bioretention cell (108 L/s-ha) occurs concurrently with the 4-min peak rainfall depth of 0.533-cm.

The maximum outflow rate (18.4 L/s-ha) occurred during Hurricane Hanna on 9/6/2008, which lasted 0.45 days and produced 7.34 cm of rainfall as shown in Figure 3.29. The maximum 4-min rainfall depth during this storm was 0.438 cm, which is a little less than the 0.533 cm corresponding to the maximum inflow rate. The peak inflow rate for this storm event was 77.1 L/s-ha.

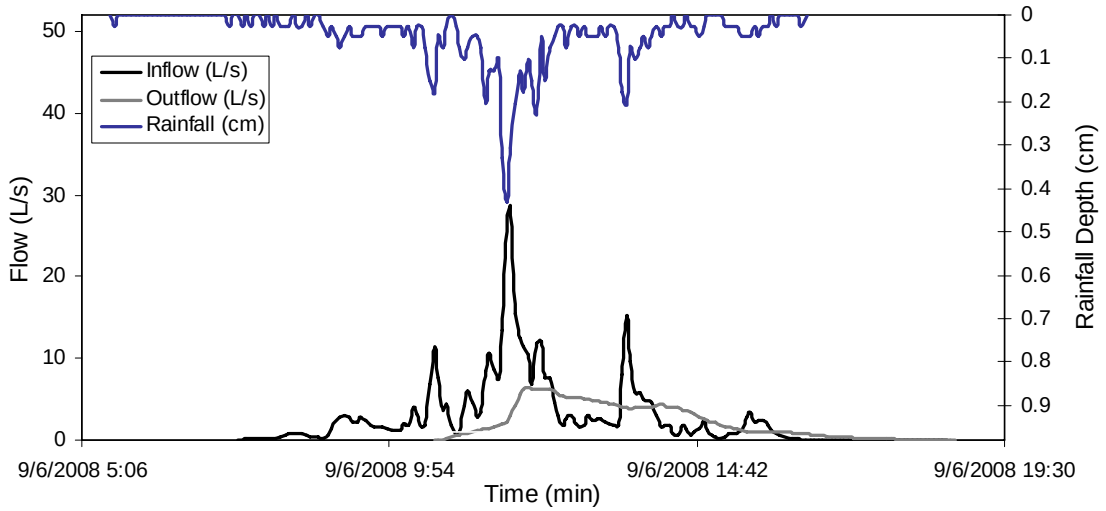

Figure 3.29 Hydrograph from storm event producing 7.34 cm of rainfall, occurring on 9/6/08. This storm produced the maximum outflow value from the data set (16.8 L/s-ha).

Higher inflow rates result from rainfall reaching the parking lot more quickly and running off into the cell. Therefore inflow rates should depend heavily on rainfall intensity. This relationship is shown in Figures 3.19 and 3.20 as well as Figure 3.15. Rainfall and inflow peaks coincide in each hydrograph.

These data suggest that while the inflow rates may depend heavily on the intensities within a storm event, the outflow and Pond Branch are buffered by the media infiltration of the watershed and therefore more dependent on total rainfall depth rather than intensity. The bioretention cell and Pond Branch seem to mitigate runoff similarly with respect to flow reduction. Both systems promote storage and infiltration before outflow occurs, dampening the effect of rainfall intensity. With rainfall depth as the major performance factor, the storage capacity of the cell is important. A larger cell would require more runoff to meet capacity and therefore more efficiently dampen the effects of rainfall intensity.

The total volume under each flow-duration curve was also determined through integration. While the total volume of water per ha from Pond Branch was larger than both the inflow and outflow curves, it occurred over a much longer period of time. The cell inflow curve spans for about 40,000 min while the Pond Branch curve spans for over 1,000,000 min. This discrepancy is due to the fact that Pond Branch is a stream with continuous flow and the cell is designed to be dry between storm events. Despite removing baseflow, Pond Branch still had a significantly longer flow-duration than the cell inflow and outflow. While forested watersheds provide more storage and infiltration and therefore less overall flow, this flow can also be distributed over a longer period of time due to slower overall flowrates. Therefore, predicting how long the Pond Branch stream flows due to storm events is difficult without analyzing each storm from the data set. In order to better compare the cell and Pond Branch volumes, two methods were used.

The first method compared the relative volumes up to the end of the cell inflow duration. The second looked at the volumes up to the end of the cell outflow duration. Because the Pond Branch flow is continuous, it is difficult to determine what flows are due specifically to storm events and which are baseflow between events with flows >0.057 L/s-ha, which was estimated to be the overall baseflow for the Pond Branch system. Pond Branch and the cell also did not see all the same storm events due to their relative locations. Some larger storms were not captured at the cell due to equipment failure and could therefore also affect the comparison.

Table 3.8 Overall volumes of runoff from cell inflow, cell outflow, and the Pond Branch given different possible flow durations. After the total duration of inflow into the cell (39,200 min), the cell produced about 400 m^3/ha less runoff than Pond Branch. However, after the total duration of cell outflow (20,600 min), the cell produced about 30 m^3/ha more runoff than Pond Branch.

	Duration (min)	Total Volume (m^3/ha)	Volume (39,232-min) [m^3/ha]	Volume (20,460-min) [m^3/ha]
Inflow	39,200	5450	5450	5160
Outflow	20,600	1130	1130	1130
Pond Branch	1,054,000	6330	1530	1100

From Table 3.8, after a shorter period (the duration of cell outflow), Pond Branch performs almost the same as the cell volumetrically, producing about 1100 m^3/ha vis-à-vis 1130 m^3/ha from cell outflow. However, after the total duration of cell inflow, Pond Branch produces more overall flow than the cell with 1530 m^3/ha, while the cell produces 1130 m^3/ha (a 400 m^3/ha difference). As shown in Section 3.6.1, Pond Branch flow durations tended to be >15 hr, and were often much longer than the cell outflow durations. The second estimate (using the cell inflow duration) may be more accurate, demonstrating that Pond Branch produced slightly more flow per hectare than the cell outflow.

This difference in flow volume may be due to a difference in the number and size of storms at each site. Because the exact storm records were not determined for the Pond Branch site, how much rain actually fell at Pond Branch is unknown. 10 storm events were also excluded from Sligo-Dennis data set due to equipment malfunctions, which may have reduced the overall, cell outflow volume. Pond Branch also produced outflow in all analyzed storm events while the cell only produced outflow after 1.27 cm of rainfall. From Table 3.1, 69% of all storm events

produced ≤1.27 cm of rainfall, representing storms that would produce flow at Pond Branch but not cell outflow. While Pond Branch produced small volumes of flows (< 2,500 L according to Figure 3.25), these storms could account for about 190,000 L (190 m^3) of flow if 127 total storm events are assumed. Therefore, this high percentage of smaller storm events may result in a higher overall flow volume at Pond Branch.

While the cell outflow and Pond Branch flows often produced similar volumes of water for storms producing <2 cm of rainfall, they were distributed differently over time. This difference in flow-duration is crucial to understanding the performance of the Sligo-Dennis cell. Figure 3.30 shows a simple model of the overall flow distributions of both the cell outflow and of the Pond Branch flow. Both systems produced comparable volumes of water. The Pond Branch flow, however, was distributed over a much longer time period (typically twice as long as the cell outflow for individual storm events), producing flows about half those observed in the cell outflow.

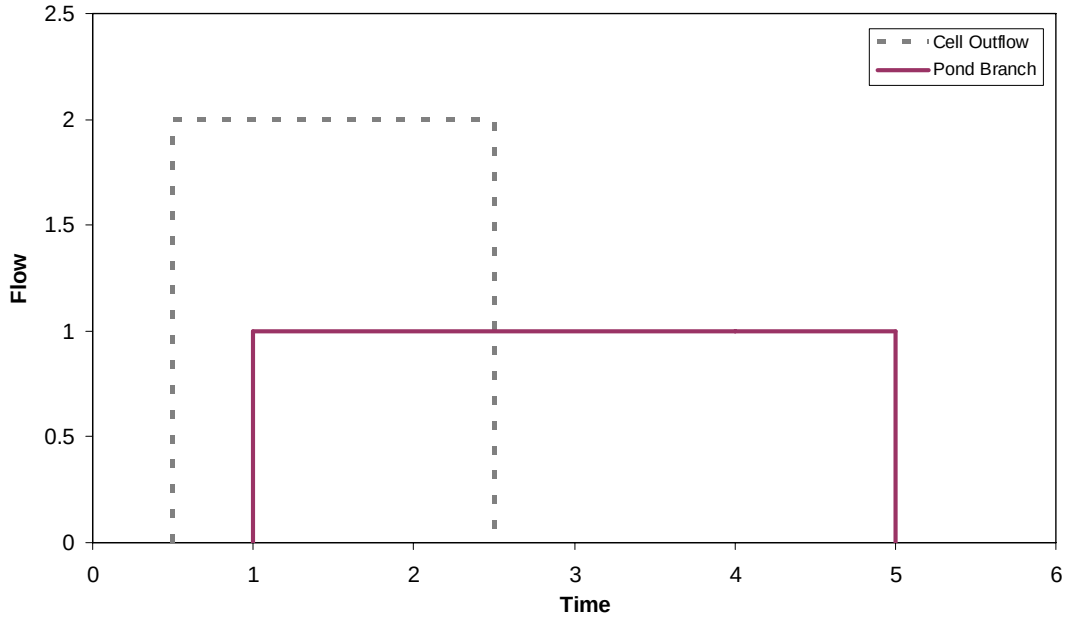

Figure 3.30 Simple representation of the overall flow distribution over the course of the current study for cell outflow and Pond Branch flow.

3.7 Water Quality Results

Total Phosphorous (TP) and Total Suspended Solids (TSS) tests were completed on samples from selected storms beginning July 23, 2009. Total Kjedahl Nitrogen (TKN), and nitrate tests were also run on all selected samples beginning in November 2009. A total of 15 samples were tested for phosphorous, 13 for TSS, and 5 for total nitrogen. Because 74% of all storm events entering the cell were completely captured, sampling outflowing storms was difficult. Only three storm events sampled produced outflow.

As previous studies have found, the actual outflowing concentrations of pollutants are favored over percent removals are necessary to evaluate BMP performance (Strecker et al. 2001). Both metrics, therefore, will be analyzed in this study. However, because no minimum nutrient levels have been established for

stormwater, it is difficult to evaluate how these effluent concentrations compare to pre-development values. Removals were based on all samples. Therefore, completely captured storm events reduced pollutant outflow levels by 100%.

Significant removal of both total phosphorous and TSS were found using both the Paired Student's Test and the Wilcoxon Signed-Rank Test. With relative influent and effluent means of 134 mg/L and 1 mg/L for TSS, the cell reduced TSS levels to below the excellent water quality criteria of 25 mg/L for the Potomac River Basin (Li and Davis 2009). Median values for TSS levels were 61 and 0 mg/L for influent and effluent water, showing most storm events had lower influent TSS levels. This trend is also shown in the large standard deviation of 208 mg/L for cell inflow, reflecting the large variance in TSS influent levels based on storm size and antecedent dry time. Longer dry periods between storm events should allow for greater build-up of pollutants, causing greater TSS influent levels. The effluent standard deviation of 0.563 mg/L is a function of very little TSS leaving the cell.

A mean value of 0.181 mg/L of TP entered the cell, while 0.026 mg/L left the cell over the course of the current study. The relative influent and effluent medians were 0.136 mg/L and 0. Both the mean and median effluent values are below 0.05 mg/L, which is the suggested level for excellent water quality in the Potomac River Basin (Li and Davis 2009). The standard deviation was relatively high for both influent and effluent water, with a value of 0.129 mg/L for cell inflow and 0.063 mg/L for cell outflow. This high variability in the data reflects the dependence of TP levels on storm size and antecedent dry time.

The Student's t-test showed significant removal within 0.05% for total phosphorous and within 2.5% for TSS. The Wilcoxon Signed-Rank Test found removal significance within 0.5% for both TP and TSS. Results for all pollutants analyzed for both tests are compiled in Tables 3.9 and 3.10.

Table 3.9. Statistical water quality results from Paired Student's t Test for water quality results.

	n	# Outflowing Events	computed t-value	Within a probability (%)	Significant Difference in population means?
Total Phosphorous	15	3	5.53	0.05	Yes (Removal)
TSS	13	3	2.32	2.5	Yes (Removal)
TN	5	2	-0.003	>10	No
TKN	5	2	0.693	>10	No
Nitrate	5	2	-0.951	>10	No

Table 3.10 Statistical water quality results from Wilcoxon Signed-Rank Test for water quality results.

	n	# Outflowing Events	computed t-value	Within a probability (%)	Significant Difference in population means?
Total Phosphorous	15	3	0	0.5	Yes (Removal)
TSS	13	3	0	0.5	Yes (Removal)
TN	5	2	5	---	No
TKN	5	2	5	---	No
Nitrate	5	2	6	---	No

The overall influent and effluent TSS EMC values from each storm event are shown in the exceedance plot in Figure 3.31. The cell showed significant removal of TSS. While only 3 of the 13 sampled storms produced outflow, two of these outflowing events were found to have effluent TSS concentrations of <1 mg/L, which was the detection limit. All effluent TSS concentrations were below the water criteria

of 25 mg/L (Li and Davis 2009). These results match well with a previous study done on the Sligo-Dennis cell, which found good TSS removal and a median effluent TSS concentration of 1 mg/L (Li and Davis 2009).

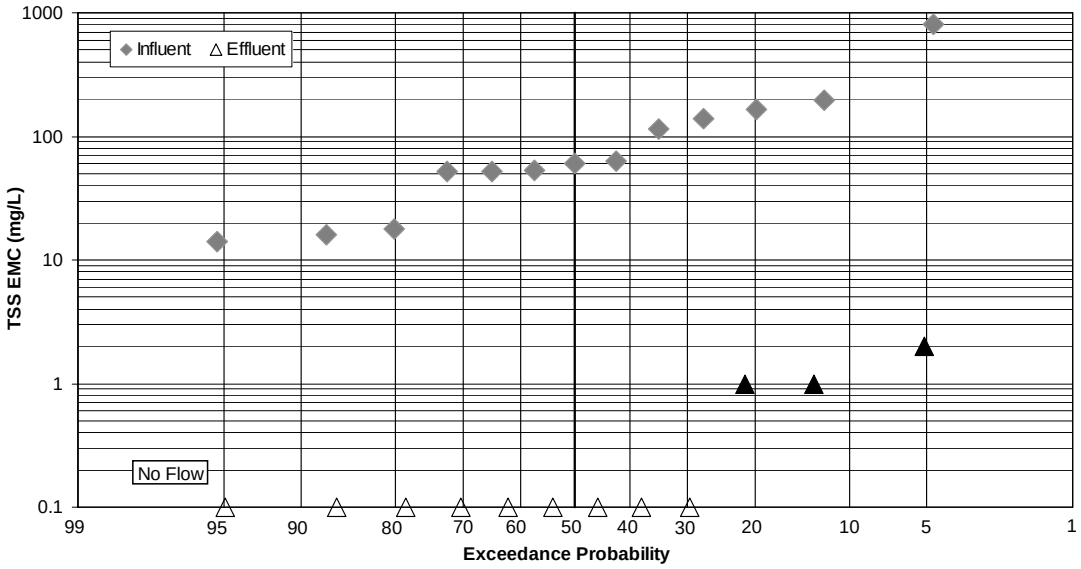

Figure 3.31 TSS exceedance plot for influent and effluent water from Sligo-Dennis bioretention cell. Significant removal was seen overall due to 10 out of 13 samples storms being completely captured. Outflowing events resulted in effluent TSS values around the minimum detection limit. Solid black triangles represent effluent values from storms producing outflow and black, outlined triangles represent effluent values from non-outflowing storms.

The cell also showed significant removal of total phosphorous based on the samples collected. The TP exceedance plot is shown in Figure 3.32. Only 3 out of the 15 sampled storms produced outflow. All 3 outflowing storms showed a significant reduction between influent and effluent TP concentrations. Both influent and effluent concentrations were moderate (< 0.55 mg/L), however, strict water quality criteria require an effluent concentration of 0.05 mg/L (Li and Davis 2009). Only one outflowing event produced a TP concentration lower than 0.05 mg/L. A previous study on the Sligo-Dennis cell found similar TP results. A number of other

studies actually found phosphorous concentration export in bioretention cells (Dietz and Clausen 2005; Hunt et al. 2006).

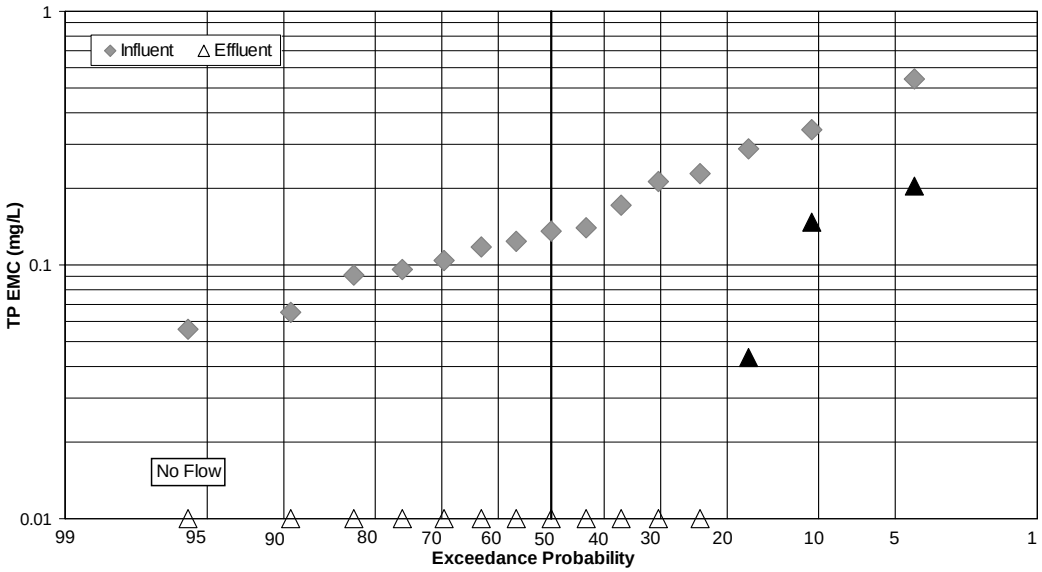

Figure 3.32 Total Phosphorous exceedance plot for influent and effluent water from Sligo-Dennis cell. Significant TP removal was seen. 12 out 15 sampled storm events completely captured all inflow and as a result all influent phosphorus. Solid black triangles represent effluent values from storms producing outflow and black, outlined triangles represent effluent values from non-outflowing storms.

Only 5 storm events were tested for total nitrogen (comprised of TKN and Nitrate), 2 of which were outflowing events. There was no significant difference between the influent and effluent TN, TKN, or Nitrate concentrations. The TN exceedance plot shown in Figure 3.33 shows that the effluent TN concentrations were greater than those of the influent for both outflowing events. This export of TN was primarily due to high concentrations of nitrate (around 4 times greater than influent levels) in the outflow. One storm event also exported TKN. While it is difficult to make conclusions the cell's behavior due to the small data set, the data points suggest denitrification did not occur during these outflowing events. These results differ with those found in a previous study done on the site, which found significant reduction in

TN (Li and Davis 2009). While this removal was accredited to the higher organic content of the cell media, the same reductions were not seen in the current study.

Samples taken on 3/12/2010 were representative of two consecutive storm events occurring just over 6 hours apart. The total duration of these storms was over 2.5 days. Because water continued to move through the cell throughout this period, conditions may have allowed for nitrification from NH_4-N to NO_3^-, but prevented anoxic regions from forming, which would have promoted denitrification from NO_3^- to N_2 gas. This behavior could explain the significant decrease of TKN from 3.36 mg/L in the influent to 0.98 mg/L in the effluent as well as the increase of Nitrate from 0.830 mg/L in the influent to 2.93 mg/L in the effluent. These results suggest that the cell does not remove and may even export nitrate during longer storm events, which do not allow anoxic regions to form. However, because only TKN and Nitrate samples were taken from only five storm events, no conclusions can be made about the overall cell performance with respect to nitrogen.

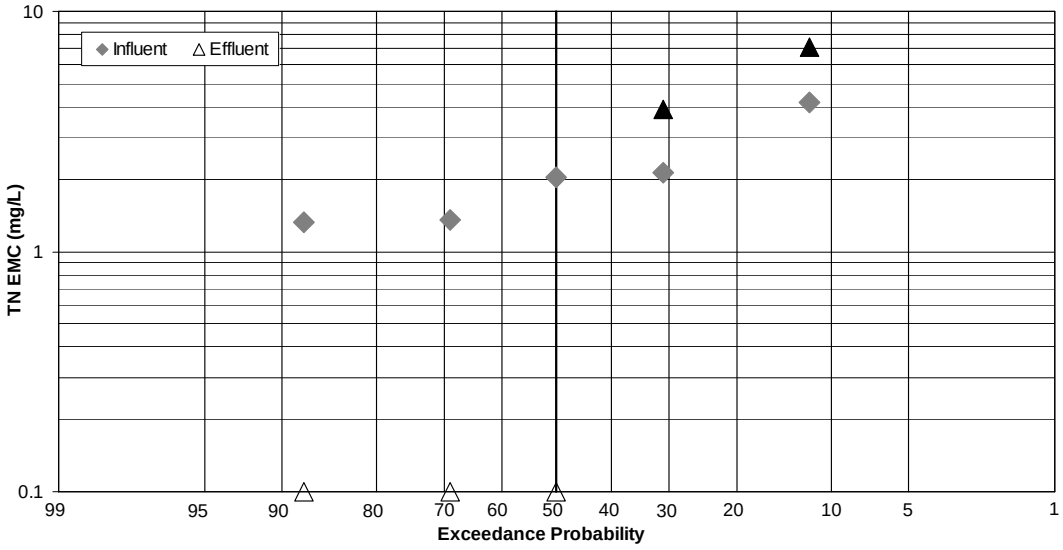

Figure 3.33 Total Nitrogen exceedance plot for influent and effluent water from Sligo-Dennis cell. Due to lack of data, no trends were observed in the behavior of TN in the cell. Two storm events were found to export TN. Solid black triangles represent effluent values from storms producing outflow and black, outlined triangles represent effluent values from non-outflowing storms.

The overall pollutant mass loads over the course of the study as well as the estimated yearly loads are compiled in Table 3.11. TSS removal was the most notable, being reduced from 2730 kg/ha-year to 0.44 kg/ha-year. While all sampled pollutants are reduced, these reductions are due mainly to water volume reduction rather than treatment processes within the cell. Therefore, no real conclusions can be made about the biological and chemical behavior of the cell due to lack of effluent samples. However, from a hydrological perspective, the cell removes all sampled pollutants well in a mass load basis.

More research is needed to better understand the behavior of phosphorous and nitrogen in bioretention cells. Media type, cell saturation, underdrain configuration (Hunt et al. 2006), and even storm size all play a role in the nitrogen reactions within a bioretention cell. Because only three storm events samples produced outflow, most

pollutant reduction were linked to the cell's hydrologic performance. Completely captured storm events also captured all associated pollutants. Therefore, overall cell size and storage capacity also affect the water quality of the cell. However, because bioretention cells promote infiltration into groundwater, it is also crucial to promote nitrogen and phosphorous degradation in order to avoid groundwater contamination.

Table 3.11 Comparison of the influent and effluent water quality and pollutant mass load for all water quality samples.

	Input EMC (mg/L)	Output EMC (mg/L)	Pollutant Mass Load Lin (kg/ha year)	Pollutant Mass Load Lout (kg/ha year)
TSS	316	1.12	2730	0.44
TP	0.279	0.095	2.41	0.04
TKN	1.28	0.594	11.1	0.23
Nitrate	0.393	1.40	3.40	0.55
TN	1.67	1.99	14.5	0.78

Chapter 4: Conclusions and Recommendations

4.1 Conclusions

The Sligo-Dennis bioretention cell successfully reduced runoff volumes, flowrates, and flow-durations, as well as TSS and total phosphorous EMC's of the Sligo-Dennis drainage area. Such improvements could have positive impacts on downstream ecosystem health by reducing turbidity, pollutant content, erosion, and channel degradation.

The cell has improved the overall hydrology of the site by altering how the site deals with rainfall and runoff from the parking lot. Rather than reacting directly to rainfall and rainfall intensity like the cell inflow, the cell outflow depends on cell saturation and ponding depth. This indirect relationship with rainfall makes outflow rates significantly smaller and more constant than inflow rates.

A storage capacity of 1.27 cm of rainfall depth, which corresponds to about 18,800 L of inflow, was estimated for the cell. Events smaller than this did not produce outflow. For larger events, a linear relationship with a slope of 0.549 (dimensionless) was observed between inflow and outflow volumes. Similar outflow trends were seen in both the current data set and a previous data set from the same cell collected in 2006 and 2007 (Li 2007). This storage capacity accounted for 20% of the total cell volume and about half of the estimated porosity. Therefore, increasing cell volume as well as available pore space would increase runoff storage.

In order to determine how well the cell performed volumetrically compared to pre-development values, the relative runoff depths were compared with those of CN

derived uses Woods B (CN=60), Woods C (CN=73), and Pavement (CN=98). The overall Sligo-Dennis site was estimated to have a CN of 79 (reduced from an initial CN=96 for the parking lot), performing slightly worse than woods C, which had a CN of 73. The cell, therefore significantly reduced the hydrologic impact of the site from a CN perspective.

Storage capacities and corresponding cell sizes were estimated based on each land use. Assuming the same cell depth, the current cell-to-drainage area ratio would have to be increased from 2.7% to 4.5% in order for the Sligo-Dennis site to perform the same hyrdologically as a Woods C land use. In order to achieve Woods B values, a ratio of 8.3% would be needed.

When assessed as a separate land use, the cell was found to have a CN=92. While the cell itself did not hydrologically mimic close to either woods land use, it reduced a CN=100 land use to CN=92. In order to achieve Woods C hydrologic performance, a cell size equal to 10.7% of the overall drainage area would be needed. Increasing the relative size of the cell would reduce both the cell's and the overall site's CN. Using these CN storage estimates as pre-development, volumetric goals could help to standardize bioretention performance. Such goals would allow for future studies to better define bioretention success as reducing a drainage area's hydrology values to those of pre-development rather than basing performance solely on percent reductions.

The cell inflow and outflow was also compared to flows from a forested stream, Pond Branch with an estimated CN of 76. Overall, for storm events producing < 2 cm of rainfall, the Sligo-Dennis cell performs similarly volumetrically

to the Pond Branch stream (a forested stream near Baltimore, MD), but produces much higher flowrates, maintaining them for longer durations. Pond Branch peak flows were quickly reduced, and were preceded and followed by long durations of low flows. This difference in flow-duration and flowrate may result from greater interception, infiltration, and time of concentration in the larger (31.1 ha) Pond Branch drainage area.

While the cell only produced outflow after 1.27 cm of rainfall, the Pond Branch stream produced flow in all storm events analyzed, suggesting no such storage threshold exists in forested streams, even after removal of a baseflow contribution. The cell performed volumetrically better than Pond Branch for rainfall events producing < 1.27 cm by completely capturing all runoff from the Sligo-Dennis site. However, the linear relationship observed between rainfall depth and cell outflow was steeper than that found between rainfall depth and Pond Branch flow. After about 2 cm of rainfall, cell outflow (per drainage area) became significantly greater than Pond Branch flow volumes due to this difference in slopes. The cell outflow was estimated to have flowrates twice as large and flow-durations half as long as Pond Branch in storm events producing < 2 cm based on the comparison hydrographs that were analyzed.

Both TP and TSS were found to be significantly removed by the cell. TN, TKN, and nitrate outflow levels, however, were not significantly different from inflow levels. Due to the small data set of nitrogen samples (5 data points), conclusions could not be made about the behavior of the different nitrogen forms in the cell. Because only three water quality samples were taken from storm events

producing outflow, most pollutant removal was due to the runoff containment of the cell.

4.2 Recommendations

Bioretention cell performance should be compared to both post-development and pre-development values. While an emphasis is currently put on hydrologic volume and peak flow reductions, actual pre-development goals are not as stressed. Pre-development hydrologic values should be the ultimate goal for all bioretention cells. While these values may be difficult to achieve, it is important to know how closely these facilities behave compared with congruent, pre-development areas.

Cell performance should also be evaluated independent of drainage area properties in order to normalize results. By assessing cells based on water that enters the cell only, more accurate comparisons could be made between studies despite differences in sites and drainage areas.

Flow-duration, in addition to peak flow, should also be a metric by which bioretention cells are evaluated. The Sligo-Dennis flow-durations were typically half the length and double the flowrate of those of Pond Branch. While, the cell produced comparable volumes of runoff to Pond Branch, it may still cause more erosion due to the extended, high flows.

In order to better imitate the pre-development flow trends seen in the Pond Branch stream, a larger bioretention cell is needed. Greater cell surface area especially, could reduce ponding depths, and as a result reduce outflow rates. A smaller outflow weir may also both reduce flowrates and increase flow-durations but

require larger storage volume. More research is necessary to better understand exactly how bioretention cells compare hyrdologically to actual pre-development areas.

Appendix 1: Hydrological Data for Sligo Dennis Bioretention Cell

Start	Duration (days)	Time Since Last Storm (days)	Rainfall (cm)	Peak Rainfall (cm) -- 4min inc.	Inflow peak (L/s)	Outflow peak (L/s)	Inflow Volume (L)	Outflow Volume (L)	Storage Capacity (L)	f(v)	Projected Inflow Volume (L) from Rainfall (0.92ac)	Mean Air Temperature (°F) (Baltimore, MD)
5/2/08 11:50 AM	0.20	0.96	0.711	0.102	16.38	0.50	27728	143	20791	0.005	26482	68.6
5/8/08 6:18 AM	1.31	5.57	4.928	0.533	40.02	2.72	71903	19319	32980	0.269	183484	67.5
5/10/08 3:55 AM	0.43	0.59	0.762	0.051	2.69	0.00	8339	0		0.000	28374	54
5/11/08 4:22 PM	1.22	1.09	7.264	0.102	6.26	1.63	132644	72066	16635	0.543	270497	50.9
5/15/08 11:40 PM	0.37	3.08	1.981	0.076	3.85	0.42	24610	4940	17849	0.201	73772	67.9
5/17/08 11:08 PM	0.003	1.61	0.025	0.025	0.00	0.00	0	0		---	946	62.7
5/18/08 1:50 PM	0.04	0.61	0.356	0.127	6.82	0.00	3782	0		---	13241	61.4
5/20/08 3:56 AM	0.40	1.55	1.499	0.051	3.55	0.07	17217	593	15095	0.034	55802	51.2
5/21/08 9:46 PM	0.003	1.35	0.025	0.025	0.00	0.00	0	0		---	946	56.7
5/31/08 12:20 PM	0.10	9.60	1.499	0.229	14.47	0.22	21723	750	20419	0.035	55802	72.3
6/3/08 7:20 PM	0.31	3.19	0.914	0.102	4.34	0.00	6613	0		---	34049	68.3
6/4/08 3:14 PM	0.42	0.50	2.616	0.127	25.81	1.17	41873	13035	17191	0.311	97417	71.4
6/7/2008 20:58	0.02	2.82	0.457	0.127	6.95	0.00	5745	0		---	17024	82.1
6/10/2008 20:18	0.02	2.95	0.584	0.330	24.29	0.00	9495	0		---	21753	82.2
6/14/2008 16:10	0.18	3.81	0.330	0.076	2.16	0.00	1628	0		---	12295	75.8
6/16/2008 16:06	0.36	1.82	1.194	0.076	3.62	0.00	13554	0		---	44452	70.6
6/18/2008 18:06	0.07	1.73	0.305	0.076	1.60	0.00	2780	0		---	11350	63.9
6/22/2008 20:54	0.003	4.04	0.025	0.025	0.00	0.00	0	0		---	946	74.9
6/23/2008 17:36	0.21	0.86	0.635	0.076	6.98	0.00	6416	0		---	23645	72.3
6/25/2008 10:00	0.00	1.47	0.025	0.025	0.00	0.00	0	0		---	946	73.4
6/27/2008 17:48	0.03	2.32	2.515	0.457	36.16	3.52	42981	12786	37673	0.297	93634	78.8
6/28/2008 13:56	0.003	0.81	0.025	0.025	0.00	0.00	0	0		---	946	75.9
6/28/2008 21:06	0.003	0.30	0.025	0.025	0.00	0.00	0	0		---	946	75.9
6/29/2008 3:54	0.01	0.28	0.127	0.102	1.27	0.00	748	0		---	4729	79.6
6/30/2008 17:46	0.17	1.57	0.203	0.025	0.35	0.00	456	0		---	7566	73.4

7/4/2008 6:04	0.01	3.34	0.076	0.025	0.12	0.00	68	0		---	2837	74.3
7/4/2008 17:12	0.17	0.45	0.178	0.025	0.68	0.00	586	0		---	6621	74.3
7/5/2008 8:56	0.02	0.49	0.051	0.025	0.11	0.00	69	0		---	1892	73.1
7/6/2008 19:12	0.02	1.41	0.178	0.051	1.31	0.00	1078	0		---	6621	73.6
7/9/2008 18:42	0.08	2.95	2.007	0.406	34.04	0.80	29153	3432	22203	0.118	74718	76.4
7/13/2008 19:02	0.47	3.93	2.642	0.254	21.11	0.30	30266	2437	21969	0.081	98363	77.4
7/22/2008 10:02	0.05	8.15	0.254	0.127	3.99	0.00	2193	0		---	9458	80
7/23/2008 20:36	0.19	1.39	1.829	0.203	13.98	0.20	21302	1134	13294	0.053	68097	76.8
7/27/2008 13:30	0.16	3.51	0.457	0.127	6.54	0.00	4454	0		---	17024	78.5
7/29/2008 4:14	0.07	1.45	0.051	0.025	0.00	0.00	0	0		---	1892	77
8/2/2008 5:04	0.07	3.97	0.660	0.330	16.92	0.00	8733	0		---	24591	77.5
8/7/2008 11:48	0.24	5.21	0.330	0.102	2.57	0.00	2054	0		---	12295	77
8/28/2008 5:06	0.33	20.48	1.346	0.030	2.90	0.00	9690	0		---	50127	70
8/29/2008 3:18	0.49	0.59	1.448	0.070	8.11	0.00	12869	0		---	53910	72
9/5/2008 20:20	0.14	7.22	0.508	0.040	5.05	0.00	3402	0		---	18916	78
9/6/2008 5:32	0.45	0.24	7.341	0.170	28.52	6.37	109317	64008	16416	0.586	273335	74
9/9/2008 12:46	0.06	10.90	0.178	0.010	0.83	0.00	1005	0		---	6621	76
9/12/2008 15:56	0.003	3.07	0.025	0.000	0.00	0.00	0	0		---	946	73
9/13/2008 11:08	0.003	0.80	0.025	0.000	0.00	0.00	0	0		---	946	79
9/25/2008 15:30	0.483	12.18	0.787	0.020	2.51	0.00	4878	0		---	29320	60
9/26/2008 9:22	0.042	0.26	0.229	0.040	0.68	0.00	1015	0		---	8512	64
9/26/2008 20:58	0.357	0.44	2.083	0.150	20.81	0.92	26052	3310	14425	0.127	77555	64
9/27/2008 15:08	0.099	0.40	0.178	0.010	0.28	0.00	504	0		---	6621	74
9/28/2008 1:58	0.635	0.35	0.381	0.030	5.67	0.00	2775	0		---	14187	73
9/30/2008 20:06	0.033	2.12	0.635	0.080	14.81	0.00	8716	0		---	23645	65
10/1/2008 13:54	0.278	0.71	0.279	0.040	0.96	0.00	850	0		---	10404	63
10/8/2008 23:36	0.003	7.13	0.025	0.000	0.00	0.00	0	0		---	946	56
10/25/2008 4:24	0.597	16.20	3.505	0.381	35.45	2.92	45894	12456	34439	0.271	130520	61
10/27/2008 14:02	0.890	1.80	0.711	0.025	0.28	0.00	2391	0		---	26482	48
11/4/2008 15:50	0.403	7.18	0.381	0.051	1.94	0.00	1677	0		---	14187	55
11/5/2008 23:52	0.135	0.93	0.051	0.025	0.25	0.00	30	0		---	1892	62
11/8/2008 8:12	0.003	2.21	0.025	0.000	0.00	0.00	0	0		---	946	60
11/13/2008 8:02	0.278	4.99	1.778	0.076	3.71	0.22	18694	1195	15891	0.064	66206	48
11/13/2008 22:02	0.003	0.31	0.025	0.000	0.00	0.00	0	0		---	946	48
11/15/2008 2:28	0.624	1.18	1.270	0.076	3.20	0.00	15613	0		---	47290	68

11/24/2008 20:20	0.257	9.12	0.305	0.025	0.34	0.00	711	0		---	11350	40
11/30/2008 3:14	0.886	5.03	1.753	0.025	3.94	0.00	16233	0		---	65260	39
12/4/2008 20:46	0.054	3.84	0.127	0.025	0.09	0.00	48	0		---	4729	42
12/10/2008 5:20	2.074	5.30	4.750	0.025	10.67	1.48	72404	33246	17445	0.459	176864	57
12/15/2008 23:42	0.196	3.69	0.102	0.025	0.34	0.00	240	0		---	3783	56
12/16/2008 12:04	0.003	0.32	0.025	0.000	0.00	0.00	0	0		---	946	45
12/16/2008 19:28	0.421	0.31	1.956	0.076	4.20	0.35	29024	7118	18122	0.245	72826	45
12/19/2008 6:10	0.590	2.03	0.889	0.051	2.77	0.00	9763	0		---	33103	42
12/21/2008 11:44	0.004	1.64	0.051	0.000	0.00	0.00	0	0		---	1892	38
12/26/2008 22:56	0.043	5.46	0.203	0.076	2.45	0.00	1519	0		---	7566	33
1/6/2009 4:48	1.649	10.20	4.978	0.025	5.88	0.86	77368	30348	23833	0.392	185376	36
1/10/2009 16:04	0.461	2.82	0.483	0.025	1.05	0.00	3427	0		---	17970	37
1/11/2009 10:40	0.003	0.31	0.025	0.025	0.00	0.00	0	0		---	946	33
1/29/2009 12:58	0.171	0.56	0.203	0.025	0.00	0.00	0	0		---	7566	30
1/30/2009 11:36	0.194	0.77	0.229	0.025	0.00	0.00	0	0		---	8512	30
2/3/2009 11:42	0.017	3.81	0.102	0.025	0.00	0.00	0	0		---	3783	32
2/11/2009 23:18	0.021	8.47	0.279	0.127	8.13	0.00	3265	0		---	10404	57
2/19/2009 10:42	0.003	0.75	0.025	0.025	0.00	0.00	0	0		---	946	37
2/22/2009 12:28	0.003	3.07	0.025	0.025	0.00	0.00	0	0		---	946	35
2/28/2009 0:48	0.003	5.51	0.025	0.025	0.00	0.00	0	0		---	946	43
3/14/2009 16:06	0.422	9.14	0.229	0.025	0.00	0.00	0	0		---	8512	39
3/15/2009 14:00	0.108	0.49	0.127	0.025	0.00	0.00	0	0		---	4729	41
3/16/2009 19:24	0.358	1.12	0.533	0.025	0.61	0.00	2927	0		---	19862	45
3/17/2009 14:52	0.003	0.45	0.025	0.025	0.00	0.00	0	0		---	946	46
3/19/2009 11:24	0.051	1.85	0.102	0.025	0.00	0.00	0	0		---	3783	48
3/26/2009 7:04	0.507	6.77	0.889	0.025	0.72	0.00	4819	0		---	33103	45
3/27/2009 20:26	0.512	1.05	2.616	0.127	6.14	1.26	38978	12983	16670	0.333	97417	51
3/28/2009 17:10	0.664	0.35	0.381	0.051	1.43	0.00	2013	0		---	14187	50
4/1/2009 17:26	0.142	3.35	0.254	0.025	0.41	0.00	716	0		---	9458	50
4/2/2009 7:20	0.003	0.44	0.025	0.025	0.00	0.00	0	0		---	946	56
4/3/2009 0:08	0.432	0.70	2.438	0.203	10.05	0.74	38207	6498	17092	0.170	90796	63
4/6/2009 9:02	0.140	2.94	0.102	0.025	0.11	0.00	100	0		---	3783	52
4/11/2009 4:10	0.290	4.66	1.524	0.051	1.48	0.42	13510	4177	11607	0.309	56748	57
4/13/2009 21:08	0.438	2.42	0.330	0.025	1.00	0.00	1028	0		---	12295	46
4/21/2009 18:14	0.019	5.82	0.051	0.025	0.00	0.00	0	0		---	1892	60

4/22/2009 8:52	0.240	0.59	0.533	0.152	4.33	0.00	4558	0		---	19862	50
4/29/2009 8:10	0.101	6.73	0.381	0.025	0.28	0.00	1051	0		---	14187	64
4/29/2009 16:54	0.142	0.26	0.152	0.025	0.09	0.00	173	0		---	5675	64
5/1/2009 2:50	0.003	1.27	0.025	0.025	0.00	0.00	0	0		---	946	70
5/1/2009 13:58	0.003	0.46	0.025	0.025	0.00	0.00	0	0		---	946	70
5/5/2009 16:20	0.250	0.90	0.559	0.076	1.72	0.00	4861	0		---	20807	56
5/6/2009 5:14	0.003	0.29	0.025	0.025	0.00	0.00	0	0		---	946	62
5/7/2009 11:26	0.100	0.38	0.381	0.152	7.80	0.00	5142	0		---	14187	68
6/8/2009 13:52	0.003	2.98	0.025	0.025	0.00	0.00	0	0		---	946	74
6/9/2009 6:02	0.060	0.67	0.914	0.127	17.23	0.00	12380	0		---	34049	75
6/9/2009 17:12	0.107	0.41	0.610	0.025	6.51	0.00	6986	0		---	22699	75
6/11/2009 12:58	0.003	1.72	0.025	0.000	0.00	0.00	0	0		---	946	72
6/12/2009 3:30	0.003	0.60	0.025	0.000	0.00	0.00	0	0		---	946	77
6/13/2009 13:28	0.019	1.41	0.127	0.102	0.48	0.00	58	0		---	4729	74
6/13/2009 22:58	0.003	0.38	0.025	0.000	0.00	0.00	0	0		---	946	74
6/16/2009 0:02	0.003	2.04	0.051	0.051	0.00	0.00	0	0		---	1892	67
6/17/2009 12:48	0.060	1.53	0.170	---	0.21	0.00	248	0		---	6337	64
6/18/2009 0:34	0.568	0.43	3.759	---	36.89	0.96	56509	12371	24582	0.219	139978	72
6/20/2009 9:06	0.240	1.79	1.168	---	20.76	0.11	15986	835	15986	0.052	43507	76
6/26/2009 19:14	0.017	6.18	0.787	---	26.05	0.00	9828	0		---	29320	73
7/1/09 1:56	0.012	4.26	0.102	0.076	0.49	0.00	293	0		---	3783	74
7/1/09 20:28	0.019	0.76	0.102	0.025	0.49	0.00	469	0		---	3783	74
7/8/09 12:00	0.003	6.63	0.025	0.000	0.00	0.00	0	0		---	946	69
7/22/2009 11:18	0.003	13.97	0.025	0.000	0.00	0.00	0	0		---	946	77
7/23/2009 15:04	0.319	1.15	0.356	0.076	2.05	0.00	1325	0		---	13241	77
7/25/2009 19:22	0.154	1.86	1.194	0.254	15.28	0.00	16937	0		---	44452	77
7/27/2009 8:22	0.058	1.39	0.051	0.025	0.00	0.00	0	0		---	1892	74
7/29/2009 18:44	0.003	2.37	0.025	0.000	0.00	0.00	0	0		---	946	80
7/31/2009 13:44	0.096	1.79	1.397	0.457	25.67	0.01	20941	17	19347	0.001	52019	79
8/1/2009 16:02	0.006	1.00	0.051	0.000	0.00	0.00	0	0		---	1892	76
8/2/2009 0:44	0.422	0.36	0.813	0.127	4.87	0.00	10675	0		---	30265	75
8/4/2009 10:36	0.003	1.99	0.025	0.000	0.00	0.00	0	0		---	946	77
8/6/2009 4:02	0.236	1.72	0.178	0.025	0.49	0.00	299	0		---	6621	71
8/7/2009 17:54	0.003	1.34	0.025	0.000	0.00	0.00	0	0		---	946	71
8/11/2009 22:12	0.011	4.18	0.203	0.152	5.72	0.00	1896	0		---	7566	80

8/18/2009 15:56	0.036	6.73	0.203	0.051	0.78	0.00	690	0		---	7566	82
8/18/2009 22:52	0.317	0.25	0.864	0.229	14.67	0.00	11928	0		---	32157	82
8/21/2009 14:40	0.787	2.34	1.499	0.356	16.80	0.00	18571	0		---	55802	83
8/22/2009 15:38	0.190	0.25	0.965	0.051	2.75	0.00	14937	0		---	35940	78
8/27/2009 10:12	0.003	4.58	0.025	0.025	0.00	0.00	0	0		---	946	76
8/28/2009 1:56	0.489	0.65	1.067	0.406	20.07	0.00	14370	0		---	39723	73
8/29/2009 19:34	0.086	1.25	1.270	0.254	20.28	0.00	20201	0		---	47290	78
9/6/2009 20:46	0.085	7.96	0.508	0.076	2.24	0.00	5137	0		---	18916	69
9/7/2009 9:38	0.006	0.45	0.051	0.025	0.00	0.00	0	0		---	1892	71
9/7/2009 16:44	0.021	0.29	0.102	0.025	0.86	0.00	672	0		---	3783	71
9/8/2009 3:08	0.065	0.41	0.076	0.025	0.00	0.00	0	0		---	2837	69
9/8/2009 12:32	0.003	0.33	0.025	0.025	0.00	0.00	0	0		---	946	69
9/9/2009 1:14	0.339	0.53	0.203	0.025	0.56	0.00	1010	0		---	7566	71
9/11/2009 4:14	0.599	1.79	1.549	0.076	5.62	0.00	22247	0	21780	0.000	57693	60
9/13/2009 6:12	0.003	1.48	0.025	0.025	0.00	0.00	0	0		---	946	70
9/14/2009 11:06	0.003	1.20	0.025	0.000	0.00	0.00	0	0		---	946	70
9/15/2009 17:28	0.194	1.26	1.067	0.406	24.57	0.00	14588	0		---	39723	73
9/17/2009 11:54	0.003	1.57	0.025	0.025	0.00	0.00	0	0		---	946	64
9/24/2009 0:44	0.003	6.53	0.025	0.025	0.00	0.00	0	0		---	946	77
9/25/2009 4:22	0.181	1.15	0.102	0.025	0.00	0.00	0	0		---	3783	67
9/26/2009 14:36	0.676	1.25	3.124	0.076	4.13	0.35	48857	4847	25664	0.099	116333	60
9/27/2009 15:30	0.018	0.36	0.432	0.152	8.55	0.00	6170	0		---	16079	67
9/30/2009 15:14	0.003	2.97	0.025	0.025	0.00	0.00	0	0		---	946	57
10/2/2009 21:04	0.043	2.24	0.051	0.025	0.00	0.00	0	0		---	1892	61
10/5/2009 9:12	0.003	2.46	0.0254	0.0254	0	0	0	0		---	946	58
10/7/2009 1:38	0.003	1.68	0.0254	0.0254	0	0	0	0		---	946	59
10/10/2009 0:08	0.011	2.93	0.0508	0.0254	0	0	0	0		---	1892	60
10/21/2009 13:36	0.003	3.29	0.0254	0.0254	0	0	0	0		---	946	59
10/23/2009 21:56	0.003	2.34	0.0254	0.0254	0	0	0	0		---	946	56
10/24/2009 14:54	0.101	0.70	0.635	0.1016	3.646102	0	8730.48	0		---	23645	66
10/31/2009 3:34	0.003	2.88	0.0254	0.0254	0	0	0	0		---	946	64
10/31/2009 19:06	0.781	0.64	0.0508	0.0254	0	0	0	0		---	1892	64
11/5/2009 16:36	0.006	4.12	0.0254	0.0254	0	0	0	0		---	946	46
11/6/2009 7:38	0.003	0.62	0.0254	0.0254	0	0	0	0		---	946	41
11/13/2009 4:32	0.003	0.62	0.0254	0.0254	0	0	0	0		---	946	52

11/13/2009 11:58	0.087	0.31	0.6858	0.1016	6.590614	0	13168.45	0		---	25536	52
11/14/2009 7:30	0.003	0.73	0.0254	0.0254	0	0	0	0		---	946	56
11/24/2009 23:06	0.539	0.53	0.4318	0.0254	0.521543	0	7804.588	0		---	16079	50
11/26/2009 17:18	0.447	1.22	1.0922	0.1524	10.52683	0	19952.1	0		---	40669	46
11/27/2009 13:48	0.014	0.41	0.0508	0.0254	1.00563	0	901.9878	0		---	1892	46
11/30/2009 10:56	0.282	2.87	0.5588	0.0254	0.900994	0	7630.285	0		---	20807	48
12/2/2009 13:46	0.585	1.84	1.7526	0.1016	4.614946	0.240718	34752.82	4627.383	20541.33	0.133151	65260	46
12/8/2009 3:32	0.003	0.41	0.0254	0	0	0	0	0		---	946	38
12/8/2009 10:44	0.878	0.30	4.2672	0.1016	7.048039	0.962463	89164.14	32864.38	19504.8	0.368583	158893	38
12/9/2009 15:14	0.003	0.31	0.0254	0	0	0	0	0		---	946	45
12/13/2009 6:18	0.428	3.63	1.7018	0.0762	4.606254	0.390135	31905.15	5898.419	22969.71	0.184874	63368	36
1/17/2010 8:08	0.561	34.65	1.397	0.0508	4.152462	0	30447.88	0		---	52019	40
1/18/2010 9:46	0.006	35.72	0.1016	0.0762	0	0	0	0		---	3783	45
1/20/2010 11:20	0.003	2.06	0.025	0.025	0	0	0	0.000		---	946	38
1/21/2010 22:16	0.181	1.45	0.254	0.025	0.486804	0.00	2621	0.000		---	9458	33
1/24/2010 19:32	1.115	2.71	1.422	0.102	2.603647	0.187385	27284	2772.814	17448	0.102	52964	42
3/12/2010 1:22	1.750	8.89	3.556	0.0762	2.965013	0.187385	81526.46	3788.55	37716.43	0.04647	132411	49
3/14/2010 3:32	0.533	0.34	0.7366	0.1016	4.468816	0	14132.92	0		---	27428	50
3/15/2010 5:06	0.236	0.53	0.203	0.025	0.594255	0	2227	0.000		---	7566	46
3/16/2010 10:00	0.003	0.97	0.025	0.000	0	0	0	0.000		---	946	51
3/22/2010 5:02	0.528	5.79	1.016	0.127	4.599167	0	13384	0.000		---	37832	56
3/25/2010 22:42	0.496	3.21	0.686	0.051	3.443882	0	9268	0.000		---	25536	56
3/28/2010 20:16	0.472	2.40	1.651	0.102	6.290672	0.086126	26457	674.383	18272	0.025	61477	49
3/30/2010 3:26	0.003	0.83	0.025	0.000	0	0	0	0.000		---	946	48
4/8/2010 19:56	0.308	9.68	1.880	0.229	9.493706	0.096678	26787	469.100	22195	0.018	69989	70
4/13/2010 12:02	0.274	4.36	0.356	0.025	0.594255	0	1964	0.000		---	13241	50
4/16/2010 20:02	0.003	3.06	0.025	0.000	0	0	0	0.000		---	946	70
4/21/2010 10:12	0.310	4.59	0.483	0.051	1.680808	0	4246	0.000		---	17970	51
4/22/2010 11:02	0.200	0.72	0.051	0.025	0	0	0	0.000		---	1892	60
4/24/2010 23:42	0.300	2.33	0.254	0.025	0.77575	0	1676	0.000		---	9458	53
4/25/2010 20:32	1.094	0.57	0.7112	0.0762	3.862156	0	8357.626	0		---	26482	55
4/29/2010 16:48	0.003	2.75	0.025	0.000	0	0	0	0.000		---	946	53

Appendix 2: Water Quality Data for Sligo-Dennis Bioretention Cell

Appendix 2: Water Quality Data for Sligo-Dennis Bioretention Cell

Total Phosphorous:

Date	TP In (mg/L)	TP Out (mg/L)
7/23/2009	0.287	0
7/25/2009	0.104	0
7/31/2009	0.065	0
8/2/2009	0.340	0
8/18/2009	0.124	0
9/5/2009	0.140	0
9/9/2009	0.056	0
9/26/2009	0.136	0.043
10/24/2009	0.091	0
11/13/2009	0.117	0
11/20/2009	0.172	0
11/30/2009	0.096	0
3/12/2010	0.544	0.148
4/9/2010	0.230	0.204
4/21/2010	0.214	0

Total Suspended Solids:

Date	TSS In (mg/L)	TSS Out (mg/L)
7/23/2009	16	0
7/25/2009	14	0
7/31/2009	196	0
8/18/2009	51.6	0
9/5/2009	166	0
9/9/2009	53.2	0
9/26/2009	52	0.5
11/13/2009	61	0
11/20/2009	114	0
11/30/2009	63	0
3/12/2010	800	2
4/9/2010	140	0.5
4/21/2010	18	0

Total Nitrogen, Total Kjedahl Nitrogen, and Nitrate:

Date	TKN In (mg/L)	TKN Out (mg/L)	Nitrate In (mg/L)	Nitrate Out (mg/L)	Total N In (mg/L)	Total N Out (mg/L)
11/13/2009	1.68	0	0.35	0	2.03	0
11/20/2009	1.54	0	0.59	0	2.13	0
11/30/2009	0.84	0	0.48	0	1.32	0
3/12/2010	3.360	1	0.830	2.930	4.19	3.91
4/9/2010	0.56	3.64	0.8	3.5	1.36	7.14

Bibliography

Ackerman, D., and Stein, E. D. (2008). Evaluating the Effectiveness of Best Management Practices Using Dynamic Modeling. *J Environ Eng 134*(8), 628-639.

Asleson, B., Nestingen, R., Gulliver, J., Hozalski, R., & Nieber, J. (2009). Performance Assessment of Rain Gardens. *J Am Water Resour Assoc, 45*(4), 1019-1031.

Balascio, C., and Lucas, W. (2009). A Survey of Storm-Water Management Water Quality Regulations in Four Mid-Atlantic States. *J Environ Manage. 90*(1), 1-7.

Barco, J., Hogue, T., Curto, V., and Rademacher, L. (2008). Linking Hydrology and Stream Geochemistry in Urban Fringe Watersheds. *J. Hydrology (Amsterdam), 360*(1-4), 31-47.

Bratieres, K., Fletcher, T., Deletic, A., and Zinger, Y. (2008). Nutrient and Sediment Removal by Stormwater Biofilters: A Large-Scale Design Optimisation Study. *Water Res, 42*(14), 3930-3940.

Bukaveckas, P. A. (2007). Effects of Channel Restoration on Water Velocity, Transient Storage, and Nutrient Uptake in a Channelized Stream. *Environ Sci Technol., 41*(5), 1570-1576.

Cunnane, C. (1978). "Unbiased plotting positions- a review," *J. Hydrology*, 37, 205-222.

Davis, A., Hunt, W., Traver, R., and Clar, M. (2009). Bioretention Technology: Overview of Current Practice and Future Needs. *J Environ Eng, 135*(3), 109-117.

Davis, A. P. (2005). "Green Engineering Principles Promote Low Impact Development," *Environ. Sci. Technol.*, 39 (16), 338A-344A.

Davis, A. P. (2007) "Field Performance of Bioretention: Water Quality." *Environ Eng Sci.* 24.8: 1048-64.

Davis, A. P. (2008) "Field Performance of Bioretention: Hydrology Impacts." *J Hydrologic Eng.* 13.2: 90-5.

Davis, A.P., and McCuen, R.H. (2005). *Stormwater Management for Smart Growth.* Springer, New York.

Dietz, M. E., and Clausen, J. C. (2005). A Field Evaluation of Rain Garden Flow and Pollutant Treatment. *Water Air Soil Pollut., 167*(1-4), 123-138.

Dietz, M. E., and Clausen, J. C. (2006). Saturation to Improve Retention in a Rain Garden. *Environ Sci and Technol.,* 40.4, 1335-1340.

Fetter, C.W. (2001). *Applied Hydrology: Fourth Edition,* Prentice-Hall, Inc, New Jersey.

Guo, J., and Cheng, J. (2008). Retrofit Storm Water Retention Volume for Low Impact Development. *J Irrigation and Drainage Eng, 134*(6), 872-876.

Guo, J. (2008). Volume-Based Imperviousness for Storm Water Designs. *J Irrigation and Drainage Eng, 134*(2), 193-196.

Heasom, W., Traver, R. G., and Welker, A. (2006). Hydrologic Modeling of a Bioinfiltration Best Management Practice. *J Am Water Resour Assoc, 42*(5), 1329-1347.

Hunt, W., Jarrett, A., Smith, J., and Sharkey, L. (2006). Evaluating Bioretention Hydrology and Nutrient Removal at Three Field Sites in North Carolina. *J Irrigation and Drainage Eng, 132*(6), 600-608.

Hunt, W., Smith, J., Jadlocki, S., Hathaway, J., and Eubanks, P. (2008). Pollutant Removal and Peak Flow Mitigation by a Bioretention Cell in Urban Charlotte, N.C. *J Environ Eng, 134*(5), 403-408.

Iman, R.L. (1977). "Graphs for Use in Testing Equality of Two Correlation Coefficients." *J. Quality Tech., 9*(4), 172-175.

Jones, M. P., and Hunt, W. F. (2009). Bioretention Impact on Runoff Temperature in Trout Sensitive Waters. *J Environ Eng, 135*(8), 577-585.

Kim, H., Seagren, E. A., and Davis, A. P. (2003). Engineered Bioretention for Removal of Nitrate from Stormwater Runoff. *Water Environ Res. 75*(4).

King, K., Smiley, P.,Jr, and Fausey, N. (2009). Hydrology of Channelized and Natural Headwater Streams. [Hydrologie de cours d'eau recalibres et naturels de tete de bassin] *Hydrological Sciences Journal/Journal Des Sciences Hydrologiques, 54*(5), 929-948.

Kreeb, L.B., and McCuen, R.H. (2003). *Hydrologic Efficiency and Design Sensitivity of Bioretention Facilities*. University of Maryland, College Park, MD.

Li, H., and Davis, A. P. (2009). Water Quality Improvement through Reductions of Pollutant Loads using Bioretention. *J Environ Eng, 135*(8), 567-576.

Li, H., and Davis, Allen P.. (2008) "Urban Particle Capture in Bioretention Media. I: Laboratory and Field Studies." *J Environ Eng* 134.6, 409-18.

Li, H., and Davis, Allen P. (2009) "Water Quality Improvement through Reductions of Pollutant Loads using Bioretention." *J Environ Eng*., 135.8: 567-76.

Li, H, Sharkey, L. J; Hunt, W. F; and Davis, A. P. (2009) "Mitigation of Impervious Surface Hydrology using Bioretention in North Carolina and Maryland." *Recent References Related to Technology.*

Li, H. (2007) "Urban Particle and Pollutant Capture via Stormwater Filter Facilities and the Concomitant Water Quality and Hydrological Benefits" *Doctorate of Philosophy Thesis.* University of Maryland

Line, D. E., and Hunt, W. F. (2009). "Performance of a Bioretention Area and a Level Spreader-Grass Filter Strip at Two Highway Sites in North Carolina." *J Irrigation and Drainage Eng.* 135.2 (2009): 217-224.

Lucas, W. C., and M. Greenway. (2008) "Nutrient Retention in Vegetated and Nonvegetated Bioretention Mesocosms." *J Irrigation and Drainage Eng.* 134.5: 613-23.

Mallin, M. A., Johnson, V. L., and Ensign, S. H. (2009). Comparative Impacts of Stormwater Runoff on Water Quality of an Urban, a Suburban, and a Rural Stream. *Environ Monit Assess., 159*(1-4), 475-491.

Maryland Department of the Environment (MDE). (2009). *2009 Maryland Stormwater Design Manual Volumes I & II*. MDE, Baltimore, MD. Available at http://www.mde.state.md.us/programs/waterprograms/sedimentandstormwater/stormwater_design/index.asp

McCuen, R. H. (1985). *Statistical Methods for Engineers.* Prentice-Hall, New Jersey.

McCuen, R. H. (2005). *Hydrologic Analysis and Design,* Pearson Education, Inc, New Jersey.

Mendenhall, W.; Sincich, T. (2007). *Statistics for Engineering and the Sciences,* Prentice Hall, Inc.

Muthanna, T.M., Vikilander, M., and Thorolfsson, S.T. (2008) "Seasonal Climatic effects on the Hydrology of a Rain Garden." *Hydrological Processes* 22: 1640-1649.

Prince George's County Department of Environmental Resources (PGDER), Programs and Planning Division. (2007). *Prince George's County Bioretention Manual*. Largo, MD. Available at http://www.princegeorgescountymd.gov/Government/AgencyIndex/DER/ESG/Bioretention/pdf/Bioretention%20Manual_2009%20Version.pdf.

Roseen, R., Ballestero, T., Houle, J., Avellaneda, P., Briggs, J., Fowler, G., and Wildey, R. (2009). Seasonal Performance Variations for Storm-Water Management Systems in Cold Climate Conditions. *J Environ Eng, 135*(3), 128- 137.

Strecker, E W., Quigley, M M., Urbonas, B R., Jones, J E., Clary, J K. (2003). "Determining Urban Storm Water BMP Effectiveness." *J Water Res Planning and Manage.* 127.3, 144-149.

Larson, Phillip. United States Geological Survey. (2009). *Oregon Ridge Rainfall Data.* Personal communication.

United States Geological Survey. (2010). *Current Pond Branch Flow Data.* Retrieved from http://waterdata.usgs.gov/md/nwis/nwisman?site_no=01583570.

Dillow, Jonathan, J. United States Geological Survey. (2010).Pond Branch Flow Data from *May 2008-Jan 2009.* Personal Communication .

Van Buren, M.A., Watt, W.E, and Marsalek, J. (1997). "Application of the Lognormal and Normal Distributions to Stormwater Quality Parameters," *Water Res.*, 31 (1), 95-104.

Walsh, C., Roy, A., Feminella, J., Cottingham, P., Groffman, P., & Morgan, R. (2005). The urban stream syndrome: Current knowledge and the search for a cure. *J North Am Benthol Soc., 24*(3), 706-723.

Yang, H., Florence, D. C., McCoy, E. L., Dick, W. A., & Grewal, P. S. (2009). Design and Hydraulic Characteristics of a Field-Scale Bi-Phasic Bioretention Rain Garden System for Storm Water Management. *Water Sci Technol., 59*(9), 1863-1872.